Evaluating how spatial heterogeneity in forage chemistry and abundance influences diet and demographics in a declining moose (*Alces alces*) population in northeast Minnesota.

A Dissertation
SUBMITTED TO THE FACULTY OF THE
UNIVERSITY OF MINNESOTA
BY

John L. Berini III

IN PARTIAL FULFILLMENT OF THE REQUIREMENTS
FOR THE DEGREE OF
DOCTOR OF PHILOSOPHY

James D. Forester

May 2019

Acknowledgements

While there are only two names on the title page of this dissertation, the story that unfolds on the following pages would not have been possible without the contributions of many.

To my wonderful family - thank you for supporting me through all of my successes and failures over the course of the last eight years. Sarah, that hike in Texas many years ago planted the seeds that would eventually grow into an M.S. and now a Ph.D. studying wildlife – something I didn't realize was even a possibility before we met. Thank you for supporting me to follow my passions, no matter the cost, when you were the individual that would likely be impacted the most. Noah, thank you for being patient with me when I allowed stress to influence my ability to be a good father. Kate, thank you for being my silent supporter and for giving so much of yourself so that I could succeed. There are no words to describe how grateful I am to have each of you in my life. I love you.

To my advisor, Dr. James Forester – thank you for allowing me to have enough latitude to learn how to recover from my own mistakes that I'm sure you saw coming from a mile away. Thank you for pushing me to do things that I would never have thought myself capable of when I began this research in 2011. Struggling through these experiences has made me a better scientist, and ultimately, a better human.

To my committee – thank you for providing with the feedback that I needed and not the feedback that I wanted. Lee, your knowledge of northeastern Minnesota helped me establish and refine my sampling regime from year one. Glenn, your knowledge of

wildlife physiology has helped me acquire a deeper and richer understanding of my study system, and your passion for communicating science in a clear and direct way has given me something to aspire to. David, thank you for guiding me to a deeper understand of stable isotopes and how we can (and cannot!) use them to better understand animal ecology. Rebecca, thank you for being a constant support since I was an undergraduate working with David Mech and Dan McNulty, and for providing me with an opportunity to better understand how climate influences plants and the animals that depend on them.

The Minnesota Department of Natural Resources played a critical role in my ability to predict moose diets by providing tissue samples from both living and dead moose. Without these samples, this dissertation would have been far less meaningful. Specifically, I would like to thank everyone associated with the Wildlife Health Program, who led the adult moose mortality project. E. Hildebrand and M. Carstensen were crucial in helping me obtain moose tissue samples and the metadata required to use these samples in a meaningful way.

I would also like to thank the members of the Forester Lab, past and present, including W. Severud, G. Oliveira-Santos, A. Herberg, S. Rettler, A. Les, S. Berg, P. Castro Antunes, R. Castro-Bustamante, G. Street, L. White, and S. Pittman. I'd like to specifically thank R. Muthukrishnan, who challenged me at every corner and became a close friend through his role as an "interim-advisor." Your guidance has helped be become substantially more capable as a quantitative ecologist and a coder. I cannot thank you enough. I'd also like to thank both the Montgomery and Fox Labs, for accepting me as one of their own, and helping me expand my horizons as a scientist.

Thank you to the army of undergraduate students who helped collect, process and analyze thousands of plant samples (literally!) over the last eight years. I'd specifically like to thank C. Montgomery and D. Erickson – you guys made my life so much easier, and I'm grateful to have had you help me keep things organized and running smoothly. Finally, I want to thank Michael Wethington - you have been with me on this project since day one, and this success of this project is as much yours as it is mine. I'm excited to see where things go for you over the next couple of years as you begin your own work in Antarctica!

This study has been supported by the Environment and Natural Resources Trust Fund, the Institute on the Environment, and the Environmental Protection Agency via the Science to Achieve Results Fellowship. I was also supported by the Conservation Biology Graduate Program via the summer block grant program and the Wally Dayton Fellowship.

A version of Chapter 2 has been published as: Berini JL, Brockman SA, Hegeman AD, Reich PB, Muthukrishnan R, Montgomery RA and Forester JD (2018) Combinations of Abiotic Factors Differentially Alter Production of Plant Secondary Metabolites in Five Woody Plant Species in the Boreal-Temperate Transition Zone. Front. Plant Sci. 9:1257. doi: 10.3389/fpls.2018.01257.

Dedication

I dedicate this thesis to anyone who overcame difficult circumstances to become greater than what the world expected of you.

Abstract

Since 2006, the moose population in northeastern Minnesota has declined by nearly 50%. While recent warming has been implicated as a primary cause of this decline, there is little evidence to support this relationship. More recent evidence suggests that the influences of warming and poor nutrition may predispose moose to increased risk of mortality, including mortality attributed to predation and disease. During summer, moose begin to experience the detrimental effects of high temperatures at around 14 to 17 ºC, and mean-maximum summer temperatures in this area range from 19.5 ºC along Lake Superior, to approximately 24.5 ºC in the more central part of the region. Thus, moose in northeastern Minnesota are likely dealing with the negative effects of high temperatures on a routine basis throughout summer.

While it has been suggested that nutrition and warming may be acting in concert to influence moose demographics in Minnesota, potential synergisms between these factors have not been investigated. Thus, I evaluated how spatial variation in the thermal landscape influences forage chemistry, the abundance and distribution of forage, and the spatial variation in moose diets and overwinter survival. To determine how high temperatures might influence the chemistry of moose forage, I used untargeted metabolomics to evaluate how varying combinations of temperature, moisture, and light in both experimental and natural conditions influence the production of plant secondary metabolites in moose forage. To investigate how the abundance and chemistry of moose forage varies across NEMN, I used a mixed-effects regression kriging framework to estimate spatial variation of $\delta^{13}C$ and $\delta^{15}N$ values in plants commonly eaten by moose,

and then refined these predictions using species-specific allometric equations to estimate above-ground biomass of moose forage. Finally, to investigate the interaction between spatial variation in high summer temperatures, moose diet, and over-winter survival, I used stable isotope values from forage and hair to estimate moose diet via Bayesian mixing models, and then evaluated if diet composition and quality vary as a function of mean-maximum summer temperature, season, or winter mortality.

In general, warming and high-temperatures had variable effects on the defensive chemistry of moose forage, only a minor influence on forage abundance, and a strong effect on diet quality, composition, and overwinter survival. Specifically, when investigating the influences of warming on PSM production in moose forage, I found that the influences of temperature can be modulated by the presence or absence of other abiotic factors, such as precipitation and light. As an example, the relative abundance of compounds known to negatively influence moose herbivory increased by 250% or more when high temperatures occurred in an open canopy setting. When modeling spatial heterogeneity in the chemistry and abundance of moose forage across northeastern Minnesota, I found that while mean-maximum summer temperature played a strong role in the isotopic composition of moose forage across the region, it had only a minor effect on distribution and abundance. Finally, when investigating interactions between spatial variation in high summer temperatures, moose diet, and over-winter survival, I found that the warmest parts of the moose range in Minnesota were those where moose diets were poorest and where winter mortality rates were highest. Specifically, I found that moose in the warmest parts of the range have diets containing the highest proportion of aquatic

forage and the lowest proportion of high-preference forage. Additionally, moose that did not survive winter had diets containing substantially greater proportions of aquatic forage throughout the entire growing season when compared to moose that survived, which consumed mostly high-preference forage during early summer but increased their consumption of aquatics during late summer. Finally, while I estimated overall mortality to be at approximately 30% throughout the entire study region, mortality in the warmest parts of the range (69%) was approximately 4.5 times higher than that in the coolest parts of the range (15%).

Given the evidence I present here, habitat-improvement projects may want to focus on promoting the regeneration of forage species that can adapt to future warming scenarios, while still providing thermal refuge, and proper nutrition during late summer. Also, future studies should evaluate spatially explicit differences in habitat use as a function of the thermal landscape and how variation in habitat use-behavior (i.e., movement) within the thermal landscape may influence diet composition, quality, and nutritional restriction. Identifying mechanistic links between movement, diet, and nutritional condition within the thermal landscape would advance our basic knowledge of large mammal behavior and ecology, as well as help develop sound management strategies in how we plan for future warming.

Table of Contents

List of Tables

List of Figures

Chapter 2

Chapter 3

Chapter 4

Chapter 1: Summer Temperatures and Forage Chemistry may interact to influence Diet Composition and Moose Demographics in Northeastern Minnesota – An Introduction.

With roughly 200 species of terrestrial vertebrates going extinct in the last 100 years, there is evidence that we are currently in the midst of Earth's sixth mass extinction event (Ceballos et al. 2017). Over this same time period, more than 40% of known terrestrial vertebrate species have exhibited severe population decline (> 80% range contraction; Ceballos et al. 2017), and from 1970 to 2014, populations of terrestrial vertebrates declined by an average of 60% (Barrett et al. 2018). In mammals, population declines are often attributed to habitat loss and degradation, overexploitation, invasive species, and disease, with recent changes in climate also thought to be a major contributor (Barrett et al. 2018, Ripple et al. 2015). Although mammal species in tropical regions appear to be most vulnerable to extinction, those at high latitudes are more vulnerable to climate change than anywhere else on the planet (Barrett et al. 2018), with large mammals more likely to experience the adverse effects of climate than their smaller counterparts (Mccain and King 2014).

Global distributions of large herbivore diversity are associated with gradients of temperature and precipitation (Olff et al. 2002, Walther et al. 2002), with the negative influences of temperature largely attributed to the positive association between body size and temperature sensitivity (Gillooly et al. 2001). High-temperatures can influence large herbivores directly via a number of different mechanisms. For example, male ibex (*Capra ibex*) reduce feeding activity during periods of high temperatures (Aublet et al.

2009), presumably in an effort to minimize metabolic heat production (Turbill et al. 2011), and moose have been shown to alter habitat-use behavior as a function of ambient temperature, choosing habitats that offer thermal refugia over those that provide high-quality forage (van Beest and Milner 2013, Street et al. 2016). In addition to the direct physiological and behavioral effects that high temperatures can have on large mammals, the influences of recent warming are pervasive, thereby leading to a range of indirect effects as well (Parmesan 2006, Walther et al. 2002).

The North American moose (*Alces alces*) is a cold-adapted species that is relatively intolerant of high temperatures (Renecker and Hudson 1990), and in recent years has experienced population declines across much of the southern edge of its geographic range (Timmermann and Rodgers 2017). In northwestern Minnesota, moose exhibited a precipitous decline starting in the mid 1980s, decreasing from about 4000 animals in 1984 to less than 100 animals in 2007 (Lenarz et al. 2009, Murray et al. 2013). A study investigating this decline reported that the majority of moose fatalities (87% of radio-collared moose and 65% of non-collared moose) were ultimately due to parasites and infectious disease. However, the authors also noted that many of the recorded causes of mortality were likely acting in close association with poor nutrition and warming (Murray et al. 2006). Animals that died of natural causes exhibited notable signs of malnutrition and severe body fat depletion, and annual population growth in northwestern Minnesota from 1961-2000 was negatively correlated with mean summer temperature, which increased by 2.1 ºC during this time (Murray et al. 2006).

In recent years, the moose population in northeastern Minnesota (NEMN) has exhibited demographic trends similar to those observed in the northwestern part of the state, declining by more than 65% from 2006 to 2018 (DelGiudice 2018, Lenarz et al. 2009). Because moose are heat intolerant, when they are exposed to prolonged periods of high temperatures, they increase metabolic and respiration rates and reduce forage intake, which can lead to malnutrition, decreased body condition, and immunosuppression (Lenarz et al. 2009, McCann et al. 2013, Murray et al. 2006, Renecker and Hudson 1986). Although one study reported a negative correlation between high temperatures and survival in this population (Lenarz et al. 2009), there is little mechanistic evidence to explain a relationship between recent warming and moose declines. Moreover, the wolf population in this region has substantially increased since 2006, with a strong inverse relationship between wolf numbers and calf:cow ratios from 2001 to 2013 (Mech and Fieberg 2014). One study recently reported between 33 and 47% of monitored moose calf mortalities was due, at least in part, to wolf predation (Severud et al. 2015), while another reported that more than 30% of analyzed wolf scats from NEMN contained moose tissue (Chenaux-Ibrahim 2015). However, it is important to note that moose significantly reduce anti-predatory behavior during periods of resource limitation (Oates et al. 2019), and in a study summarizing necropsy results of 62 opportunistically collected moose carcasses from 2003 to 2013, 85% of animals were either moderately underweight or exhibiting signs of severe weight loss and muscle deterioration (Wünschmann et al. 2015).

High-temperatures could also be indirectly impacting large herbivores through their forage. This impact could yield large-scale demographic consequences (Owen-Smith 2002, Shi et al. 2003), the causes of which could be difficult to detect. At the plant level, temperature increases of < 2 ºC in Minnesota have been shown to significantly reduce crude protein and carbohydrates (Jamieson et al. 2015), while also leading to significant phenological advancement (Schwartzberg et al. 2014). At the animal level, warming of 3 to 6 ºC can lead to decreased forage intake and digestibility (Savsani et al. 2015), as well as increased sensitivity to plant defensive compounds (Kurnath et al. 2016), all of which have been shown to influence survival and reproduction in large mammals (Barboza and Parker 2008, Cook et al. 2004, Langvatn et al. 1996, McArt et al. 2009). During summer, the moose range in Minnesota spans a 5 ºC mean-maximum summer temperature gradient, going from roughly 19.5 ºC in the northeastern-most part of the range, to approximately 24.5 ºC in the more central parts of the range (PRISM Climate Group 2017). Moose begin to experience the detrimental effects of high temperatures at around 14 to 17 ºC (McCann et al. 2013, Renecker and Hudson 1986). Thus, moose in NEMN are likely dealing with the negative effects of high temperatures on a routine basis. Together, the influences of warming on moose and their forage could have a profound negative impact on demographics via their specific, synergistic influences on survival and reproduction.

While it has been suggested that nutrition and warming may be acting in concert to influence moose demographics in Minnesota (Murray et al. 2006), potential synergisms between these factors have not been investigated. Thus, I evaluated how

warming and spatial variation in the thermal landscape influences forage chemistry, the abundance and distribution of forage, and the spatial variation in moose diets and overwinter survival. To determine how high temperatures influence the chemistry of moose forage (Ch. 1), I used untargeted metabolomics to evaluate how varying combinations of temperature, moisture, and light in both experimental and natural conditions influence the production of plant secondary metabolites in moose forage. To investigate how the abundance and chemistry of moose forage varies across NEMN (Ch. 2), I used a mixed-effects regression kriging framework to estimate spatial variation of $\delta^{13}C$ and $\delta^{15}N$ values in plants commonly eaten by moose, and then refined these predictions using species-specific allometric equations to estimate above-ground biomass of moose forage. Finally, to investigate the interaction between spatial variation in high summer temperatures, moose diet, and over-winter survival (Ch. 3), I used stable isotope values from forage and hair to estimate moose diet via Bayesian mixing models, and then evaluated if diet composition and quality vary as a function of mean-maximum summer temperature, season, or winter mortality.

In general, warming and high-temperatures had variable effects on the defensive chemistry of moose forage, only a minor influence on forage abundance, and a strong effect on diet quality, composition, and overwinter survival. Specifically, when investigating the influences of warming on PSM production in moose forage (Ch. 1), I found that the influences of temperature can be modulated by the presence or absence of other abiotic factors, such as precipitation and light. As an example, the relative abundance of compounds known to negatively influence moose herbivory (i.e., diterpene

resin acids, Danell et al. 1990) increased by 250% or more when high temperatures occurred in an open canopy setting. When modeling spatial heterogeneity in the chemistry and abundance of moose forage across NEMN (Ch. 2), I found that while mean-maximum summer temperature played a strong role in the isotopic composition of moose forage across the region, it had only a minor effect on distribution and abundance. This suggests that any relationship we observe between moose diet and the thermal landscape is likely due to temperature-induced changes in behavior (i.e., habitat use and forage intake or selection) rather than variation in abundance. Finally, when investigating interactions between spatial variation in high summer temperatures, moose diet, and over-winter survival (Ch. 3), I found that the warmest parts of the moose range in Minnesota were those where moose diets were poorest and where winter mortality rates were highest. Specifically, I found that moose in the warmest parts of the range have diets containing the highest proportion of aquatic forage and the lowest proportion of high-preference forage. Additionally, moose that did not survive winter had diets containing substantially greater proportions of aquatic forage throughout the entire growing season when compared to moose that survived, which consumed mostly high-preference forage during early summer but increased their consumption of aquatics during late summer. Finally, while I estimated overall mortality to be at approximately 30% throughout the entire study region, mortality in the warmest parts of the range (69%) was approximately 4.5 times higher than that in the coolest parts of the range (15%).

Collectively, the evidence I present here suggests that high summer temperatures may underlie the recent moose decline via the synergistic effects of warming on moose

behavior and forage. Habitat-improvement projects may want to focus on promoting the regeneration of forage species that can adapt to future warming scenarios, while still providing thermal refuge, and proper nutrition during late summer. For example, replanting efforts may want to consider genetic strains of paper birch, trembling aspen, and willow (i.e., high-preference moose forage) that are adapted to warmer climates, potentially helping buffer moose against some of the temperature-induced synergies I observed here. Also, future studies should evaluate spatially explicit differences in habitat use as a function of the thermal landscape and how variation in habitat use-behavior (i.e., movement) within the thermal landscape may influence diet composition, quality, and nutritional restriction. Also, creating landscape-scale models depicting an animal's fundamental dietary niche (i.e., what the diet should be, given the composition of the landscape, in the absence of selection) and then comparing these models to spatial variation in diet would provide valuable insights into how different habitat covariates (e.g., temperature, landscape composition, predator densities) may influence diet selection. Identifying mechanistic links between movement, diet, and nutritional condition within the thermal landscape would advance our basic knowledge of large mammal behavior and ecology, as well as help develop sound management strategies in how we plan for future warming.

Chapter 2: Combinations of Abiotic Factors Differentially Alter Production of Plant Secondary Metabolites in Five Woody Plant Species in the Boreal-temperate Transition Zone.

ABSTRACT Plant secondary metabolites (PSMs) are a key mechanism by which plants defend themselves against potential threats, and changes in the abiotic environment can alter the diversity and abundance of PSMs. While the number of studies investigating the effects of abiotic factors on PSM production is growing, we currently have a limited understanding of how combinations of factors may influence PSM production. The objective of this study was to determine how warming influences PSM production and how the addition of other factors may modulate this effect.

We used untargeted metabolomics to evaluate how PSM production in five different woody plant species in northern Minnesota, USA are influenced by varying combinations of temperature, moisture, and light in both experimental and natural conditions. We also analysed changes to the abundances of two compounds from two different species – two resin acids in *Abies balsamea* and catechin and a terpene acid in *Betula papyrifera*. We used perMANOVA to compare PSM profiles and phytochemical turnover across treatments and NMDS to visualize treatment-specific changes in PSM profiles. We used linear mixed-effects models to examine changes in phytochemical richness and changes in the abundances of our example compounds.

Under closed-canopy, experimental warming led to distinct PSM profiles and induced phytochemical turnover in *B. papyrifera*. In open-canopy sites, warming had no influence on PSM production. In samples collected across northeastern Minnesota,

regional temperature differences had no influence on PSM profiles or phytochemical richness but did induce phytochemical turnover in *B. papyrifera* and *Populus tremuloides*. However, warmer temperatures combined with open canopy resulted in distinct PSM profiles for all species and induced phytochemical turnover in all but *Corylus cornuta*. Although neither example compound in *A. balsamea* was influenced by any of the abiotic conditions, both compounds in *B. papyrifera* exhibited significant changes in response to warming and canopy. Our results demonstrate that the metabolic response of woody plants to combinations of abiotic factors cannot be extrapolated from that of a single factor and will differ by species. This heterogeneous phytochemical response directly affects interactions between plants and other organisms and may yield unexpected results as plant communities adapt to novel environmental conditions.

INTRODUCTION

Plant secondary metabolites (PSMs) are one of the primary ways in which plants respond to environmental variability, and regulation of PSM production is strongly influenced by the local environment (Bennett and Wallsgrove 1994, Bray et al. 2000, Hirt and Shinozaki 2003, Wink 1988). Many interactions between plants and other organisms are mediated by PSMs (Farmer 2001, Karban 2008, Karban et al. 2006), and thus, the biochemical mechanisms that influence these interactions are modulated, at least in part, by the presence, absence, or magnitude of various environmental factors (DeLucia et al. 2012, Jamieson et al. 2012). For instance, changes in the amount and seasonality of precipitation have been shown to influence concentrations of cyanogenic glycosides (Gleadow and Woodrow 2002, Vandegeer et al. 2013), and elevated concentrations of

atmospheric CO_2 often result in increased concentrations of condensed tannins (Lindroth 2012). Evidence is mounting that recent warming may also influence the production of PSMs (Kuokkanen et al. 2001).

Studies investigating the influence of warming on PSM production suggest that temperature-induced changes to PSMs may be species, compound, or even context dependent. For example, warming has been shown to have no effect on levels of phenolics in red maple (*Acer rubrum*, (Williams et al. 2003), Norway spruce (*Picea abies*, (Sallas et al. 2003), and Scots pine (*Pinus sylvestris*, (Sallas et al. 2003) but resulted in decreased levels of phenolics in dark-leaved willow (*Salix myrsinifolia,* (Veteli et al. 2006) and silver birch (*Betula pendula*, (Kuokkanen et al. 2001). Additionally, warming has been shown to increase levels of terpene-based compounds in Norway spruce (Sallas et al. 2003), Ponderosa pine (*Pinus ponderosa*, (Constable et al. 1999), and Scots pine (Sallas et al. 2003) but has been shown to both increase (Constable et al. 1999) and decrease (Snow et al. 2003) levels of monoterpenes in Douglas fir (*Pinus menziesii*). While evidence of warming-induced changes to phytochemistry is important to our understanding of how plants will respond to future climates, in natural settings, elevated temperature often combines with other abiotic conditions to influence PSM production and potentially modulate any changes to phytochemistry that might otherwise be induced by warming alone.

As temperatures continue to rise, global precipitation patterns are expected to shift (Alexander et al. 2006, Hurrell 1995, IPCC 2014) and light availability to understory plants will likely be altered due to changes in the frequency and intensity of forest

disturbance patterns (Canham et al. 1990, Dale et al. 2001). While variability in each of these environmental factors has been shown to influence production of PSMs on their own (Bryant et al. 1983, Dudt and Shure 1994, Pavarini et al. 2012), combinations of factors can have a distinct effect (Mittler 2006, Rizhsky et al. 2002, 2004, Zandalinas et al. 2018). Moreover, plant responses to combinations of abiotic factors can be either synergistic or antagonistic (Bonham-Smith et al. 1987, Mittler 2006, Zandalinas et al. 2018). For example, drought has been shown to enhance cold tolerance (Cloutier and Andrews 1984), but also exacerbate a plant's intolerance of high temperatures (Rizhsky et al. 2002). Further, different combinations of salinity and high temperatures have been shown to have both positive and negative influences on the metabolism of reactive oxygen species and stomatal response (Zandalinas et al. 2018). Regardless, the vast majority of current research remains focused on the influences of individual conditions rather than considering potential interactions among them.

Until recently, the majority of studies investigating the potential influence of different abiotic factors largely considered the effects of these factors on individual compounds or small groups of compounds. However, individual metabolites rarely, if ever, function in isolation (Gershenzon et al. 2012). Rather, the influence of any one compound is dependent on conditions within the local environment, as well as the relative abundance of numerous other metabolites within a plant's array of chemical constituents (Dyer et al. 2003, Gershenzon et al. 2012, Jamieson et al. 2015, Richards et al. 2010). Thus, understanding how changes in the abiotic environment will influence a

plant's metabolic profile is important for interpreting how these changes will influence the abundance and biological role of individual compounds as well.

Phytochemical diversity influences how effective plants are when defending against a range of threats (Frye et al. 2013, Gershenzon et al. 2012, Richards et al. 2015). Compounds may act synergistically, thereby forming mixtures that can provide enhanced protection against potential hazards (Gershenzon 1984, Gershenzon et al. 2012, Harborne 1987). Indeed, recent evidence suggests that the number of individual compounds comprising a plant's phytochemical profile can even influence local biological diversity via the influence of changes in toxicity on rates of herbivory (Richards et al. 2015). Increased diversity of secondary metabolites may also allow for more precise communication between plants, thereby allowing for more robust protection against a range of conditions (Frye et al. 2013, Gershenzon et al. 2012, Iason et al. 2005, Poelman et al. 2008). Two metrics that are useful for assessing changes in phytochemical diversity are "phytochemical richness" (i.e., the absolute number of compounds produced) and "phytochemical turnover" (i.e., the degree of overlap among the compounds produced), as both measures provide different insights into the metabolic response of plants to a range of abiotic conditions.

Variability in phytochemistry, even within the same species, may influence ecosystem structure and function through an array of chemically driven ecological effects (Bukovinszky et al. 2008, Gillespie et al. 2012, Sedio et al. 2017). The growth-differentiation balance hypothesis (GDBH) suggests that as the local environment becomes increasingly stressful, growth processes will become limited and the production

of PSMs will increase until the point that PSM production also becomes limited by resource acquisition/availability (Lerdau et al. 1994)(Lewinsohn et al. 1993)(Lewinsohn et al. 1993) . While phytochemical diversity has not been explicitly tested in light of the GDBH, studies have shown that herbivore-induced secondary chemistry can be completely suppressed in some woody species under a range of abiotic conditions (Lewinsohn et al. 1993), rendering them vulnerable to further invasion by pests and pathogens. While the number of studies investigating the effects of warming and other abiotic conditions on PSM production is rapidly growing, we currently have a limited understanding of how different abiotic factors may interact to influence phytochemical diversity (Bidart-Bouzat and Imeh-Nathaniel 2008, Jamieson et al. 2012, 2015). The objective of this study was to determine how elevated temperatures may influence the production of PSMs and to evaluate how the addition of other abiotic factors may modulate this effect.

While a targeted approach uses standard model compounds to identify and observe changes in specific compounds selected a priori, an untargeted (i.e., global) approach makes no assumptions regarding specific metabolites, and therefore, allows one to observe global changes across the entire metabolic profile. Thus, the strength of an untargeted approach lies in the potential to discover unanticipated changes in metabolic profiles as a result of environmental perturbations (Crews et al. 2009). Although untargeted metabolomics have been used in medicine for clinical diagnosis of various diseases, including numerous forms of cancer (Jain et al. 2015, Sreekumar et al. 2009), this study is among the first to apply this method to an ecological setting.

We used an untargeted metabolomics approach to evaluate how the phytochemical profiles of five different woody plant species are influenced by temperature, soil moisture, and light. Specifically, we tested the hypothesis that elevated temperatures alter the production of PSMs by leading to phytochemical profiles that are distinct from those found at ambient temperature (H1) and that warming will change phytochemical diversity via reductions in phytochemical richness or a high degree of turnover (H2). We also tested the hypothesis that the addition of other abiotic factors, specifically high light and drought, will either magnify or nullify temperature-induced changes in phytochemical profiles and PSM diversity (H3). Finally, because individual compounds may vary greatly in response to heterogeneity in the abiotic environment, we identified two 'example compounds' from balsam fir (*Abies balsamea* – two unspecified di-terpene resin acids) and paper birch (*Betula papyrifera* – catechin and another unspecified di-terpene resin acid) and analyzed the effects of different sets of abiotic factors (high-temperature, light, and drought) on their relative abundance. Specifically, we tested the hypothesis that individual compounds will respond to different conditions and combinations of conditions by either increasing or decreasing in relative abundance, potentially in a non-uniform and unpredictable manner (H4).

MATERIALS AND METHODS

Experimental Design —The Boreal Forest Warming at an Ecotone in Danger (B4WarmED) project is an ecosystem experiment that simulates both above- and below-ground warming in a boreal forest community. The experiment was conducted at Cloquet Forestry Center (CFC; Cloquet, MN. USA) and was initiated in 2008. The experimental

design consists of a 2 (overstory – open and closed) × 3 (warming – ambient, ambient +1.7°C, and ambient +3.4°C) × 2 (precipitation – ambient and ambient -40%) factorial design with six replicates (two per block) per treatment combination, for a total of 72 – 7.1 m^2 plots (Rich et al. 2015). Within each plot, 121 seedlings of 11 tree species were planted into the remaining herbaceous vegetation in a gridded design (Rich et al. 2015). Above-ground biomass was warmed using a Temperature Free-Air-Controlled Enhancement System (T-FACE) and below-ground biomass was warmed via buried resistance-type heating cables (Rich et al. 2015). Above- and below-ground temperatures have been monitored and logged at 15-minute intervals since spring 2008. In 2012, event-based rain exclosures were installed on nine plots in the open overstory replicates of the warming experiment, which allowed for safe and reliable removal of rainfall. Mean annual rainfall exclusion from June to September ranges from 42% to 45%.

We collected plant samples from the B4WarmED project during two different time periods. On 14 July 2013, we collected samples of balsam fir and paper birch that were grown under closed overstory and three warming treatments, and on 15 July 2014, we collected samples of balsam fir, paper birch, trembling aspen (*Populus tremuloides*), and red maple (*Acer rubrum*) grown under open overstory in the three warming treatments and two precipitation treatments. Where possible, we collected recent-growth foliar tissue from two plants per species within each replicate plot. However, some replicates contained either one or no plants with enough leaf tissue to sample. Samples sizes were particularly small during 2014, so we were forced to group individual warming treatments (ambient, +1.7°C, +3.4°C) into a binary response (ambient

temperature vs. elevated temperature). All plant samples were collected within a two-hour time period. Upon collection, samples were flash frozen with dry ice, and subsequently stored in a -80 °C freezer to minimize chemical degradation. We broadly refer to samples collected from the B4WArmED project as our "experimental" samples.

To investigate how temperature and light conditions may interact to influence phytochemical production in a natural forest environment, we collected samples of balsam fir, paper birch, trembling aspen, and beaked hazel (*Corylus cornuta*) from open and closed canopy environments across two regions in northeastern Minnesota (Fig.1). These regions exhibit differences in mean-maximum summer temperature (maximum daily temperature averaged across June, July, and August) of approximately 5.5°C (Table S2-1). On 14 July 2015, we collected a minimum of 3 biological replicates from each species within each set of abiotic conditions. The sampling design consists of a 2 (overstory – open and closed) × 2 (temperature – warm and cool) design with three plot replicates per treatment combination, for a total of 12 – 400 m^2 plots. Open-canopy plots allowed us to evaluate high-light conditions on production of PSMs and were located in areas that were clear-cut in 2006 (i.e., open overstory), while closed-canopy plots were located in areas that experienced no known overstory disturbance since at least 1985 (i.e., closed overstory). Thus, light conditions for all plots were based on whether the overstory was open (i.e., high light) or closed (i.e., low light). Temperature logger data collected for a parallel study from similar plot types suggest that average high temperatures from 1 May 2015 to 14 July 2015 ranged from 30.4°C in low-light plots in the cool region to 36.6°C in high-light plots in the warm region. All field samples were collected on the

same day, within an 8-hour period. Upon collection, samples were flash frozen with dry ice, and subsequently stored in a -80 °C freezer. For brevity, we occasionally refer to samples collected throughout northeast Minnesota as "observational" samples.

Study organisms — Balsam fir is a mid- to large-sized species of conifer, growing to 26 m in height, with shallow roots (Smith 2008). It is highly vulnerable to drought, fire, and spruce budworm (*Choristoneuro fumiferana*) infestations (Engelmark 1999), and modest climate warming has been shown to decrease net photosynthesis and growth by as much as 25% (Reich et al. 2015). Paper birch can grow to 28 m in height (Smith 2008) and is drought and shade intolerant (Iverson et al. 2008, Iverson and Prasad 1998). While it can grow rapidly and live to be 250 years of age, seedlings need significant light to prosper (Kneeshaw et al. 2006). Elevated temperatures have been shown to influence foliar nitrogen, lignin, and condensed tannins in both paper birch and trembling aspen with the specific response varying as a function of species and climate (Jamieson et al. 2015). Trembling aspen is one of the most widespread tree species in North America and occurs on a wide-range of soil types and in various climatic conditions (Smith 2008). It is sensitive to both drought and shade (Iverson et al. 2008, Iverson and Prasad 1998) and may become increasingly vulnerable to other potential stressors under conditions of drought and high temperatures (Worrall et al. 2008). Red maple is a moderately large tree, growing to 29 m in height and is known to be tolerant to a wide-range of precipitation conditions, from drought to seasonal flooding (Smith 2008). While this species is expected to prosper under future climate scenarios (Iverson et al. 2008, Iverson and Prasad 1998) and performed well under experimental warming (Reich et al. 2015),

both prolonged flooding and severe drought have been shown to result in senescence and decreased growth, respectively (Nash and Graves 1993). Beaked hazel, a shade-tolerant shrub that can grow to 4 m tall, is a common understory species in both conifer and deciduous forests and occurs almost exclusively in fire prone habitats (Smith 2008). Beaked hazel is highly sensitive to fire and previous work suggests that growth may be limited by soil moisture (Johnston and Woodard 1985).

Metabolite Analysis — Tissue samples were lyophilized for 72 hours and then homogenized and extracted using 25 mg (+/- 2.5 mg) of each sample. Homogenization and extraction were performed for 5 min at a frequency of 1500 Hz with 1 mL of 70% isopropyl alcohol at –20 °C using a bead mill and 2.8 mm tungsten carbide beads (Sped Sample Prep GenoGrinder 2010, Metuchen, NJ). Samples were then subjected to centrifugation at 16,000 xg for 5 min. The supernatant was then removed and subjected to an additional centrifugation step, 16,000 xg for an additional 5 minutes, and the supernatant was collected for subsequent analysis. Finally, 20 µL of each supernatant sample was removed and pooled to use as a control. All samples were then stored at –80 °C.

We analyzed samples with liquid chromatography mass spectrometry (LC-MS) using an Ultimate 3000 UHPLC (ultra-high-performance liquid chromatography) system coupled to a Q Enactive hybrid quadrupole-Orbitrap mass spectrometer with a heated electrospray ionization (HESI) source (Thermo Fisher Scientific, Bremen, Germany). We injected 1 µL of each sample per analysis onto an ACQUITY UPLC HSS T3 column, 100 Å, 1.8 µm, 2.1 mm X 100 mm (Waters, Milford, MA, USA) using a gradient

composed of solvents A: 0.1% formic acid and B: acetonitrile. Specifically, 0-2 min, 2% B; 6 min, 24% B; 9 min, 33% B; 12 min, 65% B; 16 min, 80% B; 20 min 93% B; 21 min 98% B; 22 min 98% B; 23 min 2% B; 23-25 min 2% B. Samples were analyzed in a randomized order to minimize systematic bias from instrument variability and carryover. Full-scan analysis was performed using positive/negative ion polarity switching, a 115-1500 *m/z* scan range, a resolution of 70,000 (at *m*/*z* 200), maximum fill times of 100 ms, and target automatic gain control (AGC) of 1×10^6 charges. Ion fragmentation was performed using a higher-energy collision dissociation (HCD) cell and resulting MS/MS data were collected using a resolution of 17,500, maximum fill times of 100 ms, and an AGC target of 2×10^5 charges. Normalized collision energies (NCE) ranged from 10-45 in increments of 5. All data were collected using Xcalibur version 2.2 (Thermo Fisher Scientific, Bremen, Germany).

Example Compounds — To determine which chemical features varied consistently and significantly among each treatment and species group, we aligned, smoothed, background subtracted, and analysed all chromatographic data using analysis of variance ($\alpha = 0.001$) via Genedata 7.1 (Genedata, Basel, Switzerland). We assigned putative metabolite identities only to the features found to be significantly abundant (ANOVA, $\alpha = 0.001$) with an exact mass and higher-energy collisional dissociation (HCD) MS/MS fragmentation spectra. We determined molecular formulae by using exact mass to calculate the most probable elemental composition for each feature (Table S2-2). We then manually interpreted HCD spectra collected at numerous collision energies (Figs.S2-1 through S2-3), and compared these to the MassBank database using

MetFusion (Gerlich and Neumann 2013). Where possible, we confirmed the identity of individual compounds via comparison to an authenticated standard (Sigma-Aldrich) and assigned other putative identities by matching molecular formulae to those of previously observed metabolites in *Betula* (Julkunen-Tiitto et al. 1996) and *Abies* (Otto and Wilde 2001). Specifically, we analyzed changes in the relative abundance of catechin and an unspecified terpene acid in paper birch and two unspecified diterpene resin acids in balsam fir. The identification of catechin was confirmed by comparison of accurate mass, LC-retention and MS/MS fragmentation properties of commercially available standard compounds for both catechin and its frequently associated isomer epicatechin which were distinguishable by chromatographic separation. There has been a great deal of work investigating the biological and ecological activity of catechin and terpenoid-based metabolites (Berg 2003, Gershenzon and Croteau 1992, Stolter et al. 2005, Tahvanainen et al. 1985); and as a result, we expect our results regarding these compounds to be broadly relevant.

Data Processing & Statistical Analysis — Data processing and statistical analyses were conducted using R 3.5.0 (R Core Team 2018). To initiate data processing, we used the *xcmsRaw* function in the *xcms* package (Benton et al. 2010, Smith et al. 2006, Tautenhahn et al. 2008) to read our raw mzML files into R. After separating our data by polarity using the *split* function in the *base* package, we used the *findPeaks.centwave* function for peak detection, which we parameterized as follows: *ppm* = 2, *peakwidth* = c(5,20), *prefilter* = c(1,15000000), *mzCenterFun* = "apex", *integrate* = 1, *mzdiff* = -0.001, *fitgauss* = F, *snthresh* = 10. Once peak detection was complete, we trimmed the resulting

polarity-specific data frames based on retention time and retained only those peaks detected between 1 and 21 minutes.

A major shortfall of employing LC-MS to perform "untargeted profile analysis," as we did here, is the production of two independent but partially overlapping datasets resulting from ion polarity switching. While polarity switching is useful for detection of features that can only be detected via either positive or negative ionization, some features are detectable under both ionization modes, therefore resulting in two independent data sets containing a small subset of common features. Moreover, interpretation of statistical results is challenging due to the presence of parallel sets of analyses with common features contributing to both. To alleviate these issues, we combined positive and negative polarities using the *find.matches* function in the *Hmisc* package (Harrell and Dupont 2018). The *find.matches* function allows one to identify which rows in a data matrix align with those in a separate, identically formatted matrix by allowing the user to define a tolerance level for the numerical columns in each matrix. Thus, to determine our common features in the positive and negative ionization datasets that result from LC-MS, we created two matrices for positive and negative polarity, containing three separate columns – the mass of each detected peak, an assigned name for each peak, and retention time. To ensure that corresponding features from each ionization mode were capable of alignment, we subtracted 2.1046, roughly the mass of two protons, from all masses in the positive polarity dataset. For those features identified as common among both ionization modes, we retained peak data from the polarity exhibiting greatest mean intensity across all samples. We then assigned new peak names to identify which peaks were present in

either positive or negative polarity versus those that were found in both. All output created using the *find.matches* function was manually checked to ensure that all peaks identified as having a match in one polarity, had their mate identified as a match in the other.

We used permutational MANOVA (perMANOVA, (Anderson 2001) to compare PSM profiles between abiotic conditions. When analyzing PSM profiles, differences were estimated using Canberra dissimilarity matrices (Dixon et al. 2009). Analysis was performed with the *adonis* function (from the vegan package(Oksanen et al. 2015), which allowed us to account for our blocked sampling design via the *strata* argument. Both differences in the centroids among conditions or differences in multivariate dispersion can lead to statistically significant results when using perMANOVA. To determine if differences among centroids were contributing to perMANOVA results, we created mean dissimilarity matrices using the *meandist* function and we used the *betadisper* function to assess multivariate homogeneity of variance (i.e., dispersion, (Oksanen et al. 2015). We used non-metric multidimensional scaling (NMDS, Kruskal, 1964) to visualize differences in PSM profiles among conditions, which we performed using the *metaMDS* function in the vegan package (Oksanen et al. 2015). We set our dimensionality parameter (k) to 2 and projected condition-specific effects onto NMDS plots using the *ordiellipse* function to plot 95% confidence ellipses based on standard error (Oksanen et al. 2015).

To evaluate treatment-induced changes to PSM diversity, we calculated phytochemical richness based on the presence and absence of individual compounds, then

tested the main effect of treatment on richness with block (experimental samples) or site ID (observational samples) as our random effect using linear mixed-effects models (*lme* function within the *nlme* package, (Pinheiro et al. 2015). To analyze phytochemical turnover (i.e., the degree of overlap between the phytochemical profiles of individual plants across and between conditions) we created dissimilarity matrices based on binary datasets representing the presence or absence of each feature using Jaccard's Index. We evaluated condition-specific differences in phytochemical turnover using perMANOVA via the *adonis* function, and evaluated the influence of multivariate centroids and homogeneity of variance on perMANOVA results as detailed above (Anderson 2001, Oksanen et al. 2015).

Weather data from Cloquet Forestry Center (CFC) shows that ambient air temperature, cumulative precipitation from 1 Jan to collection date, and leaf surface temperature were not statistically different between 2012 and 2013 or between specific sample sets (2013 – closed overstory, 2014 – open overstory). However, soil moisture and soil temperature vary strongly between years and sample sets, and differences between experimental and observational samples are likely to be even greater. Thus, samples collected during different years were analyzed independently of one another as individual data sets.

For analytical and visualization purposes, the condition or set of conditions assumed to impart the least amount of metabolic change during each year was labeled as our reference group, to which all other conditions were compared for that sample year. For Year 1 (2013), we designated "ambient" as our reference category, while samples

grown under ambient temperature and ambient precipitation were designated as our reference category for Year 2 (2014). We designated samples collected from cold region, low-light conditions as our reference category for Year 3 (2015). To help visualize how different abiotic conditions may influence PSM production in different species, we calculated the number of chemical features that increased and decreased by ≥ 75%, relative to our reference category and created scaled Venn Diagrams representing these relationships.

Finally, we used linear mixed-effects models to test the main effect of abiotic condition on the relative abundance of our example compounds, with sample block as our random effect for experimental samples and plot ID as our random effect for observational samples (*lme* function within the *nlme* package, Pinheiro *et al.*, 2015). These models tested whether combinations of abiotic factors influence the abundance of our known example compounds.

RESULTS

Temperature

The influence of temperature was both species and context dependent. In closed overstory (Year 1), when compared to ambient, warming-induced changes to the phytochemical profile of balsam fir were not statistically significant, whereas paper birch exhibited warming-induced shifts to phytochemical profiles, thereby leading to distinct PSM profiles for the warming treatment. Analysis of multivariate dispersion and mean-dissimilarity matrices both suggest that differences in paper birch were due to temperature-induced changes in the centroid rather than dispersion (Table 1). NMDS

plots reveal minor overlap between temperature conditions in paper birch, and balsam fir grown under moderate and high-temperatures show strong overlap with plants grown in ambient temperatures but minor overlap with each other (Fig.2). Warming had no effect on phytochemical richness in either species but did influence phytochemical turnover in paper birch (Table 1). In open overstory (Year 2), warming had no influence on PSM profiles or PSM diversity (i.e., richness or turnover), regardless of species (Table 1). NMDS plots support these findings in that there is no discernible relationship between temperature and PSM profiles, regardless of species (Fig.3**)**. In observational samples collected throughout northeast Minnesota (Year 3), temperature on its own had no influence on plant PSM profiles or phytochemical richness values. However, phytochemical turnover was significantly different in plants from different temperature regions in paper birch (perMANOVA, $F = 5.912$, $r^2 = 0.179$, $p = 0.0003$) and trembling aspen (perMANOVA, $F = 3.322$, $r^2 = 0.156$, $p = 0.0012$). NMDS plots suggest that each species responds differently to combinations of temperature and light (i.e., canopy; Fig.4). Balsam fir produces distinct PSM profiles as a function of ambient light conditions (i.e., open vs. closed canopy), but only within the cool region, while paper birch and trembling aspen appear to have distinct PSM profiles for each combination of conditions. Conversely, beaked hazel exhibits no discernible pattern across different conditions.

Venn diagrams created to help visualize the influence of different abiotic conditions for Year-1 samples suggest that the high-temperature (+3.4°C) treatment induced a greater response from both balsam fir and paper birch than the moderate-

temperature (+1.7°C) treatment. Specifically, the high-temperature treatment led to more features that either increased or decreased in relative abundance by 75% or more when compared to ambient or moderate-temperature treatments (Table 3; Fig.S2-4).

Interactive Effects of Different Abiotic Conditions

In our Year-2 samples, the combination of drought and elevated temperature had no influence on PSM profiles nor any aspect of phytochemical diversity, regardless of species (Table 1). These results were supported by NMDS plots (Fig.3). Additionally, Venn diagrams suggest large-magnitude increases or decreases in relative abundance of PSMs did not follow an obvious pattern that could be attributed to different conditions. There appears to be a high degree of overlap across conditions in those compounds that exhibit increases in relative abundance of ≥ 75%, while less overlap occurs among compounds exhibiting large declines in relative abundance. Furthermore, the influence of drought on the decline of relative abundance by ≥ 75% appears to be more distinct than that of either warming or warming and drought together (Table 2).

In observational samples from throughout northeast Minnesota (Year 3), when evaluating the effects of high temperature and light combined, balsam fir appears to create unique PSM profiles in response to different light conditions (i.e., open vs. closed canopy), but only within the cool region, while paper birch and trembling aspen appear to have distinct PSM profiles for each condition. Beaked hazel exhibits no discernible pattern (Fig.4). Phytochemical richness did not vary as a function of light conditions or temperature region. However, phytochemical turnover in balsam fir was significantly influenced by conditions of high light (i.e., open canopy; Table 3). When analyzing the

interactive effects of light conditions and temperature region, all species exhibited significant differences in their PSM profile (Table 3), with only trembling aspen exhibiting significant differences in multivariate dispersion as a function of the combination of light condition and temperature region (Table 3). Although phytochemical richness was not influenced by the combined effects of temperature region and light conditions, phytochemical turnover was influenced in paper birch and trembling aspen and a marginal, non-significant trend was present in beaked hazel (Table 3).

Patterns in Venn diagrams detailing the influences of different conditions during Year 2 are difficult to discern, as different plant species appeared to respond to varying conditions in different ways (Fig.S2-5). Drought led to more features increasing by ≥ 75% in balsam fir and paper birch, while elevated temperature led to the large-magnitude increase of more features in trembling aspen (Table 2; Fig.S2-5). In red maple, the combination of drought and elevated temperature had the greatest influence on large-magnitude increases in relative abundance (Table 2; Fig.S2-5). The combination of drought and warming led to more large-magnitude declines in relative abundance in balsam fir and paper birch, while drought had a greater impact on red maple and trembling aspen (Table 2; Fig.S2-5). In observational samples (Year 3), the combination of high-light conditions and warmer temperatures led to more large-magnitude shifts in relative abundance (i.e., increasing and decreasing by 75% or more), regardless of species (Table 2; Fig.S2-6).

Example Compounds

In closed-overstory conditions (Year 1), warming resulted in significant declines in both catechin and terpene acid in paper birch but had no influence on either compound in balsam fir (Fig.5, Table S2-3). In high-light conditions (Year 2), neither of the compounds in either species exhibited a significant, condition-specific change in relative abundance. However, terpene acid in paper birch was completely absent from all samples collected from high-light plots (Fig.6; Table S2-3). In observational samples from throughout northeast Minnesota (Year 3), neither compound in balsam fir exhibited significant changes in relative abundance due to light conditions, temperature region, or their interaction. In paper birch, however, the interactive effects of high-light conditions and warmer-temperatures resulted in a more than 250% increase in the relative abundance of catechin, while terpene acid exhibited no response, regardless of treatment (Fig.7; Table S2-3).

DISCUSSION

Our study is among the first to explicitly show that combinations of abiotic drivers (often potential stressors) in forest plants can lead to broad phytochemical responses that are distinct from those that result from single abiotic factors and that different species of woody plants respond to complex sets of conditions in variable ways. In our experimental samples, warming under closed canopy led to distinct PSM profiles in paper birch but not balsam fir, with paper birch exhibiting increased phytochemical turnover. Warming under open canopy had no influence on PSM profiles or any aspect of phytochemical diversity. In our observational samples collected across northeast Minnesota, warmer temperatures had no influence on PSM profiles but did lead to

significant phytochemical turnover in paper birch and trembling aspen. When elevated temperature was combined with drought in Year 2 of our experimental samples, we found no influence on PSM profiles or phytochemical diversity. However, temperature variation combined with high-light conditions in our observational samples resulted in condition-specific profiles for all species and led to significant phytochemical turnover in all but beaked hazel. In general, our results indicate that the phytochemical response of plants to varying combinations of abiotic factors cannot be directly extrapolated from the response of plants to individual factors. Perhaps more importantly, our results provide evidence that heterogeneity in the abiotic environment influences secondary metabolism in woody plants via a range of complex and highly variable responses.

Few studies to date have explicitly studied the influences of heterogeneity in the abiotic environment on phytochemical diversity, and specifically, phytochemical turnover. However, it has been hypothesized that variability in which compounds are either present or absent may be an adaptation for variable environments, thereby decreasing vulnerability of plants to a range of potential stress conditions, including herbivory (Cheng et al. 2011, Laitinen et al. 2000). Here, we found that in some plant species, different combinations of abiotic factors can affect which compounds are either present or absent, thus leading to phytochemical turnover. For example, compounds that are absent in one set of conditions may become present within a slightly different set of conditions, or vice versa. The potential for this to occur was apparent when our example terpene acid decreased in paper birch plants subjected to experimentally elevated temperature in closed canopy but went completely undetected in plants subjected to

experimental warming and drought in open canopy and exhibited no change at all in our observational samples from throughout northeast Minnesota. Suppression of individual compounds due to varying stress conditions has been observed in other studies as well. For instance, proline, which is thought to play an important role in protection from drought, is severely suppressed when plants are simultaneously subjected to drought and high temperatures (Rizhsky et al. 2004). While individual compounds can play an important role in the survival of plants subjected to a range of biotic and abiotic conditions, a plant's phytochemical profile imparts a metabolic framework that can determine the biological role and strength of individual compounds (Dyer et al. 2003, Gershenzon et al. 2012, Jamieson et al. 2015, Richards et al. 2010). Here we show that individual compounds as well as the phytochemical context within which they operate can both be altered by variations in the abiotic environment.

Plants produce thousands of individual compounds, and variations in the relative abundance of many of these compounds can have a wide-range of effects on the biotic interactions plants have with other organisms. Catechin, which is a phenol-based precursor to proanthocyanidins (i.e., condensed tannins), is widely considered an antiherbivore defensive compound (Berg 2003, Stolter et al. 2005, Tahvanainen et al. 1985) and can have a significant, negative impact on the development of forest pests (Roitto et al. 2009). Catechin also has antimicrobial and allelopathic effects, and plants with decreased catechin production may be at a competitive disadvantage for nutrients within the soil as it can inhibit the growth and germination of neighboring plants (Inderjit et al. 2008, Veluri et al. 2004). Terpene acids, including diterpene resin acids, are

considered strong antifeedants (Ikeda et al. 1977), and the ingestion of forage with elevated concentrations of diterpenoids can result in slower development times and significantly higher mortality in herbivorous larvae (Larsson et al. 1986). Here we show that different compounds have individualized responses based on the micro-environmental conditions that are present.

In balsam fir, warming alone led to consistent, albeit non-significant declines in the mean relative abundances of both resin acids. When high temperatures were combined with other abiotic factors (i.e., drought and light), resin acid 1 exhibited consistent but non-significant increases, while resin acid 2 was more variable, exhibiting no consistent trend. In paper birch, both example compounds exhibited significant changes in relative abundance as a function of different factors. While elevated temperature alone led to significant declines in catechin, the combination of elevated temperature and high light led to a more than 250% increase in relative abundance. Our example terpene acid declined with warming and was undetectable when we tried to assess the effects of drought. This particular scenario provides an example of how individual compounds may "wink in or out" due to variation in the abiotic environment.

Numerous studies have reported that high-temperature and drought interact to alter PSM production in plants (Craufurd and Peacock 1993, Jiang and Huang 2001, Rizhsky et al. 2002, 2004, Savin and Nicolas 1996). Thus, we were surprised to find no interaction between drought and warming in our study. It is important to note, however, that the extremes of those treatments employed by other studies are typically greater than what we test here, sometimes increasing temperature to more than 40ºC (Rizhsky et al.

2002) and withholding water altogether for extended periods (Jiang and Huang 2001). In our study, mean soil moisture was lower during 2014 than 2013, with mean soil temperatures being higher (unpublished data). Surprisingly, air temperature and leaf-tissue surface temperature during late spring/early summer (May 1 to July 15) were indistinguishable between samples years and plot types (2013 closed canopy vs. 2014 open canopy), and cumulative precipitation during the first half of each year (January 1 to July 15) was also indistinguishable (unpublished results). Combinations of abiotic factors can have one dominant factor that defines the phytochemical response of affected plants, and drought, when present, may dominate the influence of combinations of abiotic factors. Considering this, our inability to identify any treatment-specific influence on PSM profiles or phytochemical diversity may be due to low soil moisture during 2014. If plants from which samples were collected from in 2014 were experiencing some level of drought stress due to low soil moisture, this signal may have preempted any potential phytochemical response that might have occurred due to treatment.

When considering the influence of abiotic conditions on large-scale shifts in relative abundance (increases or decreases ≥ 75% relative to our reference group), greater increases in temperature (+3.4°C) appeared to have a greater influence than moderate increases (+1.7°C). When present, drought, either alone or in combination with elevated temperature, dominated all but one of the large-scale shifts we assessed (Year 2), and in our observational samples, high-light conditions, either alone or in combination with elevated temperature, dominated all of the large-scale shifts we assessed in which it was present (Year 3). As noted above, numerous studies have reported that drought has a

defining impact on plants' phytochemical profiles, even when in combination with other abiotic drivers, such as elevated temperature and high light. Moreover, in our Year 1 samples, elevated temperature led to both large-scale increases and large-scale decreases in relative abundance. However, the number of compounds exhibiting these shifts were substantially smaller when compared to the number of compounds influenced by the abiotic conditions evaluated in either Year 2 of our experimental samples or our observational samples (Year 3). Outside of Year 1, during which we tested only the effects of elevated temperature, it was rare when the same abiotic condition simultaneously dominated both large-scale increases and large-scale decreases in relative abundance, suggesting that different combinations of abiotic factors may influence upregulation and downregulation of different compounds.

Changes in the abundance and diversity of secondary metabolites within a plant's phytochemical profile may alter biotic interactions, potentially leading to broad-scale ecological change. For example, while some herbivores respond negatively to forage with a higher diversity of PSMs, others appear to target these plants in an effort to alleviate costs associated with external stressors via their pharmacological benefits (Forbey and Hunter 2012). Additionally, numerous studies have reported that phytochemical diversity within a plant community is positively correlated with community diversity across multiple trophic levels (Jones and Lawton 1991, Richards et al. 2015), influencing invertebrate predators and parasitoids, and potentially extending to vertebrate predators as well (Dicke et al. 2012).

While the consequences of different abiotic conditions on phytochemical diversity remain unpredictable, our results demonstrate that the phytochemical response of plants to combinations of abiotic factors cannot be extrapolated from that of individual factors. For instance, while warming alone may have a very specific influence on some compounds, when in combination with additional abiotic factors such as drought and light, warming may lead to highly variable and unpredictable response (Mittler 2006), making it increasingly difficult to predict the performance of woody plants in a changing environment. Regardless, previous research suggests that changes in phytochemical production induced by variability in abiotic conditions can influence both tree resistance and pest performance traits (Jamieson et al. 2015), potentially altering the frequency and intensity of insect outbreaks (Schwartzberg et al. 2014). Elevated temperatures by themselves have been shown to reduce the competitive abilities of more southern boreal tree species when compared to co-occurring species adapted to warmer climates (Reich et al. 2015). Climate-induced changes to phytochemistry may lead to shifts in the competitive landscapes for cold-adapted trees and shrubs, potentially altering their ability to compete for resources and defend against pests and pathogens in novel climatic conditions. However, because individual compounds and the metabolic profiles of which they are a part are differentially influenced by abiotic factors and combinations of these factors, predicting how forest plants will respond to novel environmental conditions will be challenging.

The majority of biotic interactions between plants and other organisms are chemically mediated, and recent climate change has challenged our understanding of the

mechanisms underlying these interactions. The primary objective of this study was to determine how warming influences plant production of secondary metabolites and how combinations of additional abiotic factors may modulate this effect. Here, we show that heterogeneity in a range of abiotic factors broadly influence secondary chemistry in plants thereby leading to condition-specific phytochemical profiles. If our results are typical of plant responses, abiotically induced changes to secondary chemistry in woody plants could influence their rate of range expansion or contraction under novel climate scenarios. Additionally, our results contribute to current efforts to understand how continued warming will influence plants and the biotic interactions that serve as the foundation for a wide range of ecosystem processes. In the future, studies monitoring physiological changes in conjunction with global shifts in PSM profiles would provide insights into mechanisms underlying biotic interactions mediated by the local environment. As spatial and temporal patterns in the global abiotic environment continue to shift, it is imperative that we continue to learn as much as we can about the phytochemical response of plants to these changes.

Table 1. Summary of results for B4WarmED samples used to assess the influences of temperature and drought on PSM profiles and phytochemical diversity. For samples collected during 2013, "mod. temp." includes all samples collected from plots warmed to ambient + 1.7ºC, while "high temp." includes all samples collected from plots warmed to ambient + 3.4ºC. For a given condition, the mean number of chemical features identified within a species is listed under "features". "Dispersion" represents the results of our multivariate homogeneity of variance test, while "centroid" represents the mean difference in dissimilarity matrices relative to our reference group (*). A larger Δ value indicates greater distance from the reference group than those with a smaller Δ. All statistical analyses were tested against $\alpha = 0.05$, and statistically significant results are italicized and identified with an asterisk (*). Within the table, "na" indicates "not applicable".

					PSM profile						phytochemical diversity				
					perMANOVA			dispersion		centroid	$LME_{richness}$		$perMANOVA_{turnover}$		
Year	species	stress condition	n	features	f	r^2	*P*	f	*P*	delta	$\Delta_{richness}$	*P*	f	r^2	*P*
2013	balsam fir	ambient[a]	12	1903	1.223	0.073	0.103	0.576	0.567	na	na	na	1.206	0.072	0.142
		mod. temp.	13	1856						-25.800	-47	0.154			
		high temp.	9	1873						-68.500	-30	0.321			
	paper birch	ambient[a]	11	1669	1.382	0.090	*0.013**	0.765	0.470	na	na	na	1.444	0.093	*0.019**
		mod. temp.	12	1722						55.700	53	0.201			
		high temp.	8	1700						17.700	31	0.526			
2014	balsam fir	ambient[a]	5	1937	1.016	0.105	0.428	0.346	0.810	na	na	na	1.076	0.110	0.308
		temp.	11	2017						196.000	80	0.222			
		drought	5	2012						121.000	75	0.308			
		temp. + drought	9	1992						118.000	55	0.308			
	red maple	ambient[a]	5	1968	1.070	0.100	0.303	1.520	0.210	na	na	na	1.076	0.100	0.320
		temp.	11	2002						29.300	34	0.800			
		drought	4	1998						97.600	30	0.857			
		temp. + drought	13	1845						-251.300	-123	0.344			
		ambient[a]	6	1948	1.149	0.097	0.147	1.233	0.307	na	na	na	1.210	0.102	0.134

	paper birch	temp.	12	2014						32.000	66	0.232			
		drought	7	1949						-112.000	1	0.973			
		temp. + drought	11	2036						98.000	88	0.122			
	trembling aspen	ambient[a]	4	2287	0.689	0.103	0.960	0.061	0.980	na	na	na	0.622	0.094	0.980
		temp.	6	2282						17.000	-5	0.961			
		drought	5	2241						-44.000	-46	0.646			
		temp. + drought	7	2282						16.000	-5	0.957			

[a] reference group or baseline condition for the given sample year to which all other treatments within species were compared

Table 2. Number of chemical features that increase and decrease in relative abundance by ≥ 75% as a function the dominant stress condition. In most scenarios, the stress condition that led to large-scale increases in relative abundance was different than that which led to large-scale decreases. "Number affected" displays the number of chemical features that either increased or decreased by ≥ 75% for the given species and stress condition.

		increase by ≥ 75%		decrease by ≥ 75%	
year	species	stress condition	number affected	stress condition	number affected
2013	balsam fir	high temperature	6	high temperature	21
	paper birch	high temperature	28	high temperature	38
2014	balsam fir	drought	43	temperature + drought	35
	paper birch	drought	98	temperature + drought	31
	red maple	temperature + drought	36	drought	66
	trembling aspen	temperature	79	drought	37
2015	balsam fir	temperature + light	26	light	111
	beaked hazel	temperature + light	155	temperature + light	56
	paper birch	temperature + light	126	light	278
	trembling aspen	temperature + light	280	light	162

Table 3. Summary of results for observational samples (2015) used to assess the influences of temperature region and overstory on PSM profiles and phytochemical diversity. For a given condition, the mean number of chemical features identified within a species is listed under "features". "Dispersion" represents the results of our multivariate homogeneity of variance test, while "centroid" represents the mean difference in dissimilarity matrices relative to our reference group (*). A larger Δ value indicates greater distance from the reference group than those with a smaller Δ. All statistical analyses were tested against α = 0.05, and statistically significant results are italicized and identified with an asterisk (*). Within the table, "na" indicates "not applicable".

				PSM profile							phytochemical diversity			
				perMANOVA			dispersion		centroid		$LME_{richness}$		$perMANOVA_{turnover}$	
species	stress condition	n	features	f	r^2	P	f	P	delta	$\Delta_{richness}$	P	f	r^2	P
balsam fir	reference[a]	10	1371	1.579	0.119	*0.024**	0.334	0.807	na	na	na	2.152	0.156	*0.004**
	light	8	1287						27.1	-84	0.228			
	temp.	10	1373						-11.8	2	0.947			
	temp. + light	11	1361						-40.1	-10	0.844			
paper birch	reference[a]	10	1185	2.029	0.196	*0.002**	2.546	0.072	na	na	na	2.784	0.250	*0.001**
	light	7	1168						-2.5	-17	0.675			
	temp.	8	1205						88.5	20	0.708			
	temp. + light	4	1223						143.4	38	0.537			
beaked hazel	reference[a]	3	1338	1.968	0.269	*< 0.001**	0.242	0.863	na	na	na	1.313	0.120	0.109
	light	8	1220						-227.8	-118	0.467			
	temp.	12	1194						-262.1	-144	0.303			
	temp. + light	10	1252						-228.1	-86	0.546			
trembling aspen	reference[a]	3	1509	1.352	0.123	*0.028**	2.92	*0.040**	na	na	na	2.696	0.336	*<0.001**
	light	8	1466						-26.2	-43	0.556			
	temp.	3	1531						-23.8	22	0.789			
	temp. + light	6	1558						-36.4	49	0.537			

[a] reference group or baseline condition (i.e., lower temperatures, low light) to which all other treatments were compared

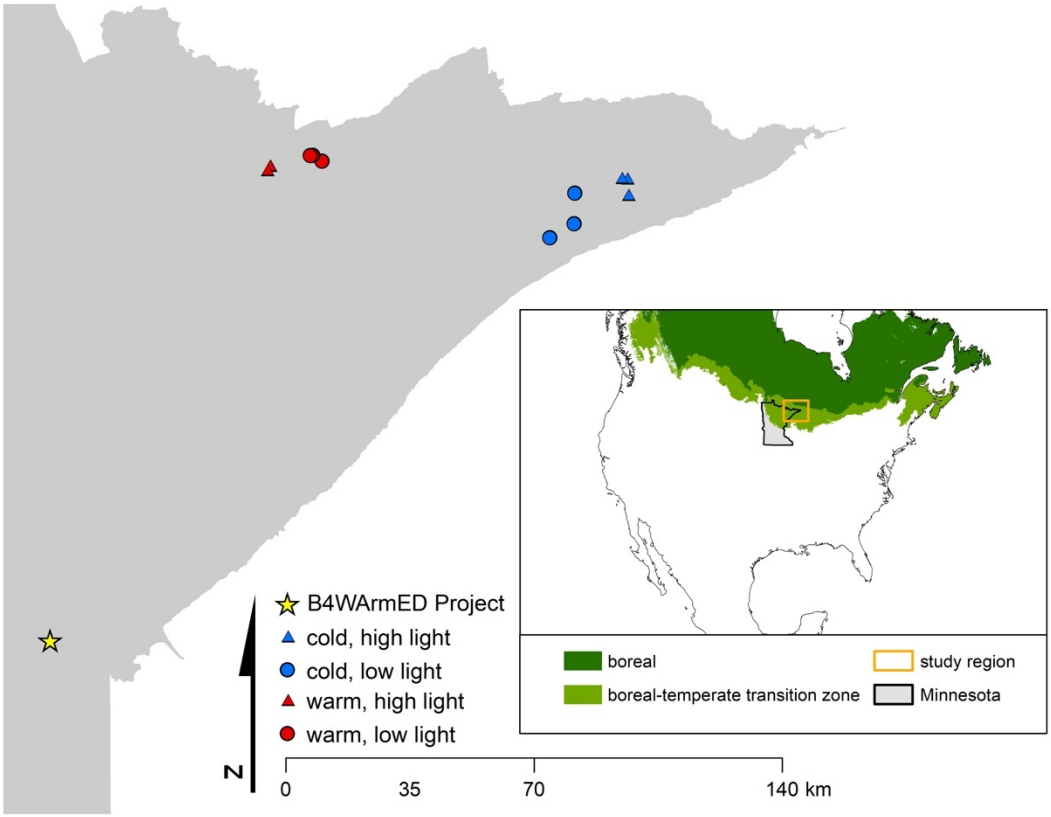

Fig.1. Location of observational sites and the B4WarmED Project at the University of Minnesota's Cloquet Forestry Center. The number of replicate plots for each set of abiotic conditions is n=3, and where only two can be seen for a given combination of abiotic factors (i.e., temperature + light conditions), locations are close enough in proximity that they appear to overlap when viewed at a broad scale. Inset map identifies the approximate location of the study area within the state of Minnesota and the boreal-temperate transition zone (Brandt, 2009).

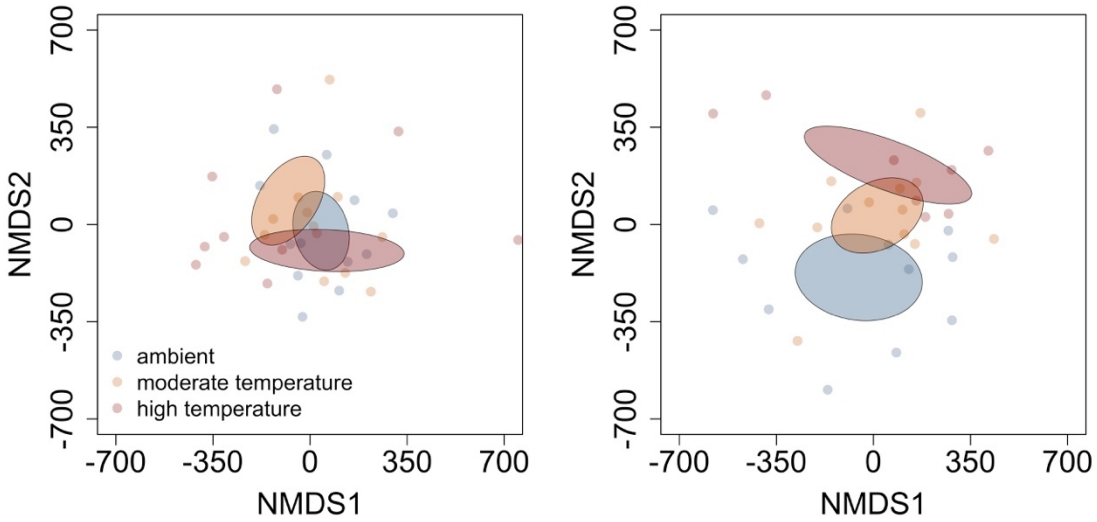

Fig.2. Non-metric multidimensional scaling (NMDS) plots detailing the influence of moderate and high-temperature on PSM profiles of (A) balsam fir and (B) paper birch in closed overstory. Ellipses represent 95% confidence intervals, based on standard error. In balsam fir, both warming treatments exhibit less overlap with each other than with ambient. In paper birch, different temperatures lead to distinct profiles when compared to each other and ambient.

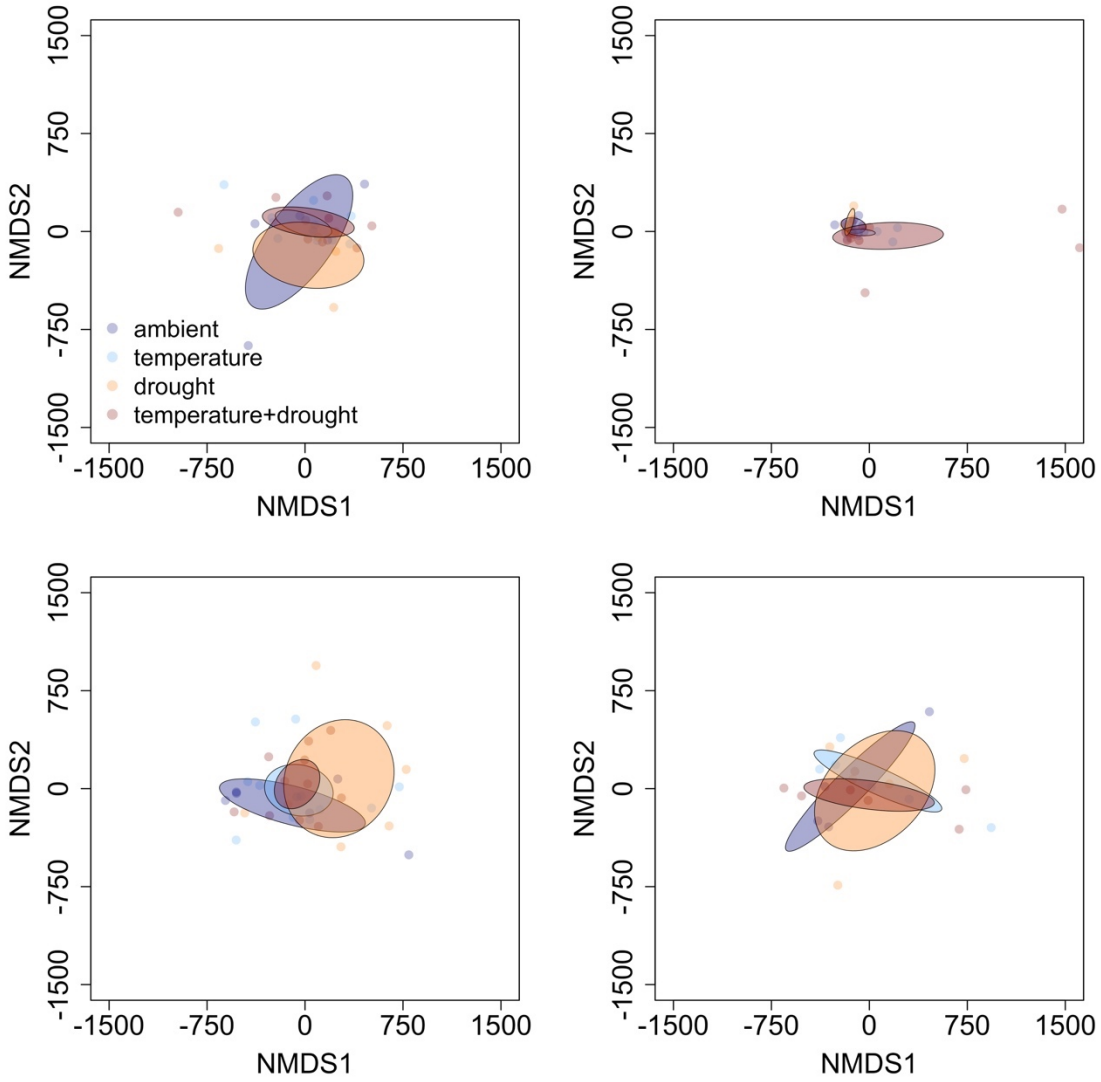

Fig.3. Non-metric multidimensional scaling (NMDS) plots detailing the influence of elevated temperature and drought on PSM profiles of (A) balsam fir, (B) red maple, (C) paper birch, and (D) trembling aspen in open overstory. Ellipses represent 95% confidence intervals, based on standard error. There appears to be no discernible pattern between sets of abiotic factors and PSM profiles, regardless of species.

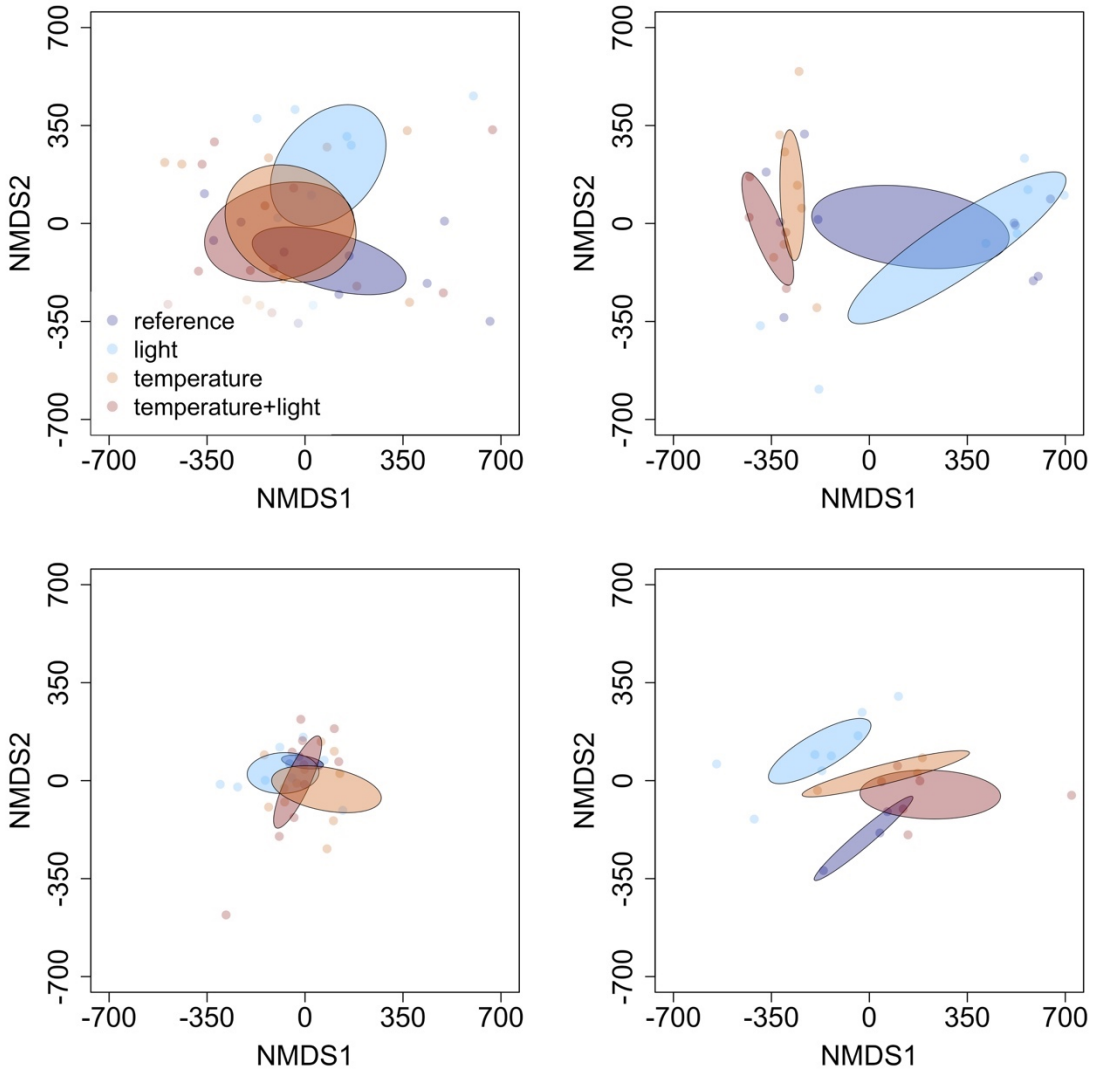

Fig.4. Non-metric multidimensional scaling (NMDS) plots detailing the influence of varying light and temperature conditions on PSM profiles of (A) balsam fir, (B) paper birch, (C) beaked hazel, and (D) trembling aspen. Ellipses represent 95% confidence intervals, based on standard error. Each species appears to respond to different abiotic conditions in a unique manner. Balsam fir appears to create unique PSM profiles in high-light conditions when compared to our reference group (closed canopy, low-temperature), while paper birch and trembling aspen appear to have distinct PSM profiles for each set of conditions. Beaked hazel exhibits no discernible pattern.

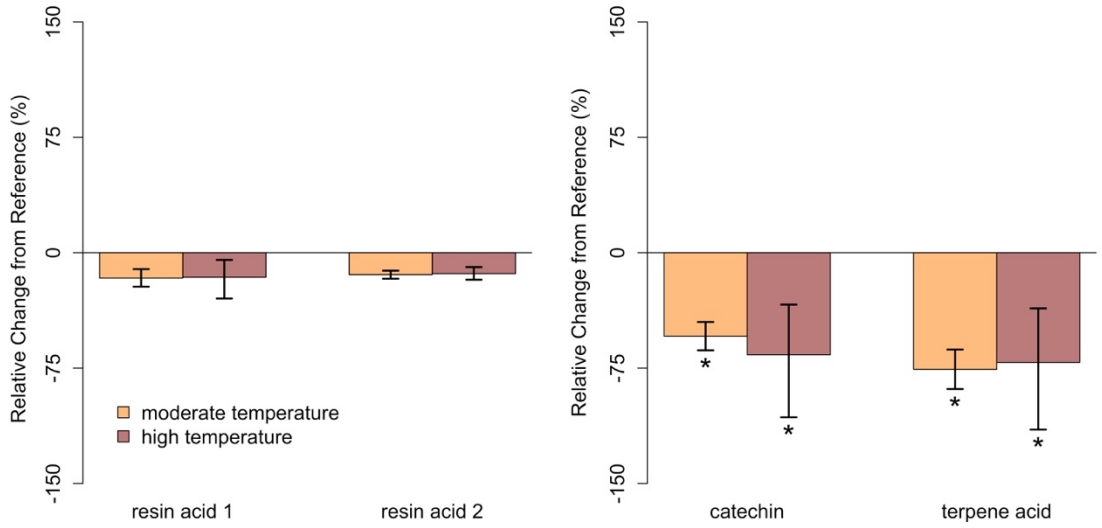

Fig.5. Relative change in abundance (%) for specific PSM compounds when compared to our reference treatment for Year 1 (ambient temperature) for (A) balsam fir and (B) paper birch in closed overstory. Neither resin acid in balsam fir was influenced by warming. In paper birch, both catechin and terpene acid declined with warming relative to ambient. Error bars represent the 95% boot-strapped confidence intervals and relative abundances significantly different than those found in the baseline treatment are identified by an asterisk (*).

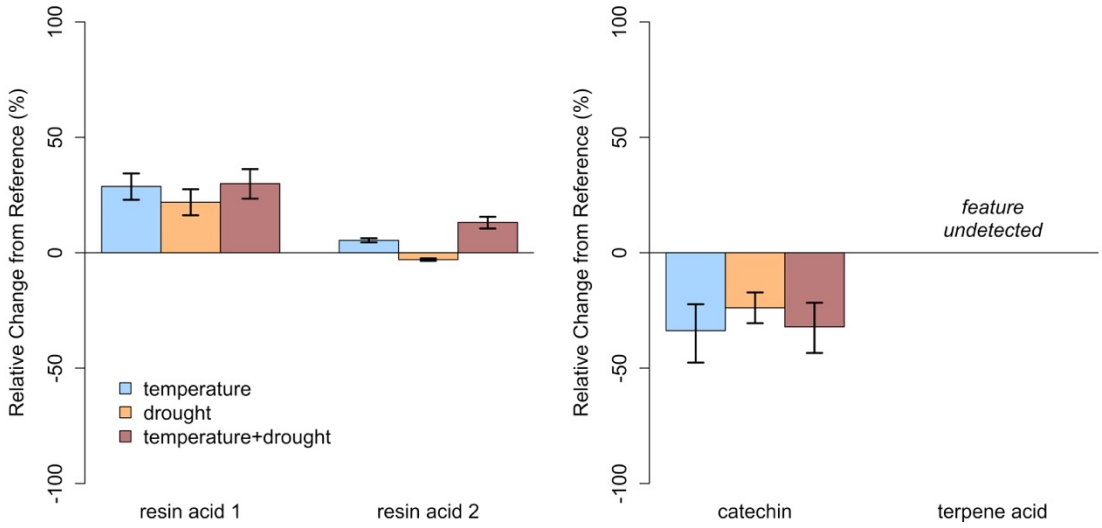

Fig.6. Relative change in abundance (%) for specific PSM compounds when compared to our baseline treatment for Year 2 (ambient temperature, ambient precipitation) for (A) balsam fir and (B) paper birch in open overstory. Neither resin acid in balsam fir was influenced by warming. In paper birch, relative abundance of catechin was not influenced by temperature, however, terpene acid was undetected. Error bars represent the 95% boot-strapped confidence intervals.

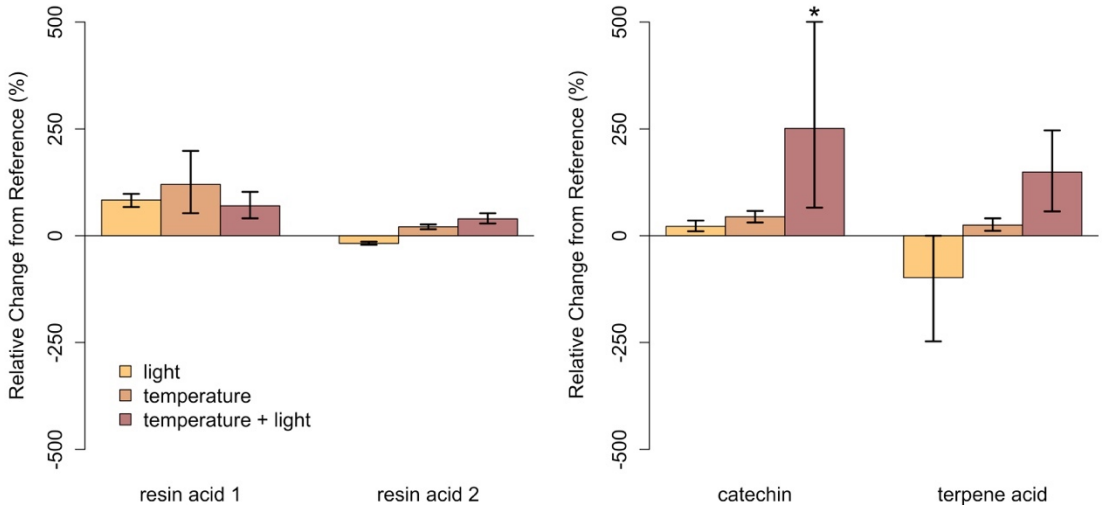

Fig.7. Relative change in abundance (%) for specific PSM compounds when compared to our baseline treatment for Year 3 (cold region, closed overstory) for (A) balsam fir and (B) paper birch. Neither resin acid in balsam fir was influenced by warming. In paper birch, relative abundance of catechin was only influenced by the combination of light and high temperatures, increasing by more than 250%. Terpene acid was unaffected, regardless of stress condition. Error bars represent the 95% boot-strapped confidence intervals and relative abundances significantly different than those found in the reference condition are identified by an asterisk (*).

Chapter 3: Incorporating Biomass Improves Predictions of Spatial Variation in $\delta^{15}N$ and $\delta^{13}C$ Across a Northern Mixed Forest.

ABSTRACT As an ecological tool, understanding the spatial variation of isotope ratios (i.e., isoscapes) has become increasingly valuable in efforts to understand various aspects of organismal behavior and ecology. To capture the most fundamental elements of isotopic variation at large spatial scales, it is essential first to predict spatial variation in the relative abundance of the materials used to estimate the isotopic landscape. Methods used to predict spatial variation at smaller spatial scales, however, have yet to include relative abundances of different materials. Moreover, when estimating the isotopic landscape, traditional regression kriging methods fail to account for the influences of environmental grouping factors (i.e., random effects) that can impact our ability to predict spatial heterogeneity accurately. We use a mixed-effects model regression kriging framework to estimate spatial variation of $\delta^{13}C$ and $\delta^{15}N$ values in plants commonly eaten by moose in northeast Minnesota. We then refined these predictions using species-specific allometric equations to estimate above-ground biomass of three different moose forage-preference groups. We determined our best-fitting mixed-effects models via two-step, AIC-based model selection and then used these models to predict spatial variation in stable carbon and nitrogen isotopes across the study region. For our final models, we kriged the regression residuals across the study region and added them to our isoscape predictions. Finally, we evaluated our prediction accuracy via spatial hold-one-out cross validation. Different preference groups exhibited substantial variation in abundance and distinct isotopic signatures. Moreover, models incorporating biomass led to predictions

that were distinct from those that did not, and the use of mixed-effects models improved our ability to predict the isotopic landscape. Regression kriging using mixed-effects models and the refinement of model predictions using measures of abundance, provides a flexible, yet mechanistically driven approach to modeling variation across space and through time. Thus, the method we present here is broadly applicable and could be adapted to many scenarios in which kriging is part of the analytical process.

INTRODUCTION

Understanding how animals interact with their environment, specifically where they go and what they eat, is foundational to the fields of ecology and animal behavior (Kingsland 1991, Owen-Smith et al. 2010). One way to study animal behavior is by using stable isotope analysis, which has become increasingly common in studies of animal movement and foraging (Cerling et al. 2006). A major advantage of using stable isotope analysis over other methods is its flexibility in allowing us to reconstruct ecological processes and activities without witnessing them firsthand (West et al. 2006). For example, the isotopic signatures of plants are reflected in the biogenic materials of the herbivores that consume them, and as a result, we can determine not only what an herbivore ate and where it went, but also why it may have gone there (Cerling et al. 2006, Raynor et al. 2016). Based on this premise, stable isotope analysis has been used to evaluate nutritional outcomes of habitat-use and dietary choice in elk (Walter et al. 2010), to show important differences in feeding behavior between migrant and resident elephants in southern Kenya (Cerling et al. 2006), and to investigate diet segregation as a function of sex-specific nutritional demands in American bison in Yellowstone National

Park (Berini and Badgley 2017). When incorporated with animal isotopes, spatial variation in the isotopic values of animal resources can provide researchers with valuable insights into animal behavior.

Spatial patterns in the variation of isotope ratios, recently described as isoscapes (West et al. 2009), have long been used to inform a range of biogeochemical and biological processes (Bowen 2010, West et al. 2009). As an ecological tool, isoscapes have become increasingly valuable in our efforts to gain a better understanding of various aspects of organismal behavior and ecology. For example, deuterium (δD) isoscapes have been used to investigate long-distance movements of butterflies across the Sahara desert (Stefanescu et al. 2016) and spatial variation in stable isotopes of strontium ($^{87}Sr/^{86}Sr$) and oxygen ($\delta^{18}O$) have been used to reconstruct caribou migrations in Alaska (Britton et al. 2009). Spatial variation in values of δD and $\delta^{13}C$ have been used to predict the most likely dispersal route of a radio-collared cougar (*Puma concolor*; Henaux et al. 2011), and heterogeneity of $\delta^{15}N$ and $\delta^{13}C$ values have been used to evaluate variation in protein inputs for geese (*Anser anser*) in Sweden (Fox et al. 2009). As the number and diversity of studies utilizing isoscapes increases, our ability to precisely and accurately predict heterogeneity in the isotopic landscape will continue to improve.

To model isotopic variation at large spatial scales, it is essential first to predict spatial variation in the abundances of different isotopic substrates used to estimate this variation (if two or more substrates differ in their isotopic composition). For example, C_3 and C_4 plants have distinct $\delta^{13}C$ signatures, and thus, the relative abundances of these two functional groups has become a critical consideration when predicting spatial variation of

$\delta^{13}C$ values (aggregated across functional groups) at regional to continental scales (Still and Powell 2010). Estimating geographic variation of $\delta^{13}C$ values at smaller spatial scales (i.e., within a single functional group), however, is more complicated, due in part to the intensive sampling required to establish relationships between $\delta^{13}C$ values and environmental covariates. Although early studies of isotopic variation in plants were unable to find significant differences in $\delta^{13}C$ among plant taxa (Craig 1953, 1954), recent work has identified differences in the isotopic composition both within and among plant species (Garten and Taylor 1992, Leavitt and Long 1986, Marshall et al. 2007). Royle & Rubenstein (2004) noted that geographic variation in species abundance is an important consideration when spatial variation in the isotopic landscape is highly non-uniform. Although their work focused on properly assigning the geographic origin of birds based on δD and $\delta^{13}C$ values, many of the arguments they make for incorporating spatial variation in species abundance into isoscape models are broadly applicable. Nevertheless, models depicting isotopic heterogeneity at smaller spatial scales have yet to include variation in abundance of different taxonomic or functional groups.

Traditionally, models depicting geographic variation in stable isotopes have relied on isotopic data derived from sampled locations, while locations without measurements were filled in via methods of spatial interpolation (Bowen and Wilkinson 2002, Cheesman and Cernusak 2016). However, the need to estimate error in isoscape models has led to the development of new geospatial modelling techniques (Bowen and Revenaugh 2003, Lott and Smith 2006). For example, regression models are now commonly used to inform spatial interpolation, which permits researchers to estimate and

potentially minimize prediction error by also kriging regression residuals (i.e., regression kriging, Bowen and Wilkinson 2002). Moreover, increased access to high-resolution spatial data has allowed for prediction of isotopic variation at higher resolutions over limited spatial extents (e.g., field-scale; Hellmann et al. 2016). With recent advancements, opportunities now exist to develop mechanistic isoscape models that have even greater accuracy and precision.

When estimating the isotopic landscape, currently employed methods often fail to account for the potential effects of environmental, categorical variables that may influence model estimates. For example, known variation of $\delta^{13}C$ within species or functional groups could easily be incorporated as a random effect in a mixed-effects regression kriging framework. At the local level, $\delta^{13}C$ in leaf tissue is known to vary as a function of canopy height, irradiance levels, and water-use efficiency (Ometto et al. 2006), all of which may be indirectly influenced by disturbance. Thus, by incorporating disturbance type as a random effect, we are better able to identify meaningful fixed-effects that might otherwise be obscured by the unmeasured influences caused by different environmental variables. Regression kriging that incorporates mixed effects models makes it possible for researchers to account for these unmeasured (and likely complicated) influences while also improving upon the prediction accuracy of currently employed methods.

As a case study, we used biomass-informed, mixed-effects models in a regression kriging framework to study how the isotopic composition of moose forage changes across space and to test whether our method improved upon the accuracy of more traditional

techniques. This study system provides a unique opportunity to test our method in a context that may also have conservation implications, as moose in this region have been declining since approximately 2005, with nutritional suppression suggested as a potential driver (Monteith et al. 2015, Wünschmann et al. 2015). While regression kriging with mixed-effects models has been applied to improve digital mapping of soil properties (Omuto and Vargas 2015), to our knowledge this method has not previously been used to predict spatial variation in stable isotopes. We use this approach to investigate four questions associated with the estimation of isotopic variation at the landscape scale. First, are different forage-preference groups isotopically distinct from one another (Q1) and second, are kriging predictions of the abundances of different preference groups distinct from one another and spatially heterogeneous (Q2)? Third, do mixed-effects models characterizing spatial variation in stable isotopes improve predictions over those created via simple linear models (Q3)? Finally, do biomass-informed isoscapes provide predictions that are distinct from those provided by uninformed isoscapes (i.e., isoscapes in which we assume equal abundance of all sampled species; Q4)? The answers to these questions will help refine our understanding of how stable isotopes vary across space and potentially, how to more accurately model this variation.

MATERIALS AND METHODS

Model System

Moose are cold-adapted, north-temperate ungulates that are at the southern edge of their bioclimatic envelope in northern Minnesota (Lenarz et al. 2009). In the northwestern part of the state moose have been all but extirpated since about 2007

(Murray et al. 2006). In the northeastern part of the state, moose have declined by more than 60% since 2005 (DelGiudice 2018), with recent warming suggested as a potential driver (Lenarz et al. 2009, 2010). Over the last century, temperatures in northern Minnesota have risen by an estimated 1.7 to 2°C (EPA 2016). While it has been hypothesized that increasing temperatures may be contributing to this decline (Lenarz et al. 2009, 2010, Murray et al. 2006), a clear connection between moose population declines and rising temperatures has yet to be established.

The study area in northeastern Minnesota covers approximately 1.3-million hectares, and is composed primarily of southern boreal forest, including large portions of Superior National Forest and the Boundary Waters Canoe Area Wilderness (BWCAW). This region is a mosaic of upland and lowland forest types characterized by black spruce (*Picea mariana*) and northern white cedar (*Thuja occidentalis*) in the lowlands and balsam fir (*Abies balsamea*), trembling aspen (*Populus tremuloides*), and paper birch (*Betula papyrifera*) on the uplands, with large stands of jack (*Pinus banskiana*), red (*P. resinosa*) and white pine (*P. strobus*) occurring throughout. While large swaths of unlogged areas remain (i.e., 169,000 ha within the BWCAW), fire and logging are common and routine forms of disturbance in this ecosystem (Heinselman 1996). Mean annual temperature is approximately 2 ºC with mean annual precipitation (rain plus snowfall water equivalent) of around 70 cm (Heinselman 1996). Summers in this region are typically short and cool, with mean temperatures of around 17.5 ºC in mid-July and an average precipitation of approximately 10 cm. Winters are characterized as long and cold, with mean temperatures of roughly -17ºC and normal annual snowfall totals ranging

from 1.4 to 1.8 m (Frelich 2002, Heinselman 1996). Topography across the study area varies from relatively flat to moderately hilly, with elevation ranging from 183 m at the surface of Lake Superior, to 701 m at Eagle Mountain, the highest point in the state. The area is sparsely inhabited, with few paved roads and much of the region accessible only by foot, logging road, or canoe (Lenarz et al. 2010).

We established 0.04 ha plots throughout northeastern Minnesota (n=70) to characterize the isotope composition (i.e., $\delta^{13}C$ and $\delta^{15}N$ values) and biomass of plant species within each plot (Fig.1). Plots covered a range of disturbance ages (i.e., 13 years, 9 years, 4 years, and undisturbed) and types (i.e., canopy burn, clear cut, and insect-defoliation), as well as a range of landcover types (i.e., wetland and wetland forest, coniferous forest, deciduous forest, mixed forest, and regenerating forest). Because temperature has been implicated as one of the leading causes of decline for moose in Minnesota (Lenarz et al. 2009, Murray et al. 2006), plots were originally established as part of a parallel study investigating the influences of high summer temperatures on moose forage. Thus, our network of plots were distributed across the study region into three discrete temperature zones (cool, moderate, and warm) that span a mean-maximum summer temperature gradient of approximately 5.5 ºC (PRISM Climate Group 2017).

Stable Isotopes

We sampled summer forage in each of the 70 plots from late May to early August during each year from 2012 to 2016 (Fig.1). In total, we collected 2,694 summer forage samples from more than 30 species (Table S3-1). We categorized all species into one of three groups, based on dietary preference – high, medium, and low (Table S3-1; Peek et

al. 1976). These groups also vary according different quality metrics (e.g., %N and C:N), with high-preference, in general, being the highest quality and low-preference forage being the lowest quality (Table S3-1). Where possible, we collected up to five samples of each species we encountered in each plot, where each sample consisted of 5-7 leaves that we stripped from a peripheral stem located between 0.5 to 1.0 m from the forest floor. Once collected, samples were placed in a cloth bag labeled with the plot and sample ID.

In preparation for stable isotopes analysis, samples were dried in a 60ºC oven for 24 to 48 hours and subsequently placed in light-proof, tin containers. A small portion of each sample was collected and ground to a homogenous powder using a Spex SamplePrep GenoGrinder bead mill with 2.8 mm stainless steel grinding beads. Once homogenized, we weighed 2.5 ± 0.1 mg of each sample into a 5x9 mm Costech tin capsule. All samples were analyzed either at the Stable Isotope Laboratory in the Department of Earth Sciences at the University of Minnesota (UMN) or the Stable Isotope Laboratory in Earth and Planetary Sciences at the University of California, Santa Cruz (UCSC). At UMN, samples were analyzed for $\delta^{15}N$ and $\delta^{13}C$ values via flash combustion in a Costech 4010 Elemental Analyzer (EA) coupled to a Thermo-Finnegan Delta V Plus isotope ratio mass spectrometer (IRMS). At UCSC, samples were analyzed via flash combustion in a CE Instruments NC2500 EA interfaced to a ThermoFinningan Delta Plus XP IRMS. At each location, the resulting gas was analyzed for elemental concentration of $^{13}C/^{12}C$ and $^{15}N/^{14}N$ ratios and expressed in standard δ notation, representing the differences between samples ratios and ratios found in international standards for carbon (VPDB) and nitrogen (atmospheric N_2). Finally, because samples

were analyzed in two different laboratories, we alleviated concerns of machine or lab specific analytical biases by running five samples from six different species in each lab and creating offset and linearity corrections that we then applied to all samples analyzed at UCSC.

Woody Biomass Calculations

While moose are known to break stems with a diameter at breast height (DBH) of ≤ 6cm in order to browse on terminal shoots, they also occasionally browse on plants that are relatively close to the forest floor (Renecker and Schwartz 2007). Thus, within each 0.04 ha plot, we measured smaller woody stems (i.e., stems ≤ 6 cm of diameter at breast height, DBH, and ≥ 15 cm in height) within three nested subplots along the 30º, 150º, and 270º azimuths, at 5.5 m from the plot centroid. Within a 25 m^2 subplot, we tallied the number of individuals of each species having a DBH ≥ 2.5 cm and ≤ 6 cm (i.e., saplings), with tallies for each species recorded for each 0.5 cm DBH interval. Within a smaller, 10 m^2 subplot, we measured diameter at 15 cm height of all woody plants that were ≥ 15 cm in height but < 2.5 cm in DBH (i.e., shrubs or advanced regeneration). We tallied the number of individuals of each species within each 0.5 cm size class, from 0.5 cm to 2.5 cm. Anything with a diameter < 0.5 cm at 15 cm height was omitted.

We calculated estimates of above-ground biomass using species-specific allometric equations based on the measurements detailed above. For saplings, we used species-specific equations from Jenkins et al. (2003), to estimate above-ground biomass using DBH. We also used species-specific equations for shrubs and small saplings, (Perala and Alban 1993, Smith and Brand 1983), which allowed us to estimate above

ground biomass based on stem diameter at 15 cm height. For some species, equations for whole, above-ground biomass were not available. For those species, we calculated biomass for stems and foliage separately, and then added those values to estimate total biomass of each species in each plot. All estimates were converted to kg/m^2.

Creating Isoscapes

To model carbon and nitrogen isotopes across the landscape, we needed to aggregate the isotope data within each preference group at each plot. We did this in two ways. First, we took a traditional approach in which we simply averaged all isotope samples within a given preference group in each plot. This approach, which did not account for sample density or available biomass, we refer to as "biomass uninformed". Our primary goal was to represent the isotopic composition of different groups of plants as those groups are perceived by a large herbivore. Because isotope samples were not collected in proportion to availability within plots or on the landscape, we used a "biomass-informed" approach, in which we generated bootstrapped samples of the isotope data (weighted by our biomass estimates) for each preference group in each plot (see "Bootstrap Sampling"). Once plot-level estimates were made for the biomass uninformed and informed approaches, we developed linear models (with and without random effects) to determine what biotic and abiotic factors influenced variation in isotope values (see "Model Selection"). Finally, we used regression kriging to make spatial predictions of how isotope compositions of each preference group vary across the landscape (see "Regression Kriging"), and then compared prediction accuracy using spatial leave-one out cross validation (see "Comparison of Models and Predictions").

Bootstrap Sampling

We used the biomass estimates from each plot to generate bootstrapped data reflecting the mean stable isotope composition of each forage preference group as a function of the relative abundance of each group within each plot. To do this, we used the *sample* function in the base package of R (R Core Team 2018), which can use a vector of probability weights (referred to below as "selection probability vector") for selecting individual values from the sampled data set (i.e., the *prob* argument within the *sample* function). Each plot had three selection probability vectors, one for each preference group. Within each plot, each vector consisted of a string of numbers representing the selection probabilities of all samples within a given preference group. Each sample had its own selection probability that was equal to the proportional abundance of that species within its preference group, divided by the number of samples collected for that species. As an example, in a hypothetical plot A, the low-preference forage samples consist of 3 balsam firs, 2 speckled alders, and 1 beaked hazel, for 6 total samples in this preference group — each species making up 72%, 19%, and 9% of the low-preference forage biomass in plot A, respectively. Given this, our selection probability vector for low-preference forage in plot A would be a string of 6 values: 3 values of 0.72/3 (0.24), 2 values of 0.19/2 (0.095), and one value of 0.09, all of which sum to 1.00. Once our selection probability vectors were established, we sampled each plot-preference group combination 500 times, with replacement. We then calculated the mean of this sample, which represents the mean stable isotope composition of a preference group within a plot. To account for potential variation from one sampling effort to the next, we repeated this

procedure 1000 times, which yielded a single vector of 1000 means. We then calculated the mean of this vector and saved it as our "biomass-informed" isotope value for that forage-preference group, within the given plot. We repeated this procedure for each plot and each forage-preference group, for both $\delta^{13}C$ and $\delta^{15}N$ values.

To summarize our uninformed data, rather than simply use mean isotope values for each preference group in each plot (i.e., mean stable isotopes values not scaled by biomass), we used a procedure similar to that described above. However, rather than incorporating species-specific proportional abundances, we assumed equal abundance across all species found within each forage-preference group at each plot. Thus, in the example above, our vector of selection probabilities for low-preference forage in plot A for uninformed data would also be a string of 6 values – 3 values of 0.33/3, 2 values of 0.33/2, and one value of 0.33, all of which sum to 1.00.

Model Selection

We selected 15 landscape covariates, 13 fixed and 2 random (Table S3-2), and performed a two-step, AIC-based backward elimination to define the best fitting linear mixed-effects model for $\delta^{15}N$ and $\delta^{13}C$ for each forage-preference group, across all plots. Our "full model" contained all fixed and random effects, and for the first step of the model-selection process, we held our random effects constant and removed one fixed covariate at a time until we reached the fixed-effects structure yielding the lowest AIC score. Once we achieved the fixed-effects structure yielding the lowest possible AIC score, we performed AIC-based backward elimination on the random effects. We used the *lmer* function in the *lme4* R package for all linear mixed-effects models (Bates et al.

2015). When defining our fixed-effects structure we set the *REML* argument in *lmer* to *FALSE*, and when defining our random effects structure we set this argument to *TRUE* (Faraway 2016). In one scenario (i.e., $\delta^{15}N$ for low-preference forage), our best fitting model was rank deficient (i.e., insufficient data to estimate the chosen model due to too many covariates). To alleviate rank deficiency, we removed the set of factor covariates that altered the model's AIC score the least.

Regression Kriging

To prepare our spatial data for regression kriging, all spatial covariate data that were originally formatted as shapefiles were converted into raster datasets in ArcGIS 10.3.1 (ESRI 2011). Once all data were converted, we needed to make sure that the cell size of all raster datasets were equal. Thus, for any raster dataset with a cell size larger than 30x30 m, we used bilinear interpolation via the *resample* tool in ArcGIS to reduce the cell size without altering the raster's extent. Next, we needed to ensure that all of our raster datasets were of the same extent. We accomplished this with the *extract by mask* function in ArcGIS, using the raster with the smallest extent as our "mask". Finally, we used the *raster to ASCII* conversion tool in ArcGIS to convert each raster to an ASCII file that could then easily be read into R as a single, multi-layered spatial grid data frame. To initiate regression kriging in R, we used the *readGDAL* function from the *rgdal* package (Bivand et al. 2018) to read in our ASCII landscape covariate data and the *read.csv* function in the *base* package to read in our plot locational data (i.e., the easting and northing of each plot's centroid). To align our plot location data with our landscape covariates, we used the *over* function from the *sp* package (Bivand et al. 2013, Pebesma

and Bivand 2005) and then combined the corresponding landscape covariate data with our plot locational data file.

By definition, regression kriging is a method of spatial interpolation that combines regression modeling with kriging of the regression residuals (Omuto and Vargas 2015). Kriging the residuals has been shown to improve spatial predictions substantially by allowing for small-scale autocorrelation while also accounting for measurement and modelling error (Alsamamra et al. 2009, Omuto and Vargas 2015, Prudhomme and Reed 1999). For spatial interpolation of the residuals from our best-fitting models, we used the *autoKrige* function in the *automap* package (Hiemstra et al. 2009). We determined the best fitting variogram model both by means of visual inspection and the sum of squared errors of the fitted model, and then incorporated the best fitting variogram model into the *autoKrige* function via the *model* argument. We then used the *predict* function in the *stats* package (R Core Team 2018) to predict $\delta^{13}C$ and $\delta^{15}N$ values across the entire study area and summed these predictions with our kriged residuals, which helps to account both for local autocorrelation and measurement and modelling error. We saved the resulting data as grid files using the *write.asciigrid* function in the *sp* package (Bivand et al. 2013, Pebesma and Bivand 2005). For visualization purposes, we then converted these ASCII files into raster data sets in ArcGIS using the *ASCII to raster* conversion tool. All R code, sample data, and resulting output for this portion of our analysis can be found at the Date Repository for the University of Minnesota (DRUM).

Comparison of Models and Predictions

In general, accounting for variation in the abundance of different substrates (e.g., forage biomass) should inherently result in estimates of the isotopic landscape that more accurately reflect the true isotopic mean at any point in space. Thus, we assume that models accounting for biomass are a better reflection of reality (i.e., the average isotope value of any point in space) than those that do not. Regardless, we used both qualitative and quantitative methods to determine which models provide better fits and predictions. We used one-way ANOVA followed by Tukey's Test for Honestly Statistical Differences to determine if different forage-preference groups are isotopically distinct from one another (Q1). To visualize spatially explicit differences in the amount and relative abundance of different forage preference groups (Q2), we calculated the absolute difference between each preference group and mapped these differences using the raster calculator in ArcGIS 10.3.1. To evaluate if mixed-effects models characterizing spatial variation in stable isotopes improve predictions over those created via simple linear models (Q3), we calculated marginal and conditional r^2. Marginal r^2 describes the proportion of variance explained by the fixed effects, while conditional r^2 describes the proportion of variance explained by both the fixed and random effects combined. Finally, to determine if biomass-informed isoscapes provide predictions that are distinct from those provided by uninformed isoscapes (Q4), we performed spatially referenced hold-one-out cross validation. Specifically, we held out an individual plot and re-kriged $\delta^{13}C$ and $\delta^{15}N$ for each preference group using the remaining plots and our best fitting linear mixed-effects models. We then compared the predicted values of the held-out plots (i.e., $\delta^{13}C$ and $\delta^{15}N$ for high-, medium-, and low-preference forage) to the true values, and

continued this process across all plots. We then calculated the root-mean-squared error (RMSE) to determine how well our regression-kriging process predicted the values of our held-out sites, for both uninformed and biomass-informed isotopes. By comparing the modeled values at each site to the "true" values, RMSE provides us with a measure of how well each model performed. Values of RMSE are in the same units as the quantities being estimated, and values closer to zero indicate better predictive power. Finally, to visualize differences among uninformed and biomass-informed models, we calculated the absolute difference between uninformed and biomass-informed isoscapes for each preference group and mapped these differences using the raster calculator in ArcGIS 10.3.1.

RESULTS

In general, different preference groups exhibited both distinct isotopic signatures and substantial variation in abundance across northeastern Minnesota (Fig.2). Moreover, the use of mixed-effects models helped improve isoscape predictions and models incorporating biomass led to predictions that were distinct from those that did not. When evaluating raw isotope data to determine if different forage preference groups were distinct (Q1, Fig.2), results of one-way ANOVA for $\delta^{13}C$ ($F_{2,2691} = 129.9$, $p < 0.00001$, $\eta^2 = 0.084$) and $\delta^{15}N$ ($F_{2,2691} = 24.9$, $p < 0.00001$, $\eta^2 = 0.085$) were statistically significant. Furthermore, Tukey HSD Tests comparing preference groups against one another for both $\delta^{13}C$ and $\delta^{15}N$ revealed that all groups were isotopically distinct, with each comparison yielding $p < 0.0001$.

When inspecting model predictions for the proportional and absolute abundance of different forage preference groups (Q2), both measures of abundance exhibited substantial variation across all preference groups (Fig.3). Predictions of low-preference forage exhibited the greatest mean abundance across the study region (49%) and predictions of medium-preference forage exhibited the smallest mean abundance (18%). Mean abundance of high-preference forage across the study region was approximately 31%. Additionally, each preference group exhibited a high degree of spatial heterogeneity across the study region. For example, proportional abundance of low-preference forage ranged from 0% to 100% with a standard deviation of 28%, while the proportional abundance of high-preference forage also ranged from 0% to 100% with a standard deviation of 23%%. Medium-preference forage ranged from 0% to 100%, with a standard deviation of 21% (Fig.3). Additionally, only two of the thirteen fixed effects (i.e., northing and mean annual precipitation) appeared in all models used to predict the abundance of different forage groups (Table 1). Furthermore, differences in abundance between low and medium-preference forage appeared to be inversely related to differences exhibited between medium- and high-preference forage. For example, those areas exhibiting large differences between low- and medium-preference forages exhibited relatively small differences when comparing medium- and high-preference foods. In general, lower-preference forages were more abundant throughout the study region than higher-preference forages (Fig.3).

When evaluating the ability of mixed-effects models to improve our predictive power (Q3), we found that incorporating random effects improved our ability to predict

$\delta^{13}C$ for medium-preference forage for our uninformed models (Table 2), and both low and medium-preference forage for our biomass-informed (Table 3) models. For $\delta^{15}N$, we found that mixed-effects models improved our ability to predict all forage-preference groups, for both uninformed (Table 4) and biomass-informed (Table 5) models. The inclusion of random effects improved r^2 values by as much as 0.20 for $\delta^{13}C$ values and by as much as 0.876 for $\delta^{15}N$.

In general, uninformed and biomass-informed isoscapes were best characterized by models that were distinct across different preference groups (Q4, Tables 2 – 4). However, there were varying degrees of overlap in the fixed effects of the best fitting models for different preference groups, and this was true for both uninformed and biomass-informed models. For example, $\delta^{15}N$ for medium-preference forage had a single fixed effect in the uninformed model, while the biomass-informed model for $\delta^{15}N$ values of the medium-preference group had six fixed effects (Tables 4 and 5). Conversely, models characterizing $\delta^{15}N$ for high-preference forage for both uninformed and biomass-informed had identical structures (Tables 4 and 5). When predicting held out data, RMSE estimates ranged from 0.69‰ to 1.05‰ for $\delta^{13}C$ and from 0.92‰ to 1.70‰ for $\delta^{15}N$ (Tables 2-5). Maps depicting the differences between uninformed and biomass informed isotopes suggest strong differences between different prediction methods. While differences among uninformed and biomass-informed isoscapes for low and high-preference foods are less pronounced for $\delta^{15}N$, predictions of the isotopic landscape for these preference groups differ by as much as 1.5 ‰ and 1.3 ‰, respectively (Fig. 6). Maps depicting the absolute difference between uninformed and biomass-informed

predictions show that accounting for biomass when estimating the isotopic landscape can yield substantially different predictions (Fig.6) that may vary by 10‰ or more (Fig.6e).

DISCUSSION

When estimating the isotopic landscape, accounting for the relative abundance of different substrates used to estimate the landscape will inherently lead to isoscape models that more accurately represent reality. The modeling approach we present here is among the first to incorporate biomass data to refine predictions of isotopic variation in plants at the landscape scale. In this study, isoscape estimates based on plant groups that vary both in their abundance and isotopic composition exhibit substantial variation between models that account for abundance (i.e., biomass) and those that do not (Tables 2-5). Moreover, accounting for the abundances of different plant groups often led to the inclusion or omission of landscape covariates resulting in models that better predict variation in the isotopic landscape (Tables 2-5). However, even though some models had identical structures (e.g., $\delta^{15}N$ for high-preference forage, both informed and uninformed), accounting for site-to-site variation in the abundance of different preference groups still led to differences in isoscape estimates (e.g., differences of up to 1.3‰, Fig.6f) that could influence the results of any study utilizing these data as an important source of inference. Overall, our results suggest that accounting for variation in the abundance of different isotopic substrates, can lead to isoscape estimates that are distinct from those that do not (Fig.6), and therefore, better reflect the actual isotopic variation present across the landscape (i.e., CV_{LMER} RMSE values in Tables 2-5).

Currently, the majority of models used to characterize variation in the isotopic landscape use simple linear models, however, we show here that incorporating environmental grouping factors (i.e., random effects) can substantially improve model fit. Incorporating random effects via the use of mixed-effects models improved the performance of nine of our 12 isoscape models, and improved model predictive ability by as much as 87% in one instance (i.e., uninformed $\delta^{15}N$ for mid-preference forage, RMSE = 0.92 ‰). While the inclusion of random covariates had no influence on the performance of three of our models, this could change with the inclusion of different covariates. We utilized bedrock geology and disturbance as random effects for both $\delta^{13}C$ and $\delta^{15}N$ values. However, given our results, values of $\delta^{15}N$ are clearly more impacted by these covariates than those of $\delta^{13}C$. The inclusion of different random covariates would likely influence how well these models perform. For instance, due to the influence of sub-canopy CO_2 recycling on $\delta^{13}C$ values (van der Merwe and Medina 1989), accounting for the amount, structure, and complexity of the space between the forest floor and the canopy could substantially improve model performance for $\delta^{13}C$ values. While the incorporation of random effects did not always help explain more of the variance, mixed-effects models are easy to implement and provide researchers with a relatively simple approach to investigating mechanistic drivers underlying spatial heterogeneity.

Different plant species vary in their isotopic composition and therefore, methods that do not account for spatial variation in the abundance of these species may lead to a misrepresentation of the isotopic landscape. Accounting for variation in the relative abundance of different preference groups altered our estimates of the isotopic landscape

by as much as 10‰ (i.e., the maximum difference between uninformed and informed isoscapes for $\delta^{15}N$ for mid-preference forage), and the average difference between uninformed and biomass-informed isoscapes ranged from 0.11‰ to 1.95‰. A more important consideration than differences in our average estimates, however, may be the refined depictions of spatial heterogeneity in these models and how it may inform our knowledge of ecological systems. For example, performance of the moose population across northeastern Minnesota is relatively heterogeneous, with some areas performing relatively well and others performing poorly (DelGiudice 2018). Because different forage-preference groups are isotopically distinct and the isotopic values for these groups are heterogeneous across the study region, moose traveling through this landscape will carry with them an isotopic signature of where they have been and what they have eaten. Thus, models that accurately characterize spatial heterogeneity in the isotopic landscape could be beneficial when evaluating how diet and habitat-use behavior of moose may be contributing to spatial heterogeneity in population performance. It is also important to note that utilizing biomass to help refine isoscape predictions will be even more useful for landscapes in which substrate groups are more isotopically distinct than that which we use here (e.g., landscapes that include C_4 grasses).

While the primary goal of this study was to provide a more accurate and precise means for modeling the isotopic landscape, models characterizing spatial variation in the abundance of different groups of plants is an additional benefit of this method. For example, data that characterize how dietary components vary in their abundance across space can provide insights into potential contributors to population decline and, therefore,

may help focus research and management efforts. In the case study we present here, statistical models characterizing spatial variation of different forage-preference groups allows us to determine which landscape covariates influence the abundance and distribution of moose forage. Those areas where the moose population is performing poorly appear to correlate with areas in which high-preference forage is relatively less abundant, and vice versa (DelGiudice 2018). If managers want to increase the abundance of high-preference moose forage, they may want to manage for high-preference species (e.g., paper birch, trembling aspen, willow) in areas with optimal solar insolation. Our models also corroborate other studies that show both temperature and precipitation influence the abundance and distribution of different boreal plants (Castro et al. 2004, Kleidon et al. 2009, Lesica and Crone 2017). Thus, changes in climate expected to occur in northeastern Minnesota over the coming decades should be considered when thinking about how to manage habitat in a way that is optimized for the future success of moose in Minnesota.

Animal behavior is, at least in part, a manifestation of how individuals respond to heterogeneity in their environment (Dall et al. 2005), and stable isotopes are a powerful tool that makes it possible to evaluate the behavioral response of animals to this heterogeneity (Rubenstein and Hobson 2004). Although we use a declining moose population in northeast Minnesota as our model system, the principles, concepts, and methods we apply throughout are applicable to a range of species across a variety of habitat types. For example, in order to reconstruct an herbivore's diet using stable isotopes, one needs only to know the stable isotope composition of the herbivore and its

potential forage (Parnell et al. 2013). However, even without stable isotope data from an herbivore, researchers could feasibly use the method we present here to create landscape-scale models depicting an animal's fundamental dietary niche (i.e., what the diet should be given the composition of the landscape, in the absence of selection). Comparing spatially explicit estimates of an animal's fundamental dietary niche to that which the animal actually consumed could provide insights that help us understand the mechanisms that drive movement and foraging behavior across a range of different model systems.

The approach to kriging that we describe here is highly flexible and broadly applicable to many scenarios in which kriging is part of the analytical process. As a result, this method could be used to model spatial variation of a range of continuous variables, not just isotopic compositions, at a wide range of spatial scales. Regression kriging using mixed-effects models has previously been applied in soil sciences (Omuto and Vargas 2015) and incorporating abundance measures like biomass of various plant species could be used to refine spatially explicit predictions of forage quality (i.e., crude protein, C:N ratios, plant secondary metabolites). Regardless of the application, regression kriging using mixed-effects models and the refinement of model predictions using measures of abundance, provides a flexible, yet mechanistically driven approach to modeling environmental covariates that vary both across space and through time.

Table 1. Model structure for mixed-effects models characterizing biomass of different moose forage-preference groups. All values were truncated to three significant digits. Covariates with no values under a given preference group indicates that the covariate was not a part of the best fitting model. Marginal r^2 explains the proportion of the variance explained by the main effects, whereas conditional r^2 explains the proportion of the variance explained by both the main and the random effects combined. Where marginal r^2 is equal to the conditional r^2, there was no benefit to using mixed-effects models over simple linear models. RMSE for cross validation (CV_{LMER}, RMSE) was derived via hold-one-out cross validation. For metadata associated with model covariates, see Table S3-2. "MMST" and "DEM" correspond to "mean maximum summer temperature" and "digital elevation map," respectively.

	low preference			medium preference			high preference		
fixed effects	β	SE	*P*	β	SE	*P*	β	SE	*P*
covertype									
wetland forest	—	—	—	-10.55	11.491	0.375	—	—	—
coniferous forest	—	—	—	-11.39	11.553	0.342	—	—	—
deciduous forest	—	—	—	-10.17	11.447	0.391	—	—	—
mixed forest	—	—	—	-10.14	11.408	0.391	—	—	—
regenerating forest	—	—	—	-10.02	11.416	0.396	—	—	—
disturbance type									
fire	—	—	—	-0.50	0.515	0.344	—	—	—
mechanical add	—	—	—	0.38	0.495	0.451	—	—	—
mechanical remove	—	—	—	-0.56	0.437	0.217	—	—	—
disturbance severity									
low	-5.90	2.864	*0.044**	—	—	—	—	—	—
medium	-5.79	2.841	*0.046**	—	—	—	—	—	—
high	-6.16	2.829	*0.033**	—	—	—	—	—	—
disturbance age	<0.01	0.038	0.986	0.01	0.040	0.777	—	—	—
easting	—	—	—	0.27	0.302	0.375	0.151	0.127	0.252
northing	0.22	0.067	*0.001**	-0.17	0.189	0.362	—	—	—
precipitation	0.27	0.123	*0.027**	-0.13	0.269	0.621	—	—	—
DEM	<0.01	<0.001	0.091	—	—	—	—	—	—
MMST	—	—	—	0.58	0.293	0.059	—	—	—
solar insolation	—	—	—	-0.07	0.088	0.414	0.112	0.079	0.079
water table depth	—	—	—	—	—	—	—	—	—

aspect	<0.01	<0.001	0.993	—	—	—	—	—	—
slope	-0.03	0.033	0.310	—	—	—	—	—	—
random effects		disturbance			bedrock geology			bedrock geology	
marginal r^2		0.339			0.236			0.064	
conditional r^2		0.339			0.736			0.374	
CV_{LMER} RMSE (kg/m^2)		0.43			0.20			0.52	

Table 2. Model structure for best-fitting mixed-effects models for uninformed δ13C. All values were truncated to three significant digits. Covariates with no values under a given preference group indicates that the covariate was not a part of the best fitting model. Marginal r^2 explains the proportion of the variance explained by the main effects, whereas conditional r^2 explains the proportion of the variance explained by both the main and the random effects combined. Where marginal r^2 equals the conditional r^2, there was no benefit to using mixed-effects models over simple linear models. RMSE was derived via spatial hold-one-out cross validation for our linear mixed-effects models (CV_{LMER}). For metadata associated with model covariates, see Table S3-2. "MMST" and "DEM" correspond to "mean maximum summer temperature" and "digital elevation map," respectively.

	low preference			medium preference			high preference		
fixed effects	β	SE	*P*	β	SE	*P*	β	SE	*P*
covertype									
wetland forest	-29.43	0.200	*<0.001**	-36.66	3.875	*<0.001**	-29.05	11.483	*0.001**
coniferous forest	-29.64	0.274	*<0.001**	-37.25	3.885	*<0.001**	-30.17	11.532	*0.001**
deciduous forest	-29.71	0.264	*<0.001**	-36.95	3.867	*<0.001**	-29.09	11.445	*0.001**
mixed forest	-30.01	0.164	*<0.001**	-37.50	3.914	*<0.001**	-29.57	11.387	*0.001**
regenerating forest	-28.66	0.153	*<0.001**	-36.41	3.890	*<0.001**	-29.03	11.535	*0.001**
disturbance type									
fire	—	—	—	—	—	—	-0.46	0.340	0.174
mechanical add	—	—	—	—	—	—	0.38	0.465	0.410
mechanical remove	—	—	—	—	—	—	0.65	0.427	0.129
disturbance severity									
low	—	—	—	—	—	—	—	—	—
medium	—	—	—	—	—	—	—	—	—
high	—	—	—	—	—	—	—	—	—
disturbance age	—	—	—	0.07	0.029	*0.009**	—	—	—
easting	-0.19	0.088	*0.028**	—	—	—	1.37	0.446	*0.003**
northing	—	—	—	—	—	—	-1.01	0.281	*<0.001**
precipitation	—	—	—	0.25	0.128	0.065	-1.34	0.368	*<0.001**
DEM	—	—	—				—	—	—
MMST	—	—	—	—	—	—	1.67	0.540	*0.002**
solar insolation	0.14	0.093	0.125	—	—	—	—	—	—
water table depth	—	—	—	—	—	—	-0.02	0.006	*<0.001**

aspect	—	—	—	—	—	—	—	—	—
slope	—	—	—	—	—	—	—	—	—
random effects	disturbance, bedrock geology			bedrock geology			bedrock geology		
marginal r^2	0.452			0.450			0.497		
conditional r^2	0.452			0.544			0.497		
CV_{LMER} RMSE (‰)	0.69			0.69			0.83		

Table 3. Model structure for best-fitting mixed-effects models for biomass-informed δ13C. All values were truncated to three significant digits. Covariates with no values under a given preference group indicates that the covariate was not a part of the best fitting model. Marginal r^2 explains the proportion of the variance explained by the main effects, whereas conditional r^2 explains the proportion of the variance explained by both the main and the random effects combined. Where marginal r^2 equals the conditional r^2, there was no benefit to using mixed-effects models over simple linear models. RMSE was derived via spatial hold-one-out cross validation for our linear mixed-effects models (CV_{LMER}). For metadata associated with model covariates, see Table S3-2. "MMST" and "DEM" correspond to "mean maximum summer temperature" and "digital elevation map," respectively.

	low preference			medium preference			high preference		
fixed effects	β	SE	*P*	β	SE	*P*	β	SE	*P*
covertype									
wetland forest	-27.13	1.087	*<0.001**	-43.12	6.234	*< 0.001**	-28.64	0.010	*0.010**
coniferous forest	-27.20	1.057	*<0.001**	-43.65	6.233	*< 0.001**	-28.55	0.010	*0.010**
deciduous forest	-27.32	1.070	*<0.001**	-43.44	6.222	*< 0.001**	-27.63	0.010	*0.010**
mixed forest	-27.47	1.097	*<0.001**	-43.81	6.245	*< 0.001**	-27.61	0.010	*0.010**
regenerating forest	-26.14	1.133	*<0.001**	-42.44	6.188	*< 0.001**	-26.71	0.010	*0.010**
disturbance type									
fire	—	—	—	—	—	—	—	—	—
mechanical add	—	—	—	—	—	—	—	—	—
mechanical remove	—	—	—	—	—	—	—	—	—
disturbance severity									
low	0.08	0.300	0.856	—	—	—	—	—	—
medium	1.03	0.551	0.161	—	—	—	—	—	—
high	-0.25	0.358	0.636	—	—	—	—	—	—
disturbance age	—	—	—	0.040	0.036	0.270	—	—	—
easting	—	—	—	—	—	—	<0.01	<0.001	*0.014**
northing	—	—	—	—	—	—	<0.01	<0.001	*0.005**
precipitation	—	—	—	0.60	0.260	*0.027**	-0.92	0.400	*0.025**
DEM	-0.01	<0.001	*0.012**	<0.01	0.001	0.078	<0.01	0.001	0.089
MMST	—	—	—	—	—	—	1.31	0.581	*0.029**
solar insolation	-0.01	<0.001	0.276	—	—	—	—	—	—
water table depth	—	—	—	—	—	—	-0.01	0.007	0.052

aspect	—	—	—	—	—	—	—	—	—
slope	—	—	—	—	—	—	—	—	—
random effects	disturbance			bedrock geology			bedrock geology		
marginal r^2	0.462			0.388			0.415		
conditional r^2	0.473			0.588			0.415		
CV_{LMER} RMSE (‰)	0.87			0.90			1.05		

Table 4. Model structure for best-fitting mixed-effects models for uninformed δ15N. All values were truncated to three significant digits. Covariates with no values under a given preference group indicates that the covariate was not a part of the best fitting model. Marginal r^2 explains the proportion of the variance explained by the main effects, whereas conditional r^2 explains the proportion of the variance explained by both the main and the random effects combined. Where marginal r^2 equals the conditional r^2, there was no benefit to using mixed-effects models over simple linear models. RMSE was derived via spatial hold-one-out cross validation for our linear mixed-effects models (CV_{LMER}). For metadata associated with model covariates, see Table S3-2. "MMST" and "DEM" correspond to "mean maximum summer temperature" and "digital elevation map," respectively.

	low preference			medium preference			high preference		
fixed effects	β	SE	*P*	β	SE	*P*	β	SE	*P*
covertype									
wetland forest	—	—	—	—	—	—	-7.674	19.431	0.699
coniferous forest	—	—	—	—	—	—	-9.349	19.483	0.639
deciduous forest	—	—	—	—	—	—	-7.826	19.400	0.693
mixed forest	—	—	—	—	—	—	-7.220	19.342	0.715
regen forest	—	—	—	—	—	—	-7.135	19.490	0.720
disturbance type									
fire	—	—	—	—	—	—	1.250	0.816	0.131
mechanical add	—	—	—	—	—	—	2.774	0.865	*0.002**
mechanical remove	—	—	—	—	—	—	1.297	0.916	0.162
disturbance severity									
high	-3.0941	0.587	*<0.001**	—	—	—	—	—	—
low	-2.0355	0.844	*0.031**	—	—	—	—	—	—
moderate	-1.6986	0.662	*0.031**	—	—	—	—	—	—
disturbance age	—	—	—	—	—	—	-0.257	0.085	*0.004**
easting	0.342	0.139	*0.001**	—	—	—	1.615	0.647	*0.017**
northing	-0.405	0.129	*0.002**	—	—	—	-1.028	0.408	*0.017**
precipitation	—	—	—	—	—	—	-1.173	0.567	*0.049**
DEM	—	—	—	—	—	—	—	—	—
MMST	—	—	—	—	—	—	1.679	0.709	*0.021**

solar insolation	—	—	—	—	—	—	—	—	—
water table depth	—	—	—	-0.031	0.008	*< 0.001**	-0.029	0.008	*0.001**
aspect	—	—	—	—	—	—	—	—	—
slope	—	—	—	—	—	—	—	—	—
random effects	disturbance			disturbance, bedrock geology			bedrock geology		
marginal r^2	0.186			0.030			0.359		
conditional r^2	0.647			0.906			0.496		
CV_{LMER} RMSE (‰)	0.92			0.92			0.98		

Table 5. Model structure for best-fitting mixed-effects models for biomass-informed δ15N. All values were truncated to three significant digits. Covariates with no values under a given preference group indicates that the covariate was not a part of the best fitting model. Marginal r^2 explains the proportion of the variance explained by the main effects, whereas conditional r^2 explains the proportion of the variance explained by both the main and the random effects combined. Where marginal r^2 equals the conditional r^2, there was no benefit to using mixed-effects models over simple linear models. RMSE was derived via spatial hold-one-out cross validation for our linear mixed-effects models (CV_{LMER}). For metadata associated with model covariates, see Table S3-2. "MMST" and "DEM" correspond to "mean maximum summer temperature" and "digital elevation map," respectively.

	low preference			medium preference			high preference		
fixed effects	β	SE	*P*	β	SE	*P*	β	SE	*P*
covertype									
wetland forest	—	—	—	—	—	—	306.20	20.64	0.160
coniferous forest	—	—	—	—	—	—	304.50	20.64	0.163
deciduous forest	—	—	—	—	—	—	306.10	20.64	0.161
mixed forest	—	—	—	—	—	—	306.70	20.64	0.160
regenerating forest	—	—	—	—	—	—	307.00	20.64	0.160
disturbance type									
fire	—	—	—	—	—	—	1.39	1.162	0.238
mechanical add	—	—	—	—	—	—	3.05	1.155	*0.012**
mechanical remove	—	—	—	—	—	—	1.58	1.208	0.197
disturbance severity									
low	172.80	95.88	0.078	—	—	—	—	—	—
medium	172.60	95.98	0.077	—	—	—	—	—	—
high	173.10	95.89	0.075	—	—	—	—	—	—
disturbance age	—	—	—	—	—	—	-3.05	0.122	*0.015**
easting	<0.01	<0.001	0.135	—	—	—	<0.01	<0.001	0.090
northing	<0.01	<0.001	0.062	<0.01	<0.001	0.693	<0.01	<0.001	0.129
precipitation	-0.37	0.417	0.367	-0.21	0.402	0.603	-1.21	0.755	0.126
DEM	<0.01	0.001	0.745	<0.01	0.002	0.111	—	—	—
MMST	—	—	—	—	—	—	1.56	0.885	0.084
solar insolation	—	—	—	<0.01	<0.001	0.018	—	—	—
water table depth	—	—	—	-0.01	0.009	0.270	-0.02	0.012	*0.025**

aspect	—	—	—	—	—	—	—	—	—
slope	—	—	—	-0.07	0.058	0.182	—	—	—
random effects	disturbance			disturbance, bedrock geology			bedrock geology		
marginal r^2	0.146			0.142			0.243		
conditional r^2	0.583			0.666			0.512		
CV_{LMER} RMSE (‰)	1.24			1.41			1.70		

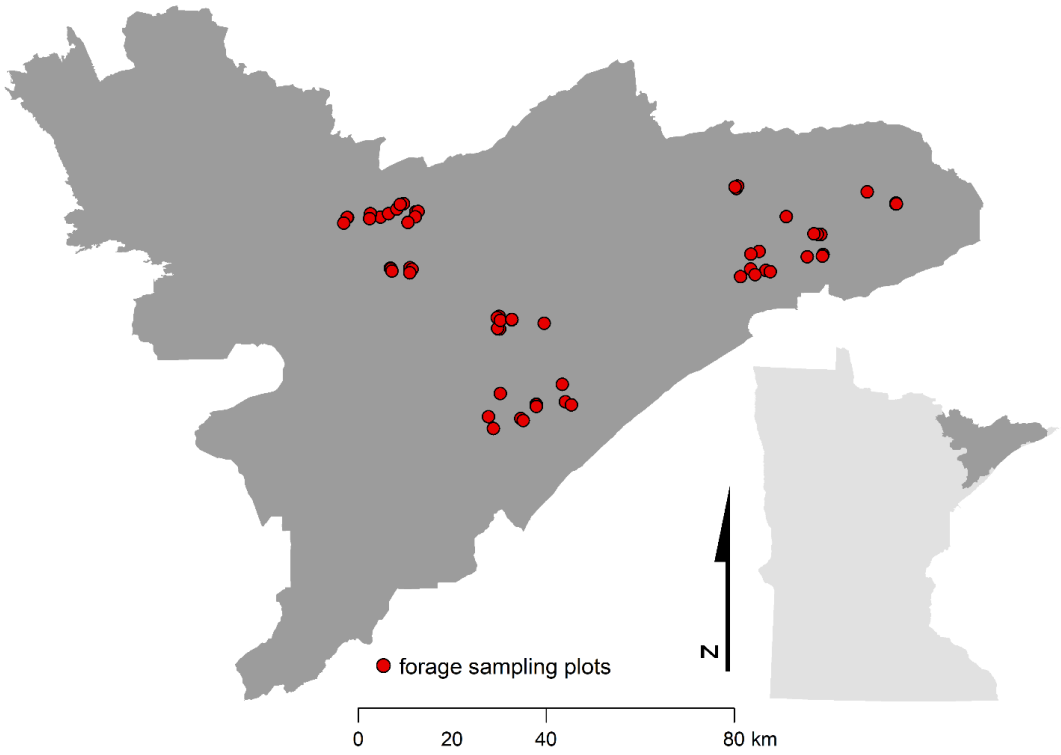

Fig.1. Forage sampling plots across northeastern Minnesota. Dark grey area in inset map represents the study region and Minnesota Moose Management Area as determined by the Minnesota Department of Natural Resources.

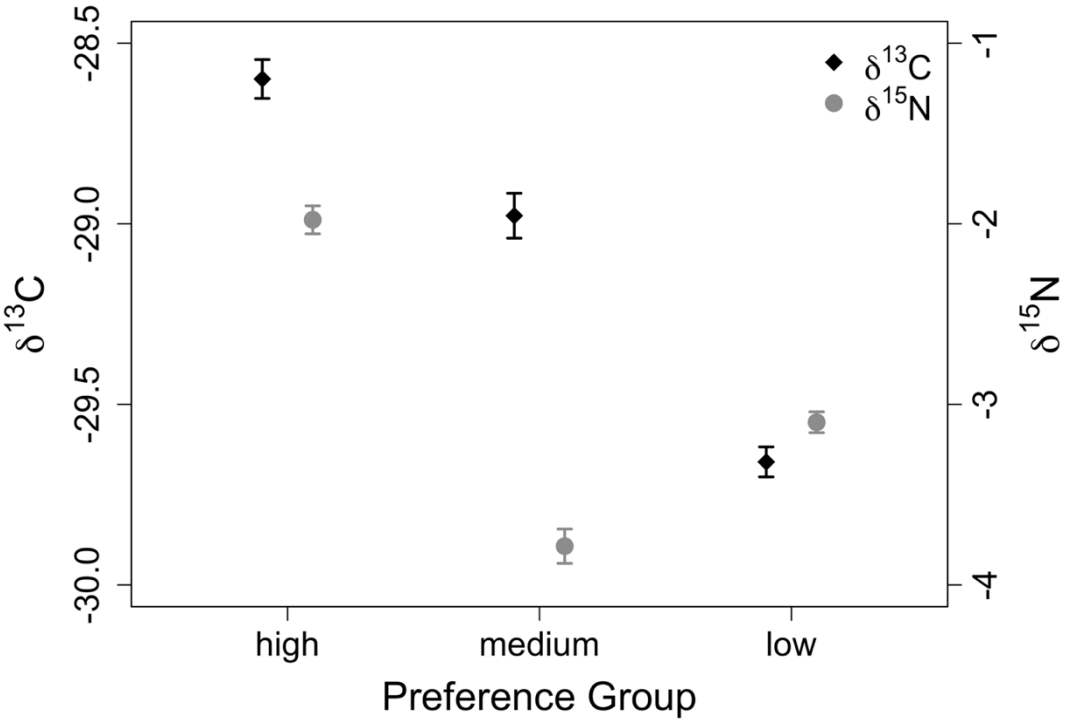

Fig.2. Isotopic variation of raw $\delta^{13}C$ and $\delta^{15}N$ values (‰) across preference groups. Mean values are represented by symbols, while error bars represent standard error.

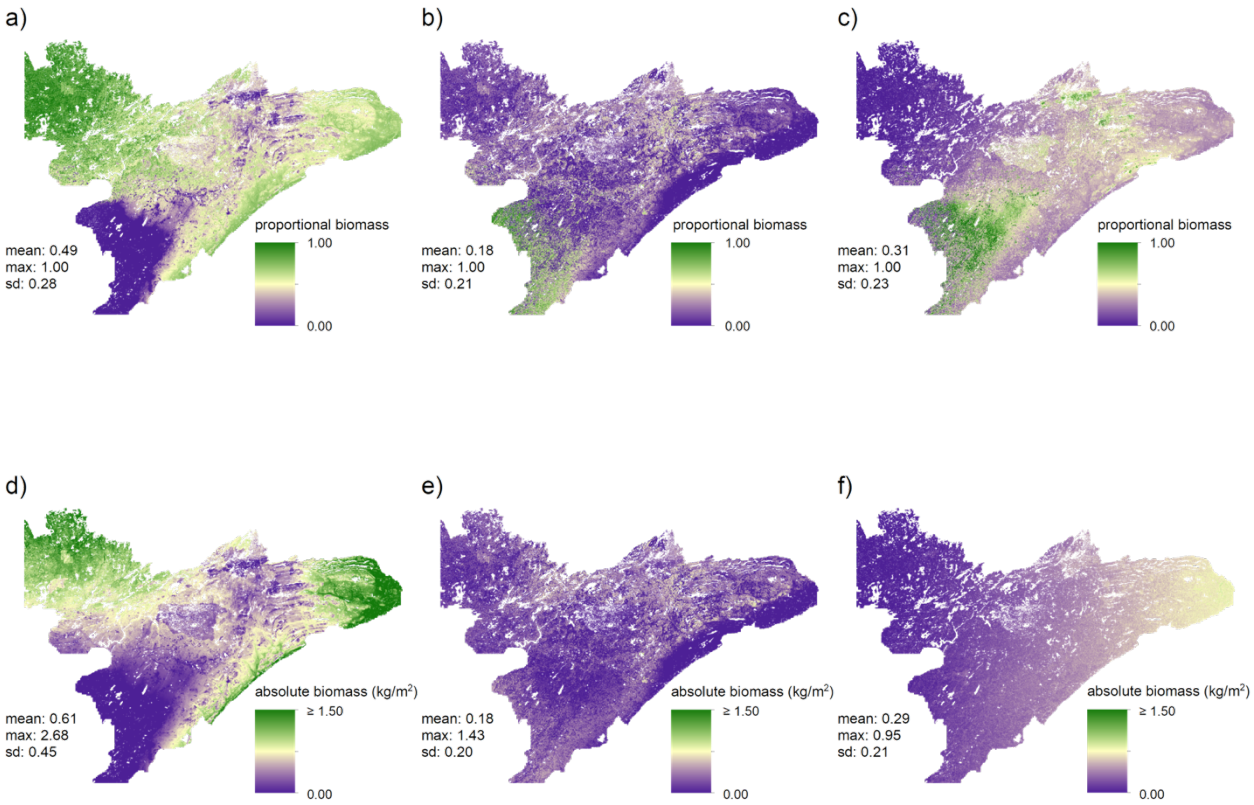

Fig.3. Predictions of proportional abundances and absolute amounts (kg/m^2) of biomass for low (a. and d., respectively), medium (b. and e., respectively), and high-preference forage (c. and f., respectively). Visual inspection of these maps suggests substantial differences in both the proportional abundances and the absolute amounts of biomass of all three forage-preference groups.

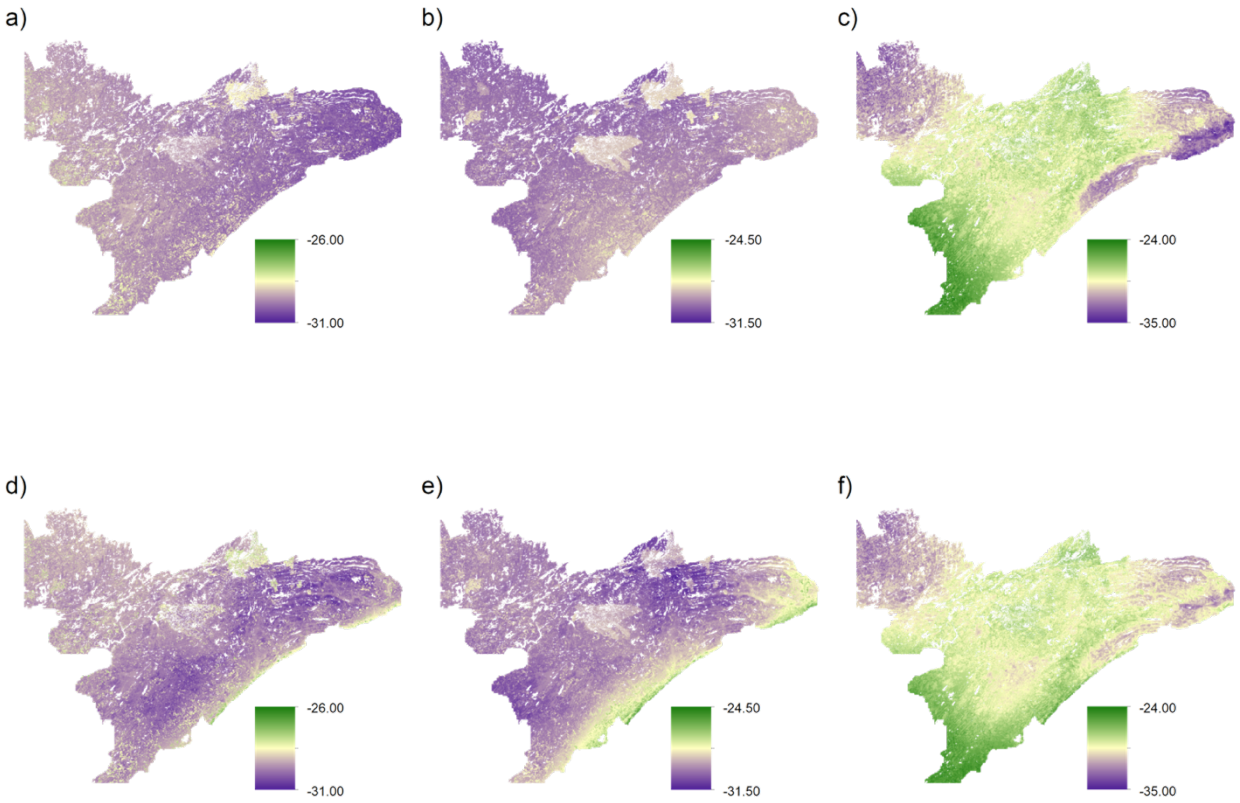

Fig.4. Isoscapes depicting spatial variation in $\delta^{13}C$ (‰) across northeastern Minnesota. Visual inspection of prediction maps reveals distinct differences when comparing uninformed isoscapes for low (a), medium (b), and high-preference forage (c) to those derived from biomass-informed models for low (d), medium (e), and high-preference forage (f).

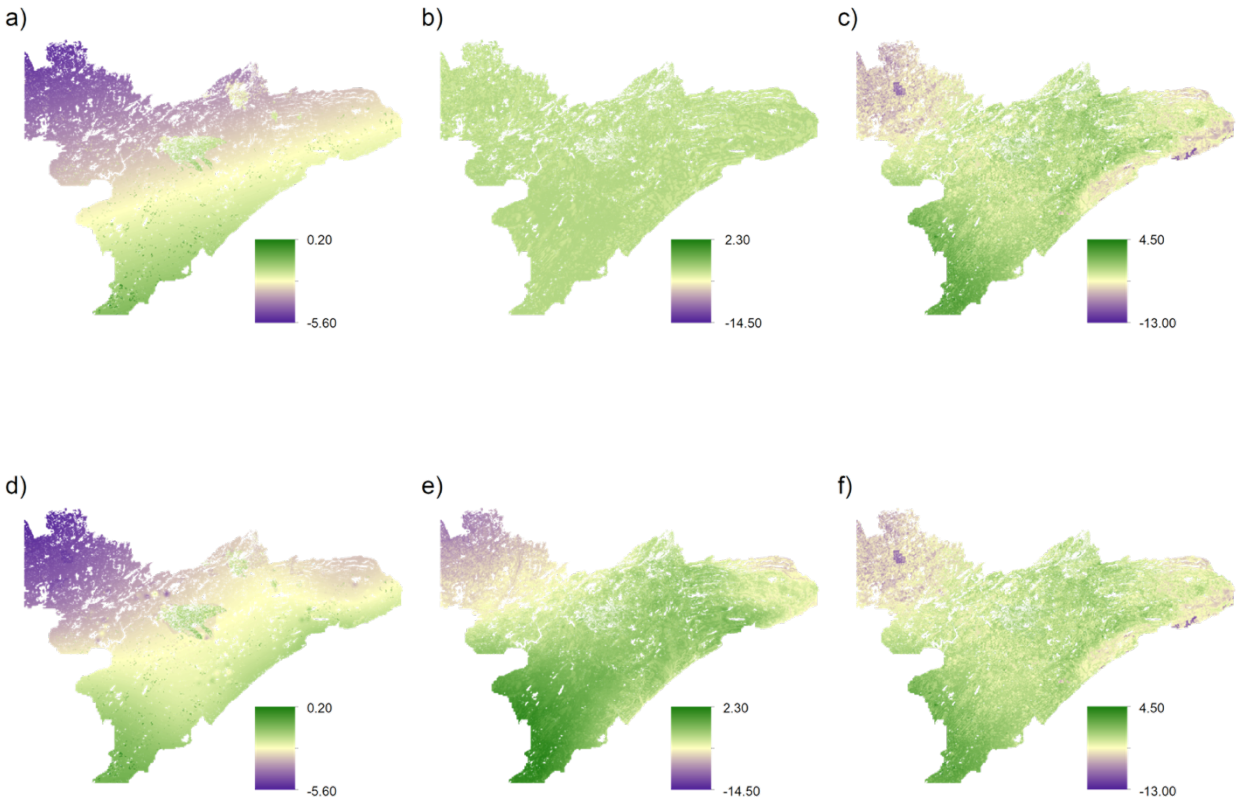

Fig.5. Isoscapes depicting spatial variation in $\delta^{15}N$ (‰) across northeastern Minnesota. Visual inspection of prediction maps reveals distinct differences when comparing uninformed isoscapes for low (a) and medium-preference forage (b) to those informed by biomass estimates (d and e, respectively). However, isoscapes predictions for high-preference forage, both uninformed (c), and biomass-informed (f), appear to be very similar.

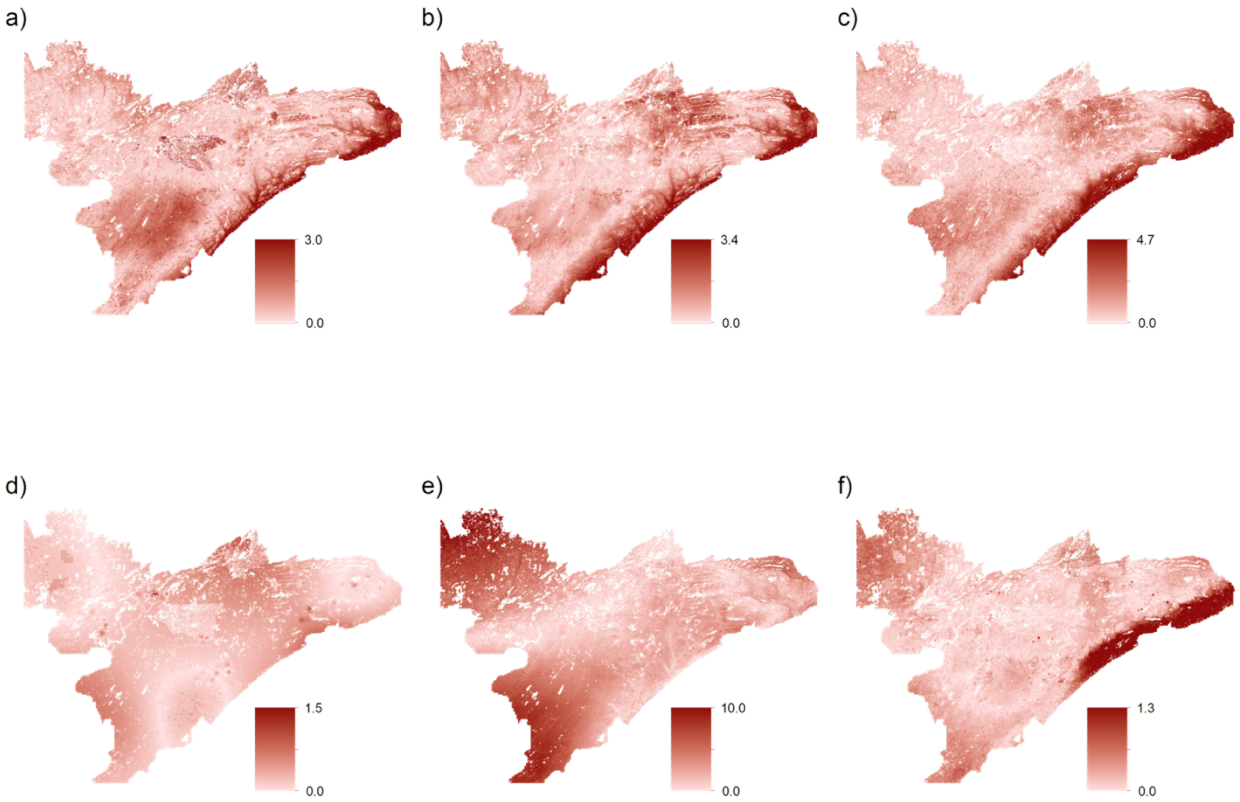

Fig.6. Differences in isoscape predictions (‰) utilizing uninformed-isotope data and biomass-informed isotopes. Maps depict the absolute values of unformed predictions minus biomass-informed predictions for $\delta^{13}C$ and $\delta^{15}N$ for low (a. and d., respectively), mid (b. and e., respectively), and high-preference forage (c. and f., respectively). Darker colors represent those areas of the study region in which predictions based on uninformed isotopes are farthest away from biomass-informed predictions, whereas lighter colors represent those areas of the study region where predictions are more similar.

Chapter 4: High Temperatures and Diet During Summer Influence Overwinter Survival in a Declining Moose Population.

ABSTRACT The North American moose (*Alces alces*) is a cold-adapted species that has recently experienced population declines at various points along the southern edge of its range. The moose population in northeast Minnesota (NEMN) declined by more than 65% from 2006 to 2018, and the combined effects of poor nutrition and high temperatures may predispose moose to higher risk of mortality. The primary objective of this study was to investigate the interaction between spatial variation in summer temperatures and moose diet and to evaluate if the relationship between these variables influenced over-winter survival.

We collected terrestrial and aquatic plant samples as well as hair samples from dead and living moose and categorized all samples into one of three temperature regions (i.e., warm, moderate, and cool) based on collection location within the thermal landscape. We also categorized forage into one of four groups based primarily on preference (high-, medium-, low-preference, and aquatics). We analyzed all forage samples for %N, $\delta^{13}C$ and $\delta^{15}N$ values, and all hair samples for $\delta^{13}C$ and $\delta^{15}N$ values. We estimated nitrogen availability in forage throughout the study region and used Bayesian mixing models to estimate diet composition. We then tested whether diets varied as a function of temperature region, winter mortality, or season, and evaluated if winter mortality varied as a function of temperature region.

In general, the warmest parts of the moose range in Minnesota are those that offered forage of lower quality, where moose diets were poorest, and where winter

mortality was highest. Nitrogen availability in terrestrial forage declined with mean-maximum summer temperature, and moose in the warmest parts of the range had diets containing the highest proportion of aquatic forage and the lowest proportion of high-preference forage. Additionally, winter mortality was almost 4.5 times greater in the warmest parts of the range when compared to the coolest. Finally, probability of over-winter survival increased with increasing proportions of high- and medium preference forage during early summer and high- and low-preference forage during late summer. Collectively, our results suggest that the interaction between temperature and diet during summer may increase risk of over-winter mortality, including mortality associated with predation and disease.

INTRODUCTION

Large mammalian herbivores are declining globally at an unprecedented rate, and while hunting, competition with livestock, and habitat loss have been listed as some of the leading causes of decline (Ripple et al. 2015), the pervasive influences of recent climate change have also been associated with negative demographic trends of large herbivores (Olff et al. 2002). Fluctuations in the North Atlantic Oscillation have been linked to changes in body condition in sheep (*Ovis aries*, Mysterud et al. 2001), severe snowpack conditions have been associated with the near elimination of juvenile cohorts in elk (*Cervus elaphus*, Garrott et al. 2003), and changes in precipitation have been tightly correlated with changes in population size in African herbivores (Berger 1997). Global distributions of large herbivore diversity are strongly correlated with gradients of temperature and precipitation (Olff et al. 2002). Thus, spatiotemporal shifts in global

patterns of these and other climatic variables are expected to influence the abundance and distribution of large herbivores (Schloss et al. 2012), with high-latitude species at greater risk of climate-induced declines than their more southerly counterparts (ACIA 2004, Garcia et al. 2014, Walther et al. 2002). Northern latitudes are likely to experience disproportionate warming compared to the rest of the globe (IPCC 2007), and large mammals are thought to be incapable of rapid micro-evolution or sufficient range shifts necessary to adjust to increasing temperatures (Hetem et al. 2014).

The North American moose (*Alces alces*) is a cold-adapted species that is relatively intolerant of high temperatures (Renecker and Hudson 1990), and has experienced population declines at various points along the southern edge of its geographic range (Timmermann and Rodgers 2017). In northwestern Minnesota, moose exhibited a precipitous decline starting in the mid 1980s, decreasing from about 4000 animals in 1984 to less than 100 animals in 2007 (Lenarz et al. 2009, Murray et al. 2013). A study investigating the potential causes of this decline reported that the majority of moose fatalities (87% of radio-collared moose and 65% of non-collared moose) were ultimately due to parasites and infectious disease. However, the authors also noted that many of the recorded causes of mortality were likely facilitated by a combination of poor nutrition and warmer ambient temperatures. Animals that died of natural causes exhibited notable signs of malnutrition and severe body fat depletion, and annual population growth in northwestern Minnesota from 1961-2000 was negatively correlated with mean summer temperature, which increased by 2.1 ºC during this time (Murray et al. 2006).

Since 2006, demographic trends of moose in northeast Minnesota (NEMN) have resembled those previously observed in the northwestern part of the state, with one study reporting a negative correlation between ambient temperature and annual survival (Lenarz et al. 2009). Because moose are heat intolerant, when they are exposed to even modestly warm temperatures (e.g., 14 to 17 ºC), they increase metabolic and respiration rates and reduce forage intake, which can lead to malnutrition, decreased body condition, and immunosuppression (Lenarz et al. 2009, McCann et al. 2013, Murray et al. 2006, Renecker and Hudson 1986). Despite these relationships, there is little mechanistic evidence directly linking increasing temperatures with the observed population decline.

While changing climate over the last decade has been implicated as a major driver of moose demographics in NEMN, the wolf population in this region has substantially increased over this same time period, potentially contributing to the current decline (Mech and Fieberg 2014). One study recently reported between 33 and 47% of monitored moose calf mortalities were due, at least in part, to wolf predation (Severud et al. 2015), and another study reported that more than 30% of analyzed wolf scats from NEMN contained moose tissue (Chenaux-Ibrahim 2015). However, there is evidence that wolf predation on moose is spatially heterogeneous, with higher rates of predation in the coolest parts of the range and lower predation rates in warmer parts of the range (Chenaux-Ibrahim 2015). Additionally, a study summarizing necropsy results of 62 opportunistically collected moose carcasses from 2003 to 2013, 85% of animals were either moderately underweight or exhibiting signs of severe weight loss and muscle

deterioration (Wünschmann et al. 2015). The authors noted the important role that nutritional state likely played in the fates of these animals (Wünschmann et al. 2015).

Evidence suggests that as ambient temperatures increase, large herbivores may alter habitat-use in a way that decreases thermal loads, while also leading to a lower nutritional state (Albon and Langvatn 1992). Moose are well-adapted for cold, but become heat stressed and potentially hyperthermic when temperatures rise above 14 ºC in the summer (Renecker and Hudson 1986). Typically, moose respond to high temperatures in one of two ways, both of which may result in important nutritional tradeoffs. First, moose may increase their use of densely forested conifer habitat (Renecker and Hudson 1990, Street et al. 2016), bedding down in lowland forest canopies with high soil-water content (McCann et al. 2016), presumably in an effort to dissipate metabolic heat by increasing contact with the cool ground (Merrill 1991). During prolonged periods of extreme heat, moose may remain bedded for extended periods of time and forgo multiple feeding bouts, thereby putting themselves at risk of starvation (Renecker and Hudson 1986). Alternatively, moose may increase their use of aquatic or wetland habitats during extended periods of high temperatures (Renecker and Hudson 1989, Street et al. 2016). While these habitats can offer an abundance of forage, aquatic forage tends to be high in protein but low in carbohydrates compared to terrestrial forage (Tischler 2004). If moose are spending extended periods of time either bedded in dense cover or in aquatic habitats, they may have a difficult time accumulating enough body fat to survive winter (Chan-McLeod et al. 2000, Julander et al. 1961, Parker et al. 2009).

A recent study investigating the relationship between winter nutritional status of moose in NEMN and regional population growth reported that estimates of abundance and calf production were closely correlated with population-wide nutrition (DelGiudice et al. 2017). Moreover, from 2013 to 2015, winter nutritional restriction was closely related to high temperatures during winter (DelGiudice et al. 2017). Although studies of other large herbivores suggest that poor summer nutrition can also detrimentally impact reproduction and overwinter survival (Cook et al. 2004), the impact of summer diet on the moose population in NEMN is unknown.

The primary objective of this study is to investigate the interaction between spatial variation in high summer temperatures and moose diet, and to evaluate if the relationship between these two variables might influence over-winter survival. Northeast Minnesota is an ideal location in which to evaluate this relationship because there is a ~ 5.5 ºC gradient in mean-maximum temperature across the region (Fig.1). To evaluate how high temperatures and diet may interact during summer to influence over-winter survival, we hypothesized that: 1) Forage quality is greater in areas with cooler temperatures, 2) Moose in cooler parts of the range have diets of higher quality than those from warmer parts of the range, 3) The number of moose that do not survive winter is disproportionately higher in the warmest parts of the range, and 4) The diets of moose that do not survive winter are of lower quality than those that do.

STUDY AREA

Our study area in northeastern Minnesota covers approximately 1.3-million hectares, and is composed primarily of southern boreal forest, including large portions of Superior

National Forest and the Boundary Waters Canoe Area Wilderness (BWCAW). This region is a mosaic of upland and lowland forest types characterized by black spruce (*Picea mariana*) and white cedar (*Thuja occidentalis*) in the lowlands and balsam fir (*Abies balsamea*), trembling aspen (*Populus tremuloides*), and paper birch (*Betula papyrifera*) on the uplands, with large stands of jack (*Pinus banskiana*), red (*P. resinosa*) and white pine (*P. strobus*) occurring throughout. While large swaths of unlogged areas remain (i.e., 169,000 ha within the BWCAW), fire and logging are common and routine forms of disturbance in this ecosystem (Heinselman 1996). Mean annual temperature is approximately 2ºC with mean annual precipitation (rain plus snowfall water equivalent) of 70 cm (Heinselman 1996). Summers in this region are typically short and cool, with mean temperatures of 17.5 ºC in mid-July and an average precipitation of 10 cm. Winters are characterized as long and cold, with mean temperatures of -17ºC and normal winter snowfall ranging from 50 to 70 cm (Frelich 2002, Heinselman 1996). Topography across the study area varies from relatively flat to moderately hilly, with elevation ranging from the 183 m at the surface of Lake Superior, to 701 m at Eagle Mountain, the highest point in the state. The area is sparsely inhabited, with few paved roads and much of the region accessible only by foot, logging road, or canoe.

METHODS

Overview

We used a variety of sampling and analytical techniques to evaluate how warmer summer temperatures and diet may interact to influence over-winter survival in moose across northeast Minnesota. We sampled terrestrial forage from 0.4 ha plots (n = 70) located

across the study region (Fig.1), and aquatic forage from 17 different lakes across the study region. We also collected moose hair samples from living and dead moose during a parallel study designed to evaluate adult moose mortality (see *Sample Collection* below). We measured woody plants in all plots and used species and size-class-specific allometric equations to estimate forage biomass within each plot (see *Woody Biomass Calculations* below), and used elemental and stable isotope analysis to determine values of %N, $\delta^{13}C$, and $\delta^{15}N$ in forage and values of $\delta^{13}C$ and $\delta^{15}N$ in hair (see *Stable Isotopes Analysis* below). We used stable isotope values from forage and hair to estimate the contributions of each forage group to moose diets using Bayesian mixing models, and then tested whether diets vary as a function of temperature region, winter mortality, and season (see *Data Analysis* below).

Sample Collection

We established 70 circular plots, each 0.4 ha in size, throughout northeast Minnesota and collected samples of known and potential forage species to characterize the isotopic composition of moose forage throughout the study region. Sample plots covered a range of disturbance ages (i.e., 13 years, 9 years, 4 years, and undisturbed) and types (i.e., canopy burn, clear cut, and insect-defoliation), as well as a range of landcover types (i.e., wetland and wetland forest, coniferous forest, deciduous forest, mixed forest, and regenerating forest). From 2012 to 2016, we collected annual samples of forage species in each of the plots from late May to early August, with a small subset of individual plants collected at multiple time periods throughout summer. In total, we collected 2,694 terrestrial forage samples from more than 30 species (Table S4-1). We

categorized all species into one of three groups, based primarily on dietary preference: high-, medium-, and low-preference (Table S4-1; Peek et al. 1976). Where possible, we collected up to five samples of each species in each plot, where a sample consisted of 5-7 leaves that we stripped from a peripheral stem located between 0.5 to 1.0 m from the forest floor. Once collected, samples were placed in a cloth bag, which was then labeled with the plot and sample ID. For diet composition estimates, we also collected samples of submerged and emergent aquatic forage (n=105) from 17 different lakes throughout the warm (n=7) and cold (n=10) temperature regions. We collected aquatic samples by dragging an aquatic sampling rake at depths ranging from 1 to 2 meters. Where possible, we collected up to five samples of each species from each lake. Once collected, samples were placed in a cloth bag, which was then labeled with the lake name and sample ID.

Moose hair samples were collected from both live and dead animals by the Minnesota Department of Natural Resources (MNDNR) from 2012 to 2017 (Fig.1a). Hair from live animals (n = 127) was collected during radio-collar deployment, which took place as part of a parallel study to investigate adult moose mortality (Carstensen et al. 2015). Hair from animals that died during winter (n=35) was collected from a combination of radio-collared animals (n=18) and opportunistically sampled carcasses (n=17). Because we wanted to focus solely on the potential influences of diet on winter mortality, we included only those animals that died between November 1st and May 1st of each year.

Woody Biomass Calculations

Moose are known to break stems with a diameter at breast height (DBH) of ≤ 6cm in order to browse on terminal shoots, but also occasionally browse on plants that are relatively close to the forest floor (Renecker and Schwartz 2007). Thus, within each 0.4 ha plot, we measured smaller woody stems (i.e., stems ≤ 6 cm of diameter at breast height, DBH, and ≥ 15 cm in height) within three, nested, 25 m^2 subplots along the 30º, 150º, and 270º azimuths, at 5.5 m from the plot centroid. Within a 25 m^2 subplot, we tallied the number of individuals of each species having a DBH ≥ 2.5 cm and ≤ 6 cm (i.e., saplings), with tallies for each species recorded for each 0.5 cm DBH interval. Within a smaller, 10 m^2 subplot, we measured diameter at 15 cm height of all woody plants that were ≥ 15 cm in height but < 2.5 cm in DBH (i.e., shrubs or advanced regeneration). We tallied the number of individuals of each species within each 0.5 cm size class, from 0.5 cm to 2.5 cm. Anything with a diameter < 0.5 cm at 15 cm height was omitted.

We calculated estimates of above-ground biomass using species-specific biomass equations based on the measurements detailed above. For saplings, we used species-specific equations from Jenkins et al. (2003) to estimate above-ground biomass using DBH. We also used species-specific equations for shrubs and advanced regeneration, (Perala and Alban 1993, Smith and Brand 1983), which allowed us to estimate above ground biomass based on stem diameter at 15 cm height. For some species, equations for whole, above-ground biomass were not available. For those species, we calculated biomass for stems and foliage separately, and then added those values to estimate total biomass of each species in each plot. All estimates were converted to kg/m^2.

Stable Isotope Analysis

In preparation for stable isotopes analysis, plant samples were dried in a 60ºC oven for 24 to 48 hours and subsequently placed in light-proof, tin containers. A small portion of each sample was collected and ground to a homogenous powder using a Spex SamplePrep GenoGrinder bead mill with 2.8 mm stainless steel grinding beads. Once homogenized, we weighed 2.5 ± 0.1 mg of each sample into a 5x9 mm Costech tin capsule. All samples were analyzed either at the Stable Isotope Laboratory in the Department of Earth Sciences at the University of Minnesota (UMN) or the Stable Isotope Laboratory in Earth and Planetary Sciences at the University of California, Santa Cruz (UCSC). At UMN, samples were analyzed for %N, %C, $\delta^{15}N$ and $\delta^{13}C$ values via flash combustion in a Costech 4010 Elemental Analyzer (EA) coupled to a Thermo-Finnegan Delta V Plus isotope ratio mass spectrometer (IRMS). At UCSC, samples were analyzed via flash combustion in a CE Instruments NC2500 EA interfaced to a ThermoFinningan Delta Plus XP IRMS. At each location, the resulting gas was analyzed for elemental concentration of $^{13}C/^{12}C$ and $^{15}N/^{14}N$ ratios and expressed in standard δ notation, representing the differences between samples ratios and ratios found in international standards for carbon (VPDB) and nitrogen (atmospheric N_2). Finally, because samples were analyzed in two different laboratories, we addressed machine or lab specific analytical biases by running five samples from six different species in each lab and creating offset and linearity corrections that we then applied to all samples analyzed at UCSC.

The isotopic composition of animal materials (e.g., scat, hair, bone) reflects that of the food that was ingested and assimilated during the formation of these materials

(Cerling and Harris 1999, Deniro and Epstein 1978). Moose begin molting their winter coat during mid- to late-May and completely replace their winter coat with a thinner, lighter coat by late June (Franzmann et al. 1975, Samuel 1991, Tankersley and Gasaway 1983, Welch et al. 1990). Beginning in early June, moose also begin to develop winter hair, including that which is grown on their withers, with their winter coat typically complete by mid- to late September (Samuel et al. 1986). Because hair growth occurs only during summer, hair collected from late fall through early spring can be used to evaluate the diet from the previous summer, with stable isotopes in the proximal end of the hair reflecting that of late-summer diet and the distal end reflecting that of early-summer diet. Differences in mean $\delta^{13}C$ values have been used to analyze population differences in diet (Angerbjörn et al. 1994), and individual variation in values of $\delta^{13}C$ from animal materials provides a measure of dietary breadth within a group or population (Berini and Badgley 2017). As animals ingest a greater range of plant species and plant parts, the variance of $\delta^{13}C$ increases (Newsome et al. 2009, Stewart et al. 2003). In general, the mean $\delta^{15}N$ of animal tissues reflects the protein content of the animal's diet (Ambrose 1991, Schoeninger and DeNiro 1984), with a negative correlation between the nitrogen content of ingested plants and $\delta^{15}N$ values of herbivore tissues (Adams and Sterner 2000). Thus, animals consuming forage with greater N content will have more negative $\delta^{15}N$ values in their tissues, with N limitation indicated via more positive $\delta^{15}N$ values (Sealy et al. 1987).

To prepare moose hair samples for stable isotope analysis, we rinsed all hairs with deionized (DI) water and sonicated them in a DI water bath for approximately 10

minutes. Samples were then given another rinse and placed in a 2:1 chloroform/methanol mixture for approximately 2 hours to remove lipids. Once lipid extraction was complete, we rinsed off any residual solution with DI water, soaked the hairs in a DI bath for an additional 30 minutes, and then gave them a final rinse. All samples were then dried in an oven at 40ºC for a minimum of 48 hours.

Hair samples were analyzed for stable isotopes of carbon and nitrogen either at UMN or the Center for Stable Isotopes at the University of New Mexico (CSI-UNM). We clipped and weighed 0.7 ± 0.1 mg at UMN and 0.5 ± 0.1 mg at CSI-UNM from the proximal and distal ends of each hair. At both laboratories, samples were then loaded into 5x9 mm Costech tin capsules and analyzed for $\delta^{15}N$ and $\delta^{13}C$ values via flash combustion in a Costech 4010 Elemental Analyzer (EA) coupled to a Thermo-Finnegan Delta V Plus isotope ratio mass spectrometer (IRMS). The resulting gas was analyzed for elemental concentration of $^{13}C/^{12}C$ and $^{15}N/^{14}N$ ratios and expressed in standard δ notation, representing the differences between samples ratios and ratios found in international standards for carbon (VPDB) and nitrogen (atmospheric N_2). Because samples were analyzed in two different laboratories, we addressed machine or lab specific analytical biases by running hair samples from five different animals in each lab and created offset and linearity corrections that we then applied to all samples analyzed at CSI-UNM. Finally, to account for minor isotopic differences between hairs from the same animal, we analyzed the ends of each hair, from each animal, in replicates of two. We then calculated the average of the two replicates and saved these values as our final $\delta^{13}C$ and $\delta^{15}N$ values, which we then used to estimate diet for early and late summer.

Data Analysis

To determine if forage quality is greater in areas with cooler temperatures (H1), we evaluated how the amount of N in moose forage varies as a function of mean-maximum summer temperature (i.e., mean maximum daily temperature over June, July, and August each year from 1980-2010). Because both %N and the abundance of different forage groups can vary differently across the study region, we needed to estimate how the amount of N available in moose forage may change as a function of our different preference groups within each plot. To do this, we multiplied the mean proportional abundance of N of each forage group within each plot by their respective biomass estimates (kg/m^2) and added these values together. Then, using the *get_prism_normals* function from the *prism* package in R (Hart and Bell 2015), we imported the 30-year averages (1981-2010) for mean-maximum summer temperature (MMST) from the PRISM Climate Group at Oregon State University (PRISM Climate Group 2017). We extracted the temperature data at each of our forage-sampling plots using the *extract* function from the *raster* package in R (Hijmans 2019). Finally, to determine if there was a significant statistical relationship ($p < 0.05$) between the amount of N available and MMST, we fit generalized linear models using the *glm* function in the base package of R (R Core Team 2018). We fit four different models – one to evaluate the total N (kg/m^2) in each plot as a function of MMST and one model for each forage group (i.e., high-, medium-, and low-preference). For each model, we set MMST as our independent variable and total N as our dependent variable.

To determine if moose in cooler parts of the range have diets of higher quality than those from warmer parts of the range (H2), we analyzed how diet composition and stable isotope values of moose hair vary as a function of MMST. First, we categorized moose hair samples from living moose into one of three temperature regions (e.g., warm, medium, cool) based on their collection location within the thermal landscape (Fig.1). We estimated diet composition during early and late summer by fitting Bayesian mixing models using the *MixSIAR* package in R (Parnell et al. 2013, Stock and Semmens 2016). *MixSIAR* allows estimation of the contributions of different isotopic sources to the composition of a material that reflects a mixture of these different sources, while also allowing the user to account for both residual and process error (Parnell et al. 2013, Stock and Semmens 2016). In our study, source data was the $\delta^{13}C$ and $\delta^{15}N$ values from plants, whereas mixture data was the $\delta^{13}C$ and $\delta^{15}N$ values from moose hair. Trophic enrichment factors (i.e., the net isotopic difference between source and mixture; Martínez del Rio et al. 2009) were based on those in Drucker et al. (2010). We arrived at the most efficient Markov chain Monte Carlo (MCMC) length by fitting our models repeatedly, starting with the shortest chain-length allowable (i.e., *run = "test", chainLength = 1000*), and gradually increasing the chain-length until we achieved a Gelman-Rubin score of < 1.10, indicating that sampling variability is negligible (Brooks and Gelman 1998). Our final models had the following MCMC parameters: *chainLength*=100000, *burn*=50000, *thin*=50, *chains*=3, *calcDIC*=TRUE. We saved the mean estimates from our posterior distributions as our final diet composition estimates.

We fit two MANOVA models that evaluated diet composition as a function of temperature region, for both early and late summer, to evaluate if animals from different temperature regions exhibit significant differences in diet composition. However, because our data are compositional in nature and therefore bound by 0 and 1, we performed an isometric log ratio transformation on our diet estimate data using the *ilr* function in the *compositions* package (van den Boogaart et al. 2018). In the event that we encountered MANOVA models resulting in $p < 0.05$, we fit univariate ANOVAs to evaluate how the proportion of each forage group (i.e., aquatic, high-, medium-, and low-preference) changes between temperature regions (R Core Team 2018). Prior to conducting univariate ANOVA, we used a centered log ratio transformation via the *clr* command (also in the *compositions* package) because isometric log transformations reduce the dimensionality of a dataset by one (van den Boogaart et al. 2018). To evaluate if animals from different temperature regions exhibit significant differences in variance of $\delta^{13}C$ (i.e., dietary breadth), we conducted Bartlett's test for homogeneity of variance via the *bartlett.test* command in the *stats* package of R (R Core Team 2018). To evaluate if animals from different regions exhibit differences in mean $\delta^{15}N$ values (i.e., nitrogen intake), we conducted analysis of variance (ANOVA) via the *aov* function (R Core Team 2018). For ANOVA tests with statistically significant outcomes ($p < 0.05$), we used the *TukeyHSD* function (R Core Team 2018) to conduct Tukey's test for honestly significant differences, which allowed us to determine which temperature regions were significantly different from one another.

To determine if the number of moose that do not survive winter is disproportionately higher in the warmest parts of the range (H3), we compared the number of moose that were radio collared in each temperature region, with the number of collared animals that died. We conducted a Pearson's χ^2 test using the *chisq.test* function in the *stats* package and applied Yate's correction for small sample sizes (Yates 1934) by setting *correct=T (R Core Team 2018)*.

We evaluated differences in diet composition as a function of winter survival (H4) using logistic regression via the *glm* function (*family = "binomial"*), for both early and late summer (R Core Team 2018). We performed centered log-ratio transformations prior to logistic regression, as described above (van den Boogaart et al. 2018). We used MANOVA to evaluate seasonal dietary shifts from early to late summer, for animals that survived winter and for those that did not, with diet composition as our dependent variable and season as our independent variable. In the event that a MANOVA resulted in $p < 0.05$, we conducted univariate ANOVA to determine which dietary items exhibited significant shifts between early and late summer. Again, we used an isometric log ratio transformation prior to conducting MANOVA and centered log ratio transformation prior to conducting ANOVA (van den Boogaart et al. 2018). To evaluate dietary breadth using $\delta^{13}C$ values, we used Bartlett's test for homogeneity of variance and to investigate nitrogen limitation using $\delta^{15}N$, we used ANOVA. Finally, we subset our diet composition estimates for those animals that we collected both live and dead hair samples from, and evaluated diet composition as a function of over-winter mortality and seasonal dietary shifts throughout summer. These analyses were conducted exactly as described above,

and allowed us to compare the diets of the same individuals both before and after their death.

RESULTS

Generalized linear models evaluating the influence of mean-maximum summer temperature on the availability of N throughout the study region (H1) revealed a statistically significant decline in overall N availability as MMST increased (Table 1). Within individual groups of terrestrial forage (i.e., high-, medium-, and low-preference forage), N availability exhibited a negative, non-significant trend with increasing MMST in high- and medium-preference forage, while low-preference forage exhibited no relationship (Table 1).

MixSIAR results revealed that during early summer, the average diet for moose that survived winter consisted of 38% high-preference forage, 28% aquatics, 22% medium-preference forage, and 11% low-preference forage. During late summer, mean estimates changed to 31% high-preference, 35% aquatics, 13% medium-preference, and 21% low-preference. For moose that did not survive winter, the average early-summer diet consisted of 27% high-preference forage, 38% aquatics, 17% medium-preference forage, and 17% low-preference forage. While during late summer, mean estimates changed to 25% high-preference, 40% aquatics, 15% medium-preference, and 20% low-preference.

MANOVA tests evaluating diet as a function of temperature region for animals that survived winter (H2) revealed significant differences in diet composition among temperature regions during early ($F_{2,123} = 3.20$, $p = 0.004$) and late summer ($F_{2,124} = 6.83$,

$p < 0.0001$). During both time periods, moose from the warm and moderate-temperature regions consumed proportionally more aquatics, but generally less high-, medium-, and low-preference forage compared to moose from the cool region (Table 2, Fig.2). Diet composition estimates of different forage groups were not significantly different between the warm and moderate regions during early or late summer. Variance of $\delta^{13}C_{hair}$ values (i.e., dietary breadth) increased with temperature during early summer but not during late summer (Table 3, Fig.3) and ANOVA results revealed a significant difference in $\delta^{15}N_{hair}$ (i.e., dietary N limitation) among temperature regions, but only during late summer ($F_{2,126} = 4.302$, $p = 0.0156$). Tukey's HSD test revealed that mean values of $\delta^{15}N_{hair}$ during late summer were greater in the moderate region when compared to cool (Table 4, Fig.3).

Our χ^2 test evaluating over-winter mortality as a function of temperature region revealed that mortality was disproportionately higher in the warmest parts of the range (H3; $\chi^2 = 6.722$, df = 2, $p < 0.0347$). While overall mortality for collared moose was 29.9% across the entire study area, 15.6% and 28.6% of radio-collared moose did not survive winter in the cool and moderate temperature regions, respectively, but 68.8% of radio-collared moose from the warm region did not survive winter.

Logistic regression analyses comparing the diets of animals with different winter fates revealed that the diet composition of moose that survived winter was significantly different than those that did not, both during early and late summer (Fig.4). Probability of overwinter survival increased with increasing contributions of high- and medium-preference forage to the overall diet during early summer, but decreased with increasing contributions of low-preference forage (Table 5, Fig.4). During late summer, probability

of survival increased with increasing contributions of high- and low-preference forage (Table 5, Fig.4). Pairwise logistic regressions comparing diets of the same animals before and after death revealed that during early summer, medium-preference forage was associated with increased probability of over-winter survival (Table 6, Fig.5). During late summer, as the proportional contributions of high-preference and aquatic forage increased, probability of overwinter survival also increased (Table 6, Fig.5). As the proportional contributions of low-preference forage increased, probability of overwinter survival decreased (Table 6, Fig.5).

MANOVA tests evaluating dietary shifts from early to late summer revealed that animals that survived winter exhibited temporal changes in diet ($F_{1,251} = 7151$, $p < 0.0001$) as did animals that died ($F_{1,69} = 15.62$, $p < 0.0001$). Animals that survived winter consumed mostly high-preference forage during early summer, but then shifted their diets in late summer to include greater proportions of aquatic forage (Table 7, Fig.6a). Despite the fact that MANOVA results suggests a significant dietary shift between seasons for animals that died, univariate ANOVAs revealed no shifts from early to late summer, with aquatic forage representing the largest proportion of their diet among all forage groups, during both time periods (Table 7, Fig.6b). During both early and late summer, moose that survived winter had smaller variance in values of $\delta^{13}C_{hair}$ (Table 8, Fig.7a) and lower mean $\delta^{15}N_{hair}$ values (Table 8, Fig.7b) than moose that died. To ensure that the differences in variance we observed were not due to our small number of mortalities, we created a bootstrapped sample of 35, $\delta^{13}C_{hair}$ values from our live sample set, calculated the variance and repeated this procedure 500 times. We then calculated the mean of these

500 variance values and the 95% confidence intervals around the mean. The resulting value for the mean variance (0.9268) and the 95% confidence interval (upper = 0.8644, lower = 0.9891) suggests that the differences we observed above were not due to the small number of mortalities.

Pairwise t-tests for those animals that we collected both live and dead hair samples from revealed that the summer before an animal died, the proportional contributions of both high- and medium-preference forage decreased while the contributions of low-preference forage increased (Table 9, Fig.8). We also found a non-significant trend of increasing aquatic forage in the diet the summer preceding winter mortality (Table 9, Fig.8).

DISCUSSION

Here we report that, in northeast Minnesota, the warmest parts of the moose range are those that offer forage of lesser quality, where moose diets are poorest, and where winter mortality is highest. Moreover, animals that do not survive winter have diets of lower quality compared to those that do, especially during late summer. While warming has been implicated as a potential driver of recent moose declines in Minnesota, our results directly link higher temperatures with negative demographic trends. Collectively, our results suggest that temperature-induced changes to summer diet are, at the very least, a contributing factor to the recent declines observed in this population.

Temperature-induced changes to forage quality are widely documented for large herbivores (Cebrian et al. 2008, Doiron et al. 2014, Lenart et al. 2002). For example, in southeastern Alaska, warmer temperatures during summer led to a decline in crude

protein and digestibility of moose forage (Lenart et al. 2002), while on Seward Peninsula, high temperatures resulted in an influx of high-quality forage for caribou during early spring due to earlier green-up dates (Cebrian et al. 2008). While earlier green-up, could benefit animals experiencing severe nutritional restriction toward the end of winter, more rapid phenology due to warming may lead to decreased nitrogen concentrations in some forage species at the end of summer (Cebrian et al. 2008, Doiron et al. 2014). Throughout the duration of this study, our experience suggests that warmer regions of NEMN may green-up as much as 7 – 10 days earlier than cooler regions, where temperatures during early summer are moderated by Lake Superior. However, a study investigating spatial heterogeneity in the phenology of NEMN would be a useful contribution in efforts to understand how the distribution and abundance of high-quality forage varies for moose and how this might influence spatially explicit demographic rates.

While it is true that only a small amount of variance in total N throughout NEMN is explained by MMST ($R^2 = 0.07$), our intentions for this model were not to predict total N based on MMST, but rather to investigate the strength of this relationship. Considering the range of different variables that are known to influence nitrogen in plants (e.g., slope, Tateno et al. 2004; canopy cover, Zackrisson et al. 2004; soil composition, Côté et al. 2000; precipitation, Yin 1993; salinity, Cheng et al. 2013), the fact that MMST explained more than 7% of this variation is surprising. It is possible that the relationship we identified here is the result of a correlation with some unmeasured variable. Regardless, if our goal was to predict spatial variation in N availability across NEMN, it is likely that MMST would be one of the variables included in the best fitting model (Berini et. al. IN

REVIEW). Heterogeneity in the thermal landscape and its effect on forage quality could lead to spatial variation in the foraging behavior of moose, and ultimately, spatially explicit differences in how animals interact with their environment. These differences, in turn, could relate to factors that influence demographic vital rates (Cook et al. 2004, Robert A. Garrott et al. 2003).

A recent study in NEMN indicated that moose increase their use of aquatic or wetland habitats with increased exposure to high temperatures (Street et al. 2016). That study suggested that use of these habitats could lead to reduced foraging efficiency if the quality of forage is lower than in other habitats (Street et al. 2016). Here, we show that moose in the warmest parts of the range consume greater quantities of aquatic forage throughout the summer. Stable isotopes of nitrogen in herbivore tissues are inversely related to N content of ingested forage (Adams and Sterner 2000), and in our study, moose from warmer regions had higher values of $\delta^{15}N_{hair}$ (i.e., lower dietary N) during late summer, when compared to animals from cooler regions. Interestingly, although our models show that moose in warmer areas are ingesting more aquatic forage, which tends to have higher N content then terrestrial forage (Tischler 2004), they are exhibiting signs of lower dietary N than moose from cooler areas. Moose are intolerant of high temperatures, and if individuals in the warmest parts of the range are becoming heat stressed, it is possible that they are limiting forage intake, which is one of the most common side effects of heat stress in large mammals (Collier and Beede 1985, Renecker and Hudson 1986) . Thus, it may be that moose are consuming the same amount of aquatic forage, but less terrestrial forage, leading to an increase in the proportional

contribution of aquatics to the overall diet. While beyond the scope of what we present here, a study comparing the body fat content of moose during winter to their diet composition during early and late summer could provide valuable insights into this relationship. Additionally, although we did not evaluate the influences of high temperatures on aquatic forage, Peek et al. (1976) suggested that higher water temperatures could lead to a reduction in quality of aquatic forage. Finally, we found that total N availability declines with increasing temperatures across the study region. Together, reduced intake along with reduced forage quality could lead to the relationship we observed here. Regardless, our results show that animals in the warmest parts of the range consume proportionally more aquatics than any other forage group during late summer, and moose with diets dominated by aquatic forage are less likely to survive winter. While aquatic forage is an important part of the moose diet, it is one of many important dietary items required for healthy moose (Belovsky 1978).

While the leading proximate causes of mortality for moose in NEMN have been attributed to predation, parasitic and bacterial infections, and severe malnutrition, these same studies have also noted that temperature and diet likely interact to predispose moose to winter mortality (Carstensen et al. 2015, Lenarz et al. 2010, 2010, Mech and Fieberg 2014, Wünschmann et al. 2015). In this study, moose that died during winter are not only exposed to higher temperatures than those that survived, but also had consistently poorer diets heading into winter. Previous work on elk has shown that body condition at the start of winter is a key determinant for overwinter survival (Cook et al. 2004), and the rate of moose mortality in the warmest parts of the range (68%) was almost 4.5 times higher

than the rate we found in the coolest parts of the range (15%). Additionally, moose that survived winter exhibited dietary shifts throughout the growing season that appear to be important for overwinter survival.

During early summer, moose that survive the following winter are consuming mostly high-preference forage (38% of their total diet), with about a quarter of their diet consisting of aquatics (27%). As summer progresses, the relative contributions of these two dietary elements becomes more equivalent, with aquatic plants making up a little more than a third of the diet (35%) and high-preference forage making up slightly less than a third (31%). Moose that die the following winter are consuming significantly less high-preference forage during early summer (27%, Fig.4a) while also consuming significantly more low-preference forage (17%, Fig.4a), with the contributions of these two elements to the overall diet changing little as summer progresses (Fig.6b). Collectively, our results provide evidence that early-summer diet is important to over winter survival in this population. It also suggests that animals consuming relatively large amounts of aquatic forage throughout the entire summer have poorer nutrition, as exhibited by higher $\delta^{15}N_{hair}$, thereby contributing to higher risk of mortality the following winter. It is possible that moose ingesting more aquatics at the beginning of summer are already experiencing heat stress due to a temporal mismatch between the shedding of the winter coat and the onset of high temperatures (Dou et al. 2013). If this is true, these animals could be at a nutritional disadvantage at the beginning of summer, and potentially fail to acquire critical nutritional stores prior to the end of the growing season and the onset of winter. The results we present here suggest that poor diet increases risk

of mortality, and high temperatures interact with, and even appear to exacerbate this effect.

It is possible that the early to late summer dietary patterns we observed here were due to behavioral predispositions rather than actual changes in behavior from one summer to the next. While hair samples from animals with different winter fates make it possible to evaluate potential correlations between summer diet and winter survival, samples from the same animal but collected before and after their death allow us to evaluate if animals that die during winter are changing their foraging behavior the summer prior to dying. While the number of animals for which we had paired samples for was small (n = 18), during summers that preceded winter mortality, moose decreased their use of medium-preference forage during early summer (Fig.5a). During late summer, these same animals decreased their use of aquatic and high-preference forage the summer prior to their death, but increased their use of low-preference forage (Fig.5b). Moreover, these same individuals exhibited no change in diet throughout the growing season – eating proportionally more aquatic forage than any other forage group throughout the entire summer.

Although the changes in diet we observed could be related to changes in forage availability, this is unlikely for multiple reasons. First, while we show above that MMST influences overall N availability, we did not observe differences within individual forage groups. Second, moose that died during winter came from all three temperature regions, yet show significant differences in their proportional consumption of all preference groups when compared to those that survived, which also come from all three

temperature regions. Finally, by evaluating differences in diet composition for those animals that we have paired hair samples for, we show that animals actually change their foraging behavior the summer prior to their death. Thus, while the small number of mortalities limits our ability to draw robust conclusions, our results suggest that over-winter survival is more likely to be influenced by temperature-induced changes to behavior than spatial variation in the availability of forage.

Although we investigated how high-summer temperatures and diet interact to specifically influence overwinter survival, potential synergies between temperature and diet could have broader impacts than what we investigate here. Prior work has found that small differences (10-20%) in digestible energy (DE) intake during summer-autumn can have substantial implications for fat accretion and growth rates in adults and calves in elk (Cook et al. 2004), and differences of roughly 13% have been reported for DE of aquatic and terrestrial forage (MacCracken et al. 1993). Additionally, previous work has suggested that fertility may be compromised by poor summer-autumn nutrition for moose in NEMN (DelGiudice et al. 2011), and in northwest Minnesota, poor nutrition was associated with pregnancy rates that were consistently below 50% (Murray et al. 2006). If high-summer temperatures are forcing moose to decide between habitats that offer thermal refugia versus those that offer high-quality food, then the thermal environment during mid to late summer may be influencing demographic rates throughout the entire year, especially during winter and early spring. While the results we present here indicate that moose in the warmest parts of their range are consuming more aquatic forage than those from the cooler parts of the range, these animals may simply be eating less

terrestrial forage in response to heat stress. Regardless of the cause, ingesting less terrestrial forage could make it difficult for moose to accrue enough body prior to the onset of winter, thereby increasing risk of over-winter mortality and other negative demographic consequences.

For animals at the southern edge of their geographic range, the detrimental effects of higher temperatures may be pervasive, having a wide range of both direct and indirect influences on demographic rates. During summer, moose experience heat stress between 17 and 24 ºC (McCann et al. 2013), and mean-maximum summer temperatures in NEMN from 1981 to 2010 ranged from roughly 20 to 25 ºC, suggesting that moose in NEMN routinely experience heat stress during summer. While numerous studies have suggested that warming and nutrition likely interact to influence moose declines in Minnesota, a clear link between these variables and demographic rates has not been established. In this study, we provide evidence that high temperatures negatively influence forage quality, foraging behavior, and nutrition, and that the interaction of these factors negatively affects overwinter survival. While moose mortality throughout NEMN has been attributed to a range of different causes, the evidence we present here suggests that high temperatures and diet during summer may, together, be a driver that predisposes moose to predation, disease, and malnutrition, along with other potential causes of winter mortality.

Table 1. Results of generalized linear models evaluating the influence of mean-maximum summer temperature on N availability for individual forage groups and for all groups combined (i.e., total N). Comparisons yielding a statistically significant difference ($p < 0.05$) are identified via italics and an asterisk (*).

forage group	β	df	r^2	*p*
low	-0.6427	68	0.0421	0.0885
medium	-0.1804	68	0.0359	0.1163
high	-0.3927	68	0.0526	0.0562
total N	-0.0288	68	0.0725	*0.0242**

Table 2. Results of Tukey's test for honestly significant differences comparing individual forage groups between temperature regions during late summer. "Comparison" indicates the temperature regions being compared, while "difference" indicates the mean difference between the two temperature regions being compared for the respective preference group. "Upper" and "lower" represent the upper and lower limits of 95% confidence interval of the mean difference. Comparisons yielding a statistically significant difference ($p < 0.05$) are identified via italics and an asterisk (*). All values were truncated to four significant digits.

time period	preference group	comparison	difference	lower	upper	*p*
early summer						
	aquatic					
		mod-cool	0.1525	0.0451	0.2600	*0.0028**
		warm- cool	0.2649	0.0762	0.4537	*0.0032**
		warm-mod	0.1124	-0.0690	0.2938	0.3090
	high					
		mod- cool	-0.0517	-0.1271	0.0237	0.2380
		warm- cool	-0.0965	-0.2290	0.0360	0.1989
		warm-mod	-0.0448	-0.1721	0.0826	0.6827
	medium					
		mod- cool	-0.1184	-0.2092	-0.0277	*0.0068**
		warm- cool	-0.1435	-0.3030	0.0159	*0.0870**
		warm-mod	-0.0251	-0.1784	0.1282	0.9203
	low					
		mod- cool	-0.1051	-0.1829	-0.0272	*0.0049**
		warm- cool	-0.1420	-0.2788	-0.0051	*0.0401**
		warm-mod	-0.0369	-0.1685	0.0946	0.7838
late summer						
	aquatic					
		mod-cool	0.0423	0.0181	0.0664	*0.0001**
		warm- cool	0.0671	0.0261	0.1081	*0.0004**
		warm-mod	0.0248	-0.0144	0.0641	0.2955
	high					

	mod- cool	-0.0110	-0.0205	-0.0015	*0.0186**
	warm- cool	-0.0232	-0.0393	-0.0071	*0.0025**
	warm-mod	-0.0122	-0.0276	0.0033	0.1516
medium					
	mod- cool	-0.0196	-0.0348	-0.0043	*0.0080**
	warm- cool	-0.0253	-0.0512	0.0006	0.0572
	warm-mod	-0.0057	-0.0305	0.0191	0.8484
low					
	mod- cool	-0.0379	-0.0574	-0.0184	*< 0.0001**
	warm- cool	-0.0586	-0.0917	-0.0255	*0.0001**
	warm-mod	-0.0207	-0.0525	0.0110	0.2712

Table 3. Variance in δ13C values for different temperature regions and results of Bartlett's test for homogeneity of variance comparing these values. Comparisons yielding a statistically significant difference ($p < 0.05$) are identified via italics and an asterisk (*).

	variance			Bartlett's test		
period	cool	moderate	warm	df	Bartlett's K^2	*p*
early summer	0.1183	0.7509	0.3421	2	99.6650	*< 0.0001**
late summer	0.4480	0.3379	0.3269	2	1.1742	0.5559

Table 4. Results of Tukey's test for honestly significant differences comparing of mean values of δ15Nhair between different temperature regions for early and late summer. "Comparison" indicates the temperature regions being compared, while "difference" indicates the mean difference between the two temperature regions being compared for the respective preference group. "Upper" and "lower" represent the upper and lower limits of 95% confidence interval of the mean difference. Comparisons yielding a statistically significant difference ($p < 0.05$) are identified via italics and an asterisk (*). All values were truncated to four significant digits.

summer period	comparison	difference	lower	upper	*p*
early					
	mod-cool	0.4903	-0.0360	1.0168	0.0734
	warm- cool	0.2644	-0.6648	1.1938	0.7783
	warm-mod	-0.2258	-1.1211	0.6694	0.8211
late					
	mod-cool	0.6488	0.1195	1.1781	*0.0119**
	warm-cool	0.5423	-0.3608	1.4454	0.3316
	warm-mod	-0.1065	-0.9704	0.7572	0.9539

Table 5. Results of logistic regressions detailing the influence of each forage group on the probability of overwinter survival. Odds ratios < 1 indicate a negative effect of that forage group on survival, while an odds ratio > 1 indicates a positive effect on winter survival. Comparisons yielding a statistically significant difference ($p < 0.05$) are identified via italics and an asterisk (*).

summer period	forage group	odds ratios	z	p
early				
	aquatics	3.6773	-1.5690	0.1170
	high	1.9758	3.7260	*< 0.0001**
	medium	3.8050	3.3230	*0.0008**
	low	-3.8171	-1.9760	*0.0482**
late				
	aquatics	3.5286	-0.1620	0.8720
	high	0.0685	4.8430	*< 0.0001**
	medium	3.5800	1.5310	0.1260
	low	-3.6518	2.7000	*0.0069**

Table 6. Results of pairwise logistic regressions comparing diets of the same animals before and after death. Odds ratios < 1 indicate a negative effect of that forage group on survival, while an odds ratio > 1 indicates a positive effect on winter survival. Comparisons yielding a statistically significant difference ($p < 0.05$) are identified via italics and an asterisk (*).

summer period	forage group	odds ratios	z	p
early				
	aquatics	1.0003	0.8080	0.4190
	high	$2.8180 \cdot 10^{-6}$	0.0010	0.9990
	medium	0.9229	2.3560	*0.0185**
	low	$3.9219 \cdot 10^{-5}$	-1.2540	0.2100
late				
	aquatics	0.6847	2.7730	*0.0055**
	high	0.4631	3.1790	*0.0014**
	medium	0.0057	-1.8930	0.0583
	low	-0.8619	-2.6870	*0.0072**

Table 7. Results of univariate ANOVAs comparing the dietary contributions of individual forage groups as a function of season, for animals that survived winter and those that died.

		early summer		late summer			
winter fate	forage group	mean (%)	sd	mean (%)	sd	F	p
alive							
	aquatics	27.9	0.08	34.5	0.02	117.500	*< 0.0001**
	high	38.5	0.03	31.0	0.01	193.100	*< 0.0001**
	medium	22.5	0.03	13.1	0.01	796.500	*< 0.0001**
	low	10.9	0.01	21.0	0.01	1687.000	*< 0.0001**
dead							
	aquatics	38.0	0.28	40.2	0.25	1.015	0.3170
	high	27.0	0.12	24.9	0.09	0.042	0.8390
	medium	17.3	0.09	14.6	0.06	0.267	0.1590
	low	17.4	0.09	20.1	0.09	2.100	0.2300

Table 8. Variance in δ13Chair values for animals with different winter fates, for both early and late summer and results of Bartlett's test for homogeneity of variance comparing these values. Comparisons yielding a statistically significant difference ($p < 0.05$) are identified via italics and an asterisk (*).

	variance		Bartlett's test		
period	alive	dead	df	Bartlett's K^2	*p*
early summer	0.5189	2.7467	1	45.034	*< 0.0001**
late summer	0.4415	13.2210	1	195.520	*< 0.0001**

Table 9. Results of pairwise t-tests for comparing differences between early and late summer diet for those animals that we collected both live and dead hair samples. The column entitled "mean difference" represents the mean difference between early and late summer, and statistical significance for each test is identified via italics and asterisk (*).

	mean difference (%)				
forage group	alive	dead	df	t	p
aquatic	-8.88	-5.08	18	-1.9471	0.0673
high	8.11	3.97	18	9.5419	*< 0.0001**
medium	10.97	3.91	18	6.7522	*< 0.0001**
low	-10.20	-2.79	18	-6.3695	*< 0.0001**

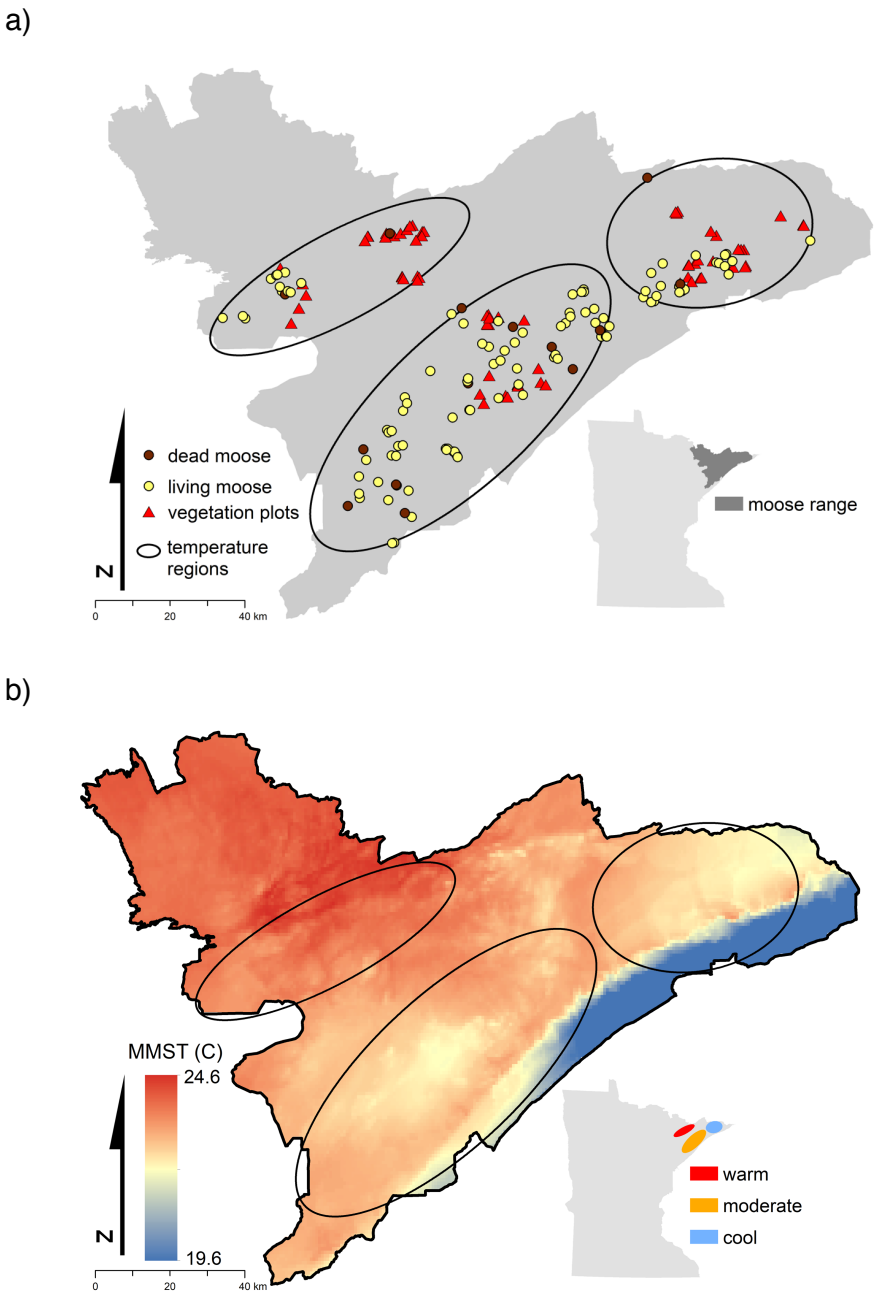

Fig.1. Sampling locations of vegetation and hair throughout the moose range of NEMN (a) and thermal landscape as depicted by mean-maximum summer temperature (JJA) from 1981-2010 (PRISM Climate Group 2017) with temperature regions (b). All sampling plots and moose hair were categorized into one of three different temperature regions (inset map, panel b) based on their location within the thermal landscape.

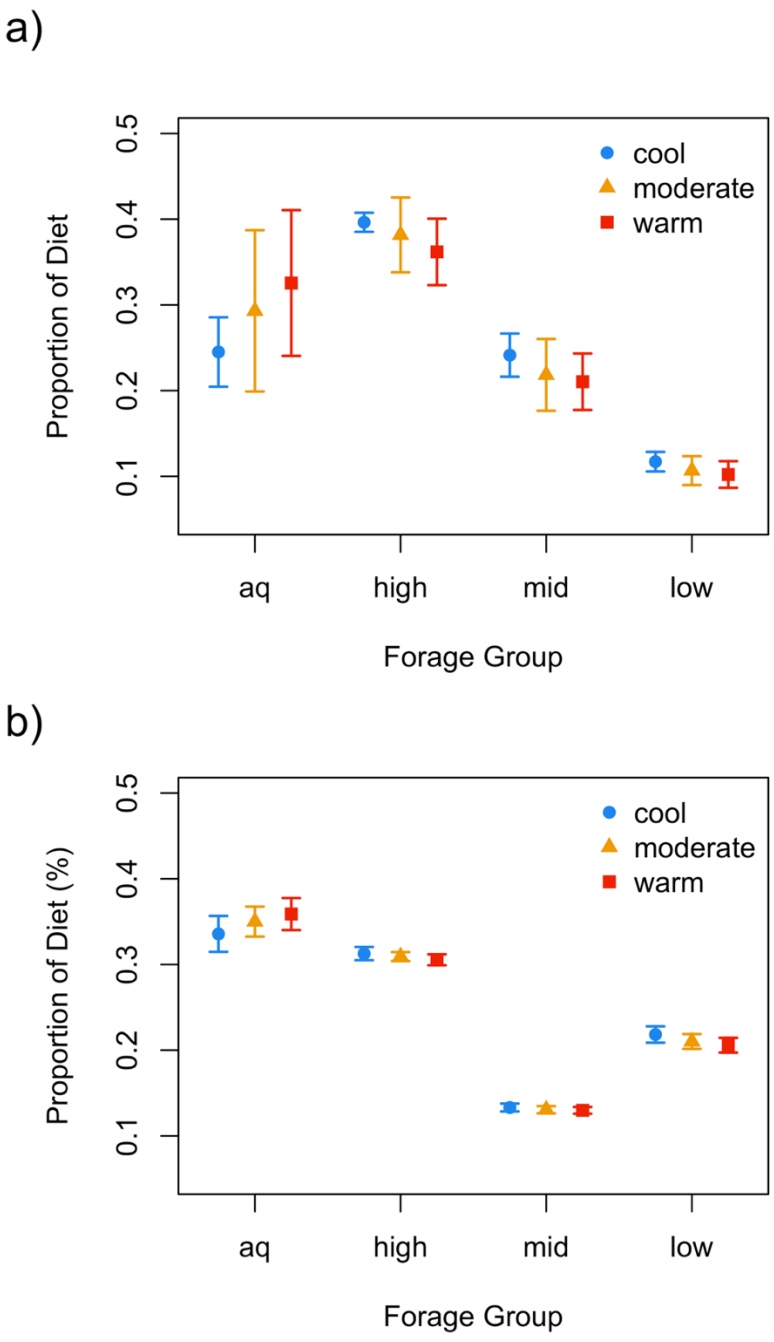

Fig.2. Variation in moose diets as a function of temperature region during both early (a) and late summer (b). MANOVA results suggest that diet composition does not vary by temperature region during early summer, but does during late summer. Points represent mean and bars ± one standard error.

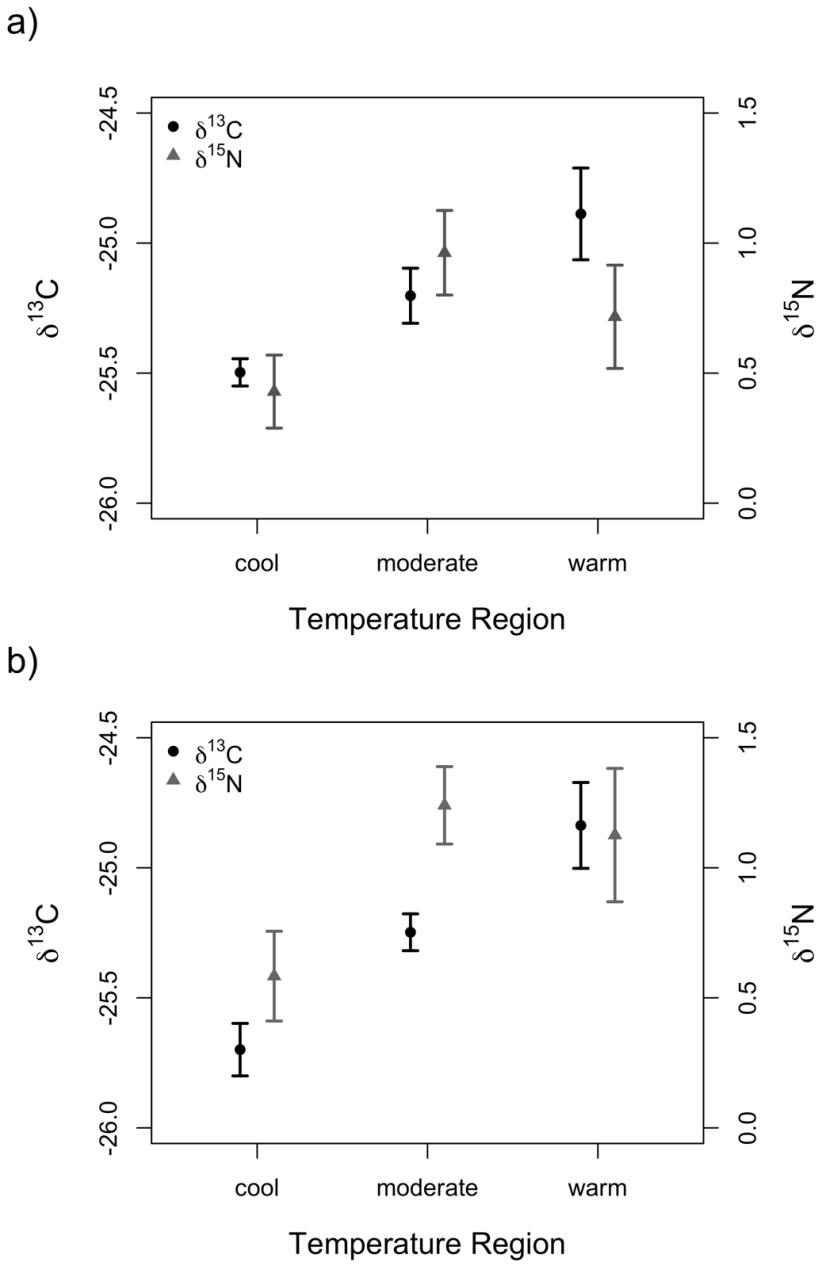

Fig.3. Mean and variance for values of δ13Chair and δ15Nhair across each temperature region for early (a) and late summer (b). Greater variance in values of $\delta^{13}C_{hair}$ suggests greater dietary breadth, while higher mean values of $\delta^{15}N_{hair}$ represent greater nitrogen limitation. Points represent mean values while error bars represent ± one standard deviation.

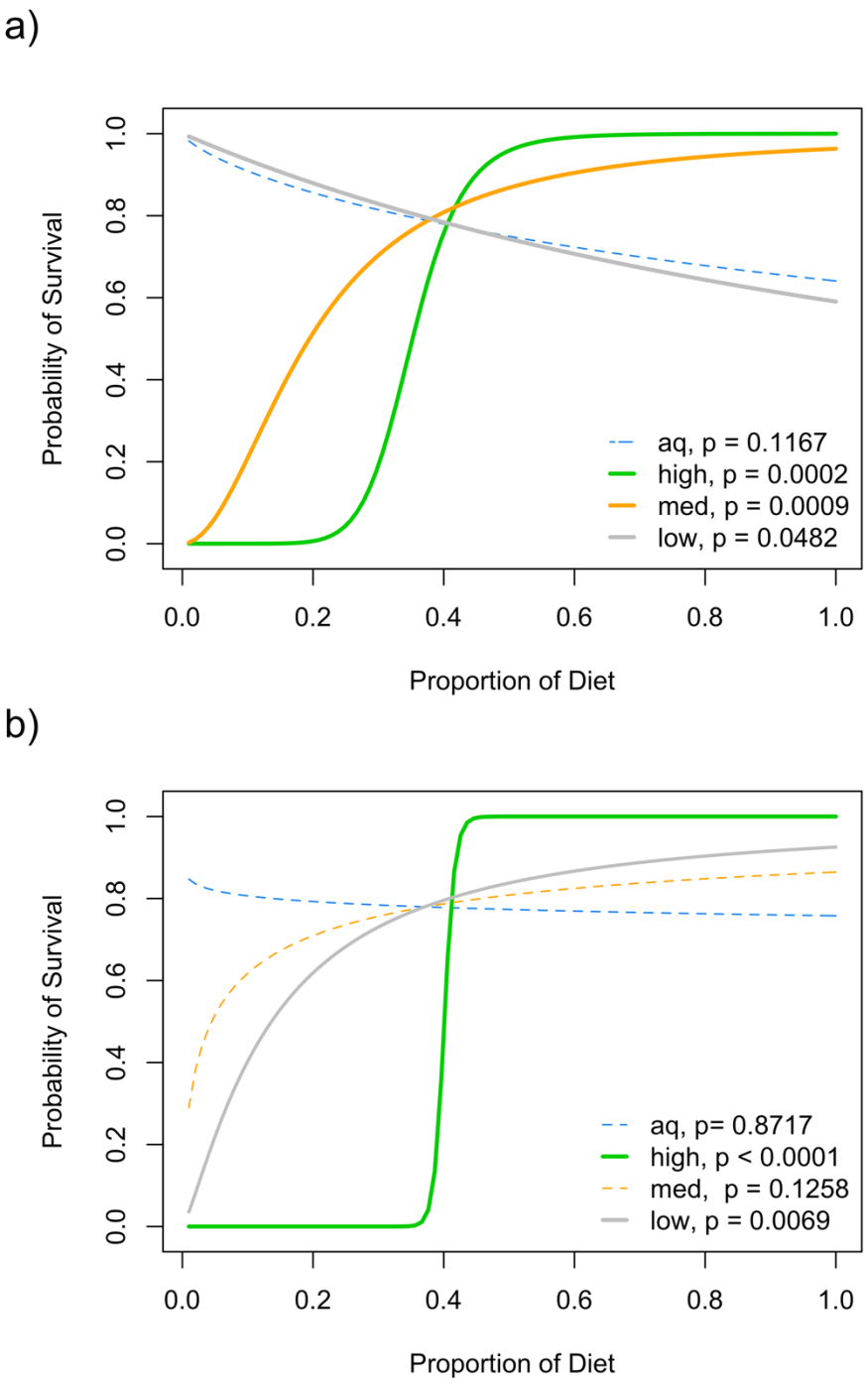

Fig.4. Results of logistic regressions evaluating how consumption of different dietary groups varies between animals that survived winter and those that did not, for both early (a) and late summer (b). Weighted lines identify significant changes ($p < 0.05$) in consumption as a function of winter mortality, while lighter, dashed lines indicate no significant relationship.

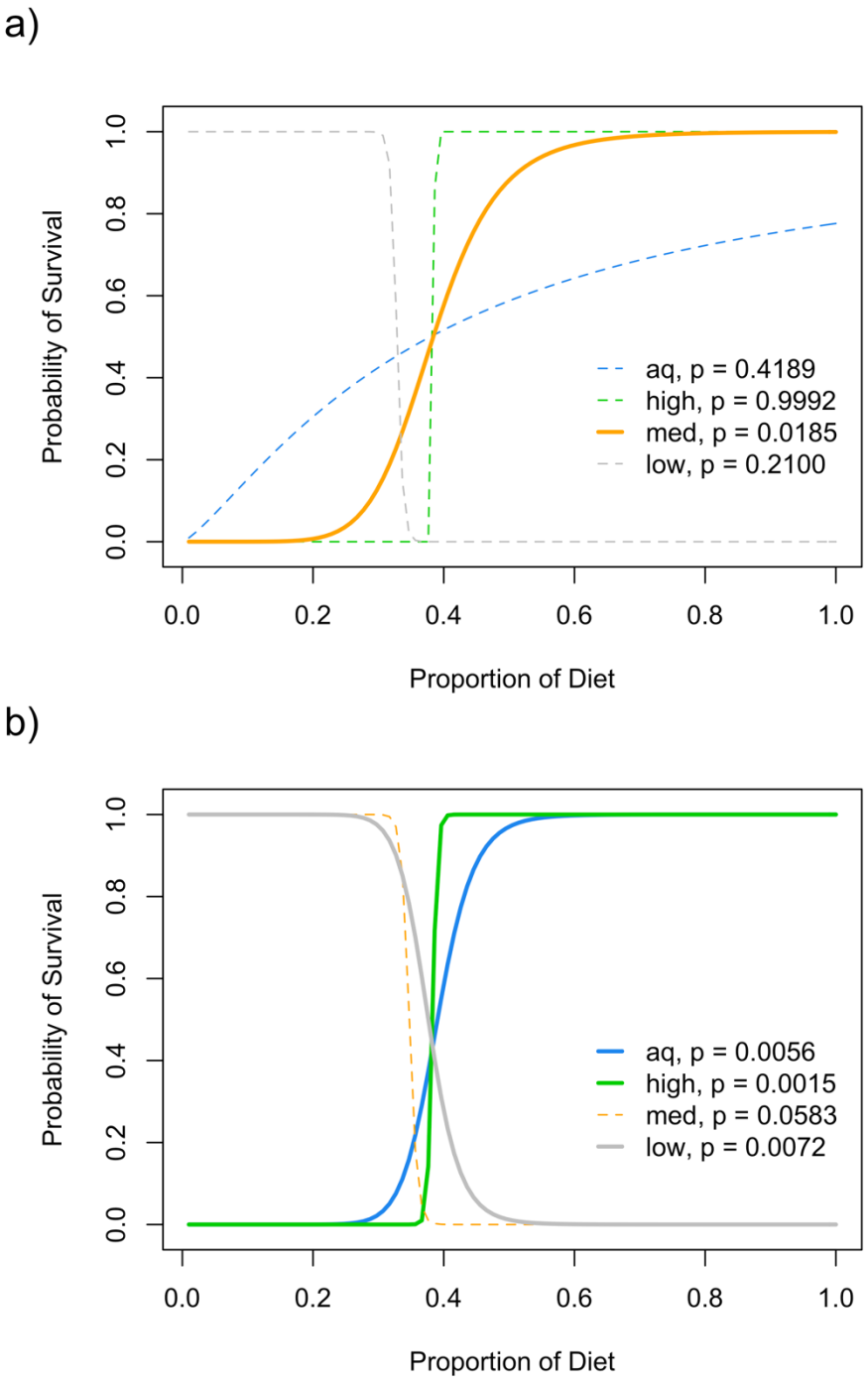

Fig.5. Results of pairwise logistic regressions for those animals that we collected both live and dead hair samples from, comparing diets before and after death, for early (a) and late summer (b). Weighted, solid lines identify significant changes ($p < 0.05$) in consumption as a function of winter mortality, while lighter, dashed lines indicate no significant relationship.

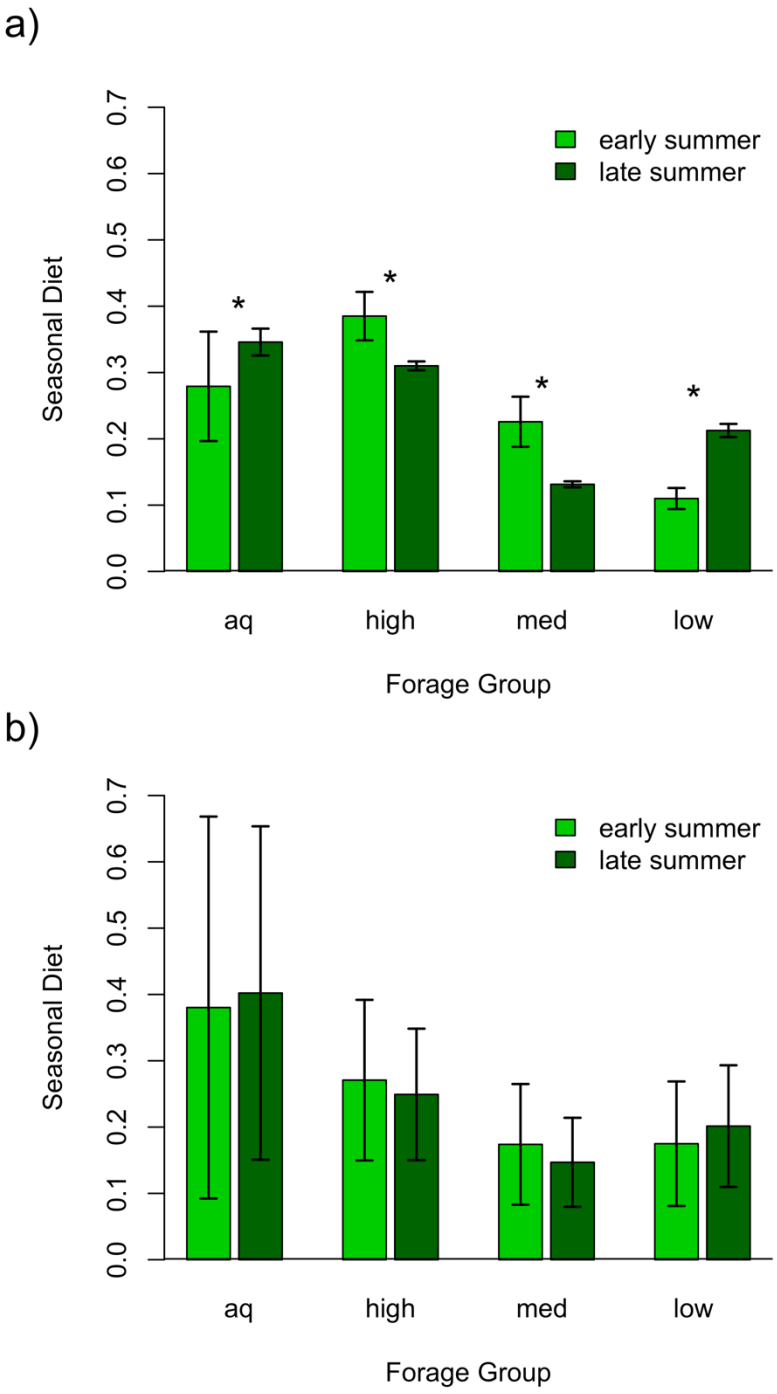

Fig.6. Bar plots representing seasonal shifts in diet for animals that survived winter (a) and those that died (b). Error bars represent ± 1 standard deviation, while bars represent the mean value. Astrices (*) represent statistically significant differences ($p < 0.05$) between the mean values of individual forage groups for early and late-summer.

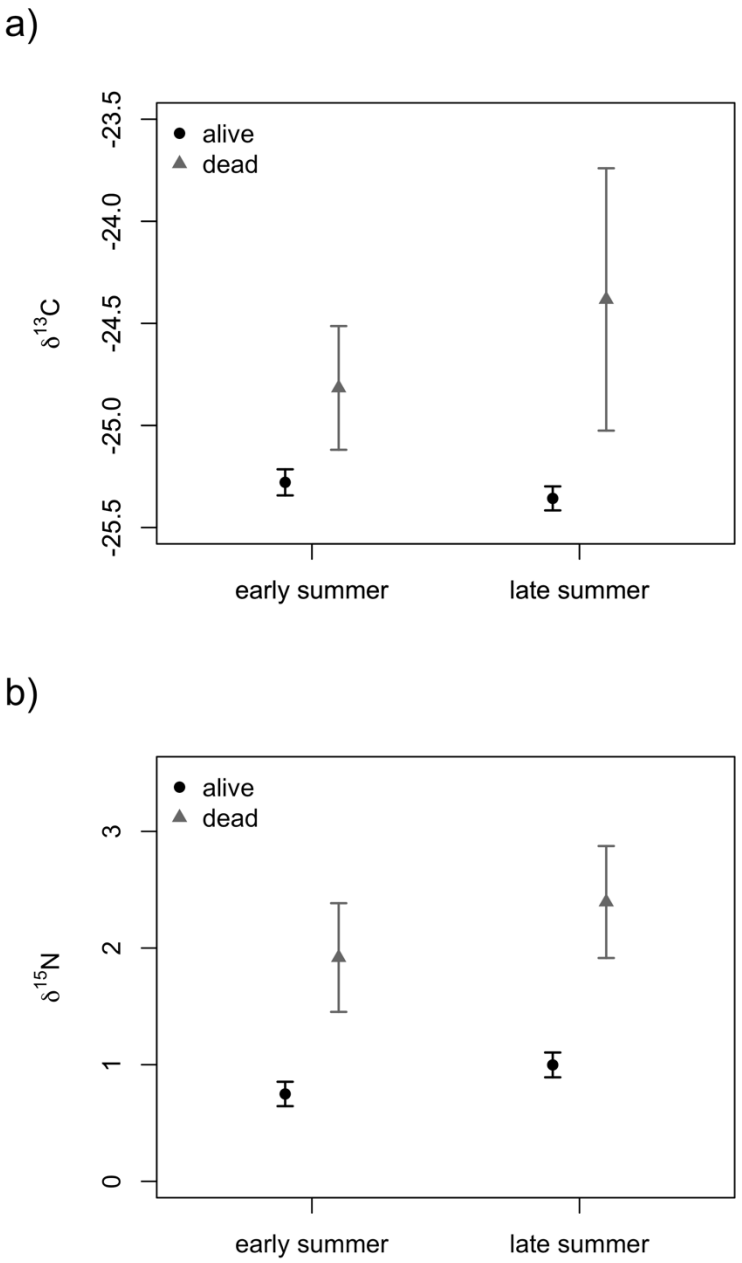

Fig.7. Mean and variance for values of δ13Chair (a) and δ15Nhair (b). Greater variance in values of $\delta^{13}C_{hair}$ suggests greater dietary breadth, while higher mean values of $\delta^{15}N_{hair}$ represent greater nitrogen limitation. Points represent mean values while error bars represent ± one standard deviation.

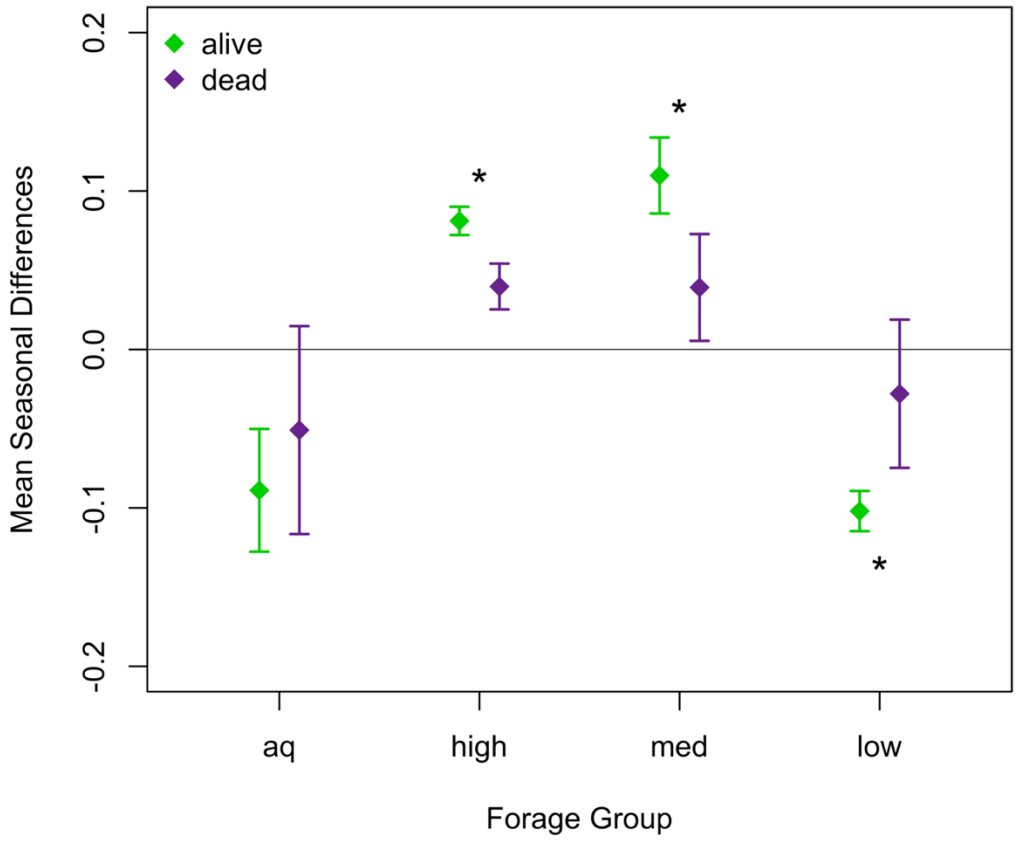

Fig.8. Mean differences in seasonal diet for those animals that we collected both live and dead hair samples from. Points represent mean difference between early and late summer diet while bars represent ± 1 standard deviation. Values below zero indicate greater proportional contributions during late summer, while values above zero indicate greater contributions of individual forage groups during early summer. Substantial overlap between paired, alive-dead error bars (i.e., aquatic) suggests no change in the contribution of that forage group during summers preceding winter survival and summers preceding winter mortality. Statistically significant differences ($p < 0.05$) are represented by an asterisk (*).

Literature Cited

ACIA. 2004. Impacts of a warming Arctic-Arctic climate impact assessment. Impacts of a Warming Arctic-Arctic Climate Impact Assessment, by Arctic Climate Impact Assessment, pp. 144. ISBN 0521617782. Cambridge, UK: Cambridge University Press, December 2004. 144.

Adams, T. S., and R. W. Sterner. 2000. The effect of dietary nitrogen content on trophic level 15N enrichment. Limnology and Oceanography 45: 601–607.

Albon, S. D., and R. Langvatn. 1992. Plant phenology and the benefits of migration in a temperate ungulate. Oikos 502–513.

Alexander, L. V., X. Zhang, T. C. Peterson, J. Caesar, B. Gleason, A. M. G. Klein Tank, M. Haylock, D. Collins, B. Trewin, F. Rahimzadeh, A. Tagipour, K. Rupa Kumar, J. Revadekar, G. Griffiths, L. Vincent, D. B. Stephenson, J. Burn, E. Aguilar, M. Brunet, M. Taylor, M. New, P. Zhai, M. Rusticucci, and J. L. Vazquez-Aguirre. 2006. Global observed changes in daily climate extremes of temperature and precipitation. J. Geophys. Res. 111: D05109.

Alsamamra, H., J. A. Ruiz-Arias, D. Pozo-Vázquez, and J. Tovar-Pescador. 2009. A comparative study of ordinary and residual kriging techniques for mapping global solar radiation over southern Spain. Agricultural and Forest Meteorology 149: 1343–1357.

Ambrose, S. H. 1991. Effects of diet, climate and physiology on nitrogen isotope abundances in terrestrial foodwebs. Journal of Archaeological Science 18: 293–317.

Anderson, M. J. 2001. A new method for non-parametric multivariate analysis of variance. Austral Ecology 26: 32–46.

Angerbjörn, A., P. Hersteinsson, K. Lidén, and E. Nelson. 1994. Dietary variation in arctic foxes (Alopex lagopus)-an analysis of stable carbon isotopes. Oecologia 99: 226–232.

Aublet, J.-F., M. Festa-Bianchet, D. Bergero, and B. Bassano. 2009. Temperature constraints on foraging behaviour of male Alpine ibex (*Capra ibex*) in summer. Oecologia 159: 237–247.

Barboza, P. S., and K. L. Parker. 2008. Allocating Protein to Reproduction in Arctic Reindeer and Caribou. Physiological and Biochemical Zoology 81: 835–855.

Barrett, M., A. Belward, S. Bladen, T. Breeze, N. Burgess, S. Butchart, H. Clewclow, S. Cornell, A. Cottam, and S. Croft. 2018. Living Planet Report 2018: Aiming Higher.

Bates, D., M. Maechler, B. Bolker, and S. Walker. 2015. Fitting linear mixed-effects models using lme4. Journal of Statistical Software 67: 1–48.

Belovsky, G. E. 1978. Diet optimization in a generalist herbivore: The moose. Theoretical Population Biology 14: 105–134.

Bennett, R. N., and R. M. Wallsgrove. 1994. Secondary metabolites in plant defence mechanisms. New Phytologist 127: 617–633.

Benton, H. P., E. J. Want, and T. M. Ebbels. 2010. Correction of mass calibration gaps in liquid chromatography–mass spectrometry metabolomics data. Bioinformatics 26: 2488–2489.

Berg, T. B. 2003. Catechin content and consumption ratio of the collared lemming. Oecologia 135: 242–249.

Berger, J. 1997. Population constraints associated with the use of black rhinos as an umbrella species for desert herbivores. Conservation Biology 11: 69–78.

Berini, J. L., and C. Badgley. 2017. Diet segregation in American bison (*Bison bison*) of Yellowstone National Park (Wyoming, USA). BMC Ecology 17: 27.

Bidart-Bouzat, M. G., and A. Imeh-Nathaniel. 2008. Global change effects on plant chemical defenses against insect herbivores. Journal of Integrative Plant Biology 50: 1339–1354.

Bivand, R. S., E. J. Pebesma, and V. Gomez-Rubio. 2013. Applied spatial data analysis with R, 2nd ed. Springer, New York.

Bivand, R., T. Keitt, and B. Rowlingson. 2018. rgdal: bindings for the "geospatial" data abstraction library.

Bonham-Smith, P. C., M. Kapoor, and J. D. Bewley. 1987. Establishment of thermotolerance in maize by exposure to stresses other than a heat shock does not require heat shock protein synthesis. Plant Physiology 85: 575–580.

Bowen, G. J. 2010. Isoscapes: spatial pattern in isotopic biogeochemistry. Annual Review of Earth and Planetary Sciences 38: 161–187.

Bowen, G. J., and B. Wilkinson. 2002. Spatial distribution of δ18O in meteoric precipitation. Geology 30: 315–318.

Bowen, G. J., and J. Revenaugh. 2003. Interpolating the isotopic composition of modern meteoric precipitation. Water Resources Research 39.

Bray, E. A., J. Bailey-Serres, and E. Weretilnyk. 2000. Responses to abiotic stresses. Biochemistry and Molecular Biology of Plants 1158: e1203.

Britton, K., V. Grimes, J. Dau, and M. P. Richards. 2009. Reconstructing faunal migrations using intra-tooth sampling and strontium and oxygen isotope analyses: a case study of modern caribou *(Rangifer tarandus granti*). Journal of Archaeological Science 36: 1163–1172.

Brooks, S. P., and A. Gelman. 1998. General methods for monitoring convergence of iterative simulations. Journal of Computational and Graphical Statistics 7: 434–455.

Bryant, J. P., F. S. Chapin, and D. R. Klein. 1983. Carbon/nutrient balance of boreal plants in relation to vertebrate herbivory. Oikos 40: 357–368.

Bukovinszky, T., F. F. van Veen, Y. Jongema, and M. Dicke. 2008. Direct and indirect effects of resource quality on food web structure. Science 319: 804–807.

Canham, C. D., J. S. Denslow, W. J. Platt, J. R. Runkle, T. A. Spies, and P. S. White. 1990. Light regimes beneath closed canopies and tree-fall gaps in temperate and tropical forests. Canadian Journal of Forest Research 20: 620–631.

Carstensen, M., E. C. Hildebrand, D. Plattner, M. H. Dexter, C. Jennelle, and R. G. Wright. 2015. Determining cause-specific mortality of adult moose in northeast Minnesota. Summaries of wildlife research findings. St. Paul: Minnesota Department of Natural Resources 161: 71.

Castro, J., R. Zamora, J. A. Hódar, and J. M. Gómez. 2004. Seedling establishment of a boreal tree species (Pinus sylvestris) at its southernmost distribution limit:

consequences of being in a marginal Mediterranean habitat. Journal of Ecology 92: 266–277.

Ceballos, G., P. R. Ehrlich, and R. Dirzo. 2017. Biological annihilation via the ongoing sixth mass extinction signaled by vertebrate population losses and declines. Proceedings of the National Academy of Sciences 114: E6089–E6096.

Cebrian, M. R., K. Kielland, and G. Finstad. 2008. Forage quality and reindeer productivity: multiplier effects amplified by climate change. Arctic, Antarctic, and Alpine Research 40: 48–54.

Cerling, T. E., G. Wittemyer, H. B. Rasmussen, F. Vollrath, C. E. Cerling, T. J. Robinson, and I. Douglas-Hamilton. 2006. Stable isotopes in elephant hair document migration patterns and diet changes. Proceedings of the National Academy of Sciences 103: 371–373.

Cerling, T., and J. Harris. 1999. Carbon isotope fractionation between diet and bioapatite in ungulate mammals and implications for ecological and paleoecological studies. Oecologia 120: 347–363.

Chan-McLeod, A. C. A., R. G. White, and D. E. Russell. 2000. Comparative body composition strategies of breeding and nonbreeding female caribou. Canadian Journal of Zoology 77: 1901–1907.

Cheesman, A. W., and L. A. Cernusak. 2016. Isoscapes: a new dimension in community ecology. Tree Physiology 36: 1456–1459.

Chenaux-Ibrahim, Y. 2015. Seasonal diet composition of gray wolves (*Canis lupus*) in northeastern Minnesota determined by scat analysis. Ph.D. Dissertation. University of Minnesota, Duluth.

Cheng, D., K. Vrieling, and P. G. Klinkhamer. 2011. The effect of hybridization on secondary metabolites and herbivore resistance: implications for the evolution of chemical diversity in plants. Phytochemistry Reviews 10: 107–117.

Cheng, Y., J. Wang, B. Mary, J. Zhang, Z. Cai, and S. X. Chang. 2013. Soil pH has contrasting effects on gross and net nitrogen mineralizations in adjacent forest and grassland soils in central Alberta, Canada. Soil Biology and Biochemistry 57: 848–857.

Cloutier, Y., and C. J. Andrews. 1984. Efficiency of cold hardiness induction by desiccation stress in four winter cereals. Plant Physiology 76: 595–598.

Collier, R. J., and D. K. Beede. 1985. Thermal stress as a factor associated with nutrient requirements and interrelationships. Nutrition of grazing ruminants in warm climates 59–71.

Constable, J., M. E. Litvak, J. P. Greenberg, R. K. Monson, and others. 1999. Monoterpene emission from coniferous trees in response to elevated CO_2 concentration and climate warming. Global Change Biology 5: 252–267.

Cook, J. G., B. K. Johnson, R. C. Cook, R. A. Riggs, T. I. M. Delcurto, L. D. Bryant, and L. L. Irwin. 2004. Effects of summer-autumn nutrition and parturition date on reproduction and survival of elk. Wildlife Monographs 155: 1–61.

Côté, L., S. Brown, D. Paré, J. Fyles, and J. Bauhus. 2000. Dynamics of carbon and nitrogen mineralization in relation to stand type, stand age and soil texture in the boreal mixedwood. Soil Biology and Biochemistry 32: 1079–1090.

Craig, H. 1953. The geochemistry of the stable carbon isotopes. Geochimica et Cosmochimica Acta 3: 53–92.

Craig, H. 1954. Carbon 13 in plants and the relationships between carbon 13 and carbon 14 variations in nature. The Journal of Geology 62: 115–149.

Craufurd, P. Q., and J. M. Peacock. 1993. Effect of heat and drought stress on sorghum (*Sorghum bicolor*). II. Grain yield. Experimental Agriculture .

Crews, B., W. R. Wikoff, G. J. Patti, H.-K. Woo, E. Kalisiak, J. Heideker, and G. Siuzdak. 2009. Variability analysis of human plasma and cerebral spinal fluid reveals statistical significance of changes in mass spectrometry-based metabolomics data. Analytical Chemistry 81: 8538–8544.

Dale, V. H., L. A. Joyce, S. McNulty, R. P. Neilson, M. P. Ayres, M. D. Flannigan, P. J. Hanson, L. C. Irland, A. E. Lugo, C. J. Peterson, and others. 2001. Climate change and forest disturbances. BioScience 51: 723–734.

Dall, S. R. X., L.-A. Giraldeau, O. Olsson, J. M. McNamara, and D. W. Stephens. 2005. Information and its use by animals in evolutionary ecology. Trends in Ecology & Evolution 20: 187–193.

Danell, K., R. Gref, and R. Yazdani. 1990. Effects of mono- and diterpenes in scots pine needles on moose browsing. Scandinavian Journal of Forest Research 5: 535–539.

DelGiudice, G. 2018. 2018 aerial moose survey. Minnesota Department of Natural Resources, St. Paul.

DelGiudice, G. D., B. A. Sampson, M. S. Lenarz, M. W. Schrage, and A. J. Edwards. 2011. Winter body condition of moose (*Alces alces*) in a declining population in northeastern Minnesota. Journal of Wildlife Diseases 47: 30–40.

DelGiudice, G. D., W. J. Severud, and T. R. Obermoller. 2017. Climate change, winter nutritional restriction, and the decline of moose in northeastern Minnesota, winters 2013-2017. Minnesota Department of Natural Resources, St. Paul, MN.

DeLucia, E. H., P. D. Nabity, J. A. Zavala, and M. R. Berenbaum. 2012. Climate change: resetting plant-insect interactions. Plant Physiology 160: 1677–1685.

Deniro, M., and S. Epstein. 1978. Influence of diet on the distribution of carbon isotopes in animals. Geochimica et Cosmochimica Acta 42: 495–506.

Dicke, M., R. Gols, and E. H. Poelman. 2012. Dynamics of plant secondary metabolites and consequences for food chains and community dynamics. The Ecology of Plant Secondary Metabolites: From Genes to Global Processes 308.

Dixon, P. M., L. Wu, M. P. Widrlechner, and E. S. Wurtele. 2009. Weighted distance measures for metabolomic data. Ames, IA ; 1–8.

Doiron, M., G. Gauthier, and E. Lévesque. 2014. Effects of experimental warming on nitrogen concentration and biomass of forage plants for an arctic herbivore. Journal of Ecology 102: 508–517.

Dou, H., G. Jiang, P. Stott, and R. Piao. 2013. Climate change impacts population dynamics and distribution shift of moose (*Alces alces*) in Heilongjiang Province of China. Ecological Research 28: 625–632.

Drucker, D. G., K. A. Hobson, J. P. Ouellet, and R. Courtois. 2010. Influence of forage preferences and habitat use on 13C and 15N abundance in wild caribou (*Rangifer tarandus caribou*) and moose (*Alces alces*) from Canada. Isotopes in Environmental and Health Studies 46: 107–121.

Dudt, J. F., and D. J. Shure. 1994. The influence of light and nutrients on foliar phenolics and insect herbivory. Ecology 75: 86–98.

Dyer, L. A., C. D. Dodson, J. O. Stireman Iii, M. A. Tobler, A. M. Smilanich, R. M. Fincher, and D. K. Letourneau. 2003. Synergistic effects of three Piper amides on generalist and specialist herbivores. Journal of Chemical Ecology 29: 2499–2514.

Engelmark, O. 1999. Boreal forest disturbances. Ecosystems of the World 161–186.

EPA. 2016. What climate change means for Minnesota. Environmental Protection Agency.

ESRI. 2011. ArcGIS 10.3.1. ESRI, Redlands, CA.

Faraway, J. J. 2016. Extending the linear model with R: generalized linear, mixed effects and nonparametric regression models, second edition. CRC Press, Boca Raton.

Farmer, E. E. 2001. Surface-to-air signals. Nature 411: 854–856.

Forbey, J., and M. D. Hunter. 2012. The herbivore's prescription: a pharm-ecological perspective on host-plant use by vertebrate and invertebrate herbivores in The

Ecology of Plant Secondary Metabolites: From Genes to Global Processes. Cambridge University Press, New York.

Fox, A. D., K. A. Hobson, and J. Kahlert. 2009. Isotopic evidence for endogenous protein contributions to greylag goose *Anser anser* flight feathers. Journal of Avian Biology 40: 108–112.

Franzmann, A. W., A. Flynn, and P. D. Arneson. 1975. Levels of some mineral elements in Alaskan moose hair. The Journal of Wildlife Management 374–378.

Frelich, L. E. 2002. Forest dynamics and disturbance regimes: studies from temperate evergreen-deciduous forests. Cambridge University Press, New York.

Frye, G. G., J. W. Connelly, D. D. Musil, and J. S. Forbey. 2013. Phytochemistry predicts habitat selection by an avian herbivore at multiple spatial scales. Ecology 94: 308–314.

Garcia, R. A., M. Cabeza, C. Rahbek, and M. B. Araújo. 2014. Multiple dimensions of climate change and their implications for biodiversity. Science 344: 1247579.

Garrott, Robert A, L. L. Eberhardt, P. J. White, and J. Rotella. 2003. Climate-induced variation in vital rates of an unharvested large-herbivore population. Canadian Journal of Zoology 81: 33–45.

Garrott, Robert A., L. L. Eberhardt, P. J. White, and J. Rotella. 2003. Climate-induced variation in vital rates of an unharvested large-herbivore population. Canadian Journal of Zoology 81: 33–45.

Garten, C. T., and G. E. Taylor. 1992. Foliar $\delta^{13}C$ within a temperate deciduous forest: spatial, temporal, and species sources of variation. Oecologia 90: 1–7.

Gerlich, M., and S. Neumann. 2013. MetFusion: Integration of compound identification strategies. Journal of Mass Spectrometry 48: 291–298.

Gershenzon, J. 1984. Changes in the levels of plant secondary metabolites under water and nutrient stress in Phytochemical Adaptations to Stress. Springer, New York.

Gershenzon, J., A. Fontana, M. Burow, U. T. E. Wittstock, and J. Degenhardt. 2012. Mixtures of plant secondary metabolites: metabolic origins and ecological benefits in The Ecology of Plant Secondary Metabolites: From Genes to Global Processes. Cambridge University Press, New York.

Gershenzon, J., and R. Croteau. 1992. Terpenoids in Herbivores: Their Interactions With Secondary Plant Metabolites, 2nd ed, Vol. 1: The Chemical Participants. Academic Press, Cambridge.

Gillespie, D. R., A. Nasreen, C. E. Moffat, P. Clarke, and B. D. Roitberg. 2012. Effects of simulated heat waves on an experimental community of pepper plants, green peach aphids and two parasitoid species. Oikos 121: 149–159.

Gillooly, J. F., J. H. Brown, G. B. West, V. M. Savage, and E. L. Charnov. 2001. Effects of size and temperature on metabolic rate. Science 293: 2248–2251.

Gleadow, R. M., and I. E. Woodrow. 2002. Defense chemistry of cyanogenic Eucalyptus cladocalyx seedlings is affected by water supply. Tree Physiology 22: 939–945.

Harborne, J. B. 1987. Chemical signals in the ecosystem. Annals of Botany 60: 39–57.

Harrell, F. E., and C. D. Dupont. 2018. Hmisc: Harrell Miscellaneous.

Hart, E. M., and K. Bell. 2015. prism: Download data from the Oregon prism project.

Heinselman, M. L. 1996. The boundary waters wilderness ecosystem. University of Minnesota Press, St. Paul.

Hellmann, C., K. G. Rascher, J. Oldeland, and C. Werner. 2016. Isoscapes resolve species-specific spatial patterns in plant–plant interactions in an invaded Mediterranean dune ecosystem. Tree Physiology 36: 1460–1470.

Henaux, V., L. A. Powell, K. A. Hobson, C. K. Nielsen, and M. A. LaRue. 2011. Tracking large carnivore dispersal using isotopic clues in claws: an application to cougars across the Great Plains. Methods in Ecology and Evolution 2: 489–499.

Hetem, R. S., A. Fuller, S. K. Maloney, and D. Mitchell. 2014. Responses of large mammals to climate change. Temperature 1: 115–127.

Hiemstra, P. H., E. J. Pebesma, C. J. Twenhöfel, and G. B. Heuvelink. 2009. Real-time automatic interpolation of ambient gamma dose rates from the Dutch radioactivity monitoring network. Computers & Geosciences 35: 1711–1721.

Hijmans, R. J. 2019. raster: Geographic data analysis and modeling.

Hirt, H., and K. Shinozaki. 2003. Plant responses to abiotic stress. Springer Science & Business Media.

Hurrell, J. W. 1995. Decadal trends in the North Atlantic Oscillation: regional temperatures and precipitation. Science 269: 676–679.

Iason, G. R., J. J. Lennon, R. J. Pakeman, V. Thoss, J. K. Beaton, D. A. Sim, and D. A. Elston. 2005. Does chemical composition of individual Scots pine trees determine the biodiversity of their associated ground vegetation? Ecology Letters 8: 364–369.

Ikeda, T., F. Matsumura, and D. M. Benjamin. 1977. Mechanism of feeding discrimination between matured and juvenile foliage by two species of pine sawflies. J Chem Ecol 3: 677–694.

Inderjit, J. L. Pollock, R. M. Callaway, and W. Holben. 2008. Phytotoxic effects of (±)-catechin in vitro, in soil, and in the field. PLoS ONE 3: e2536.

IPCC. 2007. Intergovernmental Panel on Climate Change, Climate Change 2007: Synthesis Report. Contribution of Working Groups I, II and III to the Fourth Assessment Report of the Intergovernmental Panel on Climate Change. .

IPCC. 2014. Climate change 2014–impacts, adaptation and vulnerability: regional aspects. Cambridge University Press, New York.

Iverson, L. R., A. M. Prasad, S. N. Matthews, and M. Peters. 2008. Estimating potential habitat for 134 eastern US tree species under six climate scenarios. Forest Ecology and Management 254: 390–406.

Iverson, L. R., and A. M. Prasad. 1998. Predicting abundance of 80 tree species following climate change in the eastern United States. Ecological Monographs 68: 465–485.

Jain, N. S., U. H. Dürr, and A. Ramamoorthy. 2015. Bioanalytical methods for metabolomic profiling: Detection of head and neck cancer, including oral cancer. Chinese Chemical Letters 26: 407–415.

Jamieson, M. A., A. M. Trowbridge, K. F. Raffa, and R. L. Lindroth. 2012. Consequences of climate warming and altered precipitation patterns for plant-insect and multitrophic interactions. Plant physiology 160: 1719–1727.

Jamieson, M. A., E. G. Schwartzberg, K. F. Raffa, P. B. Reich, and R. L. Lindroth. 2015. Experimental climate warming alters aspen and birch phytochemistry and performance traits for an outbreak insect herbivore. Global Change Biology 24: 2698–2710.

Jenkins, J. C., D. C. Chojnacky, L. S. Heath, and R. A. Birdsey. 2003. National-scale biomass estimators for United States tree species. Forest Science 49: 12–35.

Jiang, Y., and B. Huang. 2001. Drought and heat stress injury to two cool-season turfgrasses in relation to antioxidant metabolism and lipid peroxidation. Crop Science 41: 436–442.

Johnston, M., and P. Woodard. 1985. The effect of fire severity level on postfire recovery of hazel and raspberry in east-central Alberta. Canadian Journal of Botany 63: 672–677.

Jones, C. G., and J. H. Lawton. 1991. Plant chemistry and insect species richness of British umbellifers. The Journal of Animal Ecology 767–777.

Julander, O., W. L. Robinette, and D. A. Jones. 1961. Relation of summer range condition to mule deer herd productivity. The Journal of Wildlife Management 25: 54–60.

Julkunen-Tiitto, R., M. Rousi, J. Bryant, S. Sorsa, M. Keinänen, and H. Sikanen. 1996. Chemical diversity of several *Betulaceae* species: comparison of phenolics and terpenoids in northern birch stems. Trees 11: 16–22.

Karban, R. 2008. Plant behaviour and communication. Ecology Letters 11: 727–739.

Karban, R., K. Shiojiri, M. Huntzinger, and A. C. McCall. 2006. Damage-induced resistance in sagebrush: volatiles are key to intra-and interplant communication. Ecology 87: 922–930.

Kingsland, S. E. 1991. Defining ecology as a science. Foundations of Ecology. Classic papers with commentaries. The University of Chicago Press, Chicago & London 1–13.

Kleidon, A., J. Adams, R. Pavlick, and B. Reu. 2009. Simulated geographic variations of plant species richness, evenness and abundance using climatic constraints on plant functional diversity. Environmental Research Letters 4: 014007.

Kneeshaw, D. D., R. K. Kobe, K. D. Coates, and C. Messier. 2006. Sapling size influences shade tolerance ranking among southern boreal tree species. Journal of ecology 94: 471–480.

Kruskal, J. B. 1964. Multidimensional scaling by optimizing goodness of fit to a nonmetric hypothesis. Psychometrika 29: 1–27.

Kuokkanen, K., R. Julkunen-Tiitto, M. Keinänen, P. Niemelä, and J. Tahvanainen. 2001. The effect of elevated CO_2 and temperature on the secondary chemistry of *Betula pendula* seedlings. Trees 15: 378–384.

Kurnath, P., N. D. Merz, and M. D. Dearing. 2016. Ambient temperature influences tolerance to plant secondary compounds in a mammalian herbivore in Proc. R. Soc. B vol. 283. The Royal Society.

Laitinen, M.-L., R. Julkunen-Tiitto, and M. Rousi. 2000. Variation in phenolic compounds within a birch (*Betula pendula*) population. Journal of Chemical Ecology 26: 1609–1622.

Langvatn, R., S. D. Albon, T. Burkey, and T. H. Clutton-Brock. 1996. Climate, plant phenology and variation in age of first reproduction in a temperate herbivore. Journal of Animal Ecology 653–670.

Larsson, S., C. Björkman, and R. Gref. 1986. Responses of *Neodiprion sertifer* (*Hym., Diprionidae*) larvae to variation in needle resin acid concentration in Scots pine. Oecologia 70: 77–84.

Leavitt, S. W., and A. Long. 1986. Stable-carbon isotope variability in tree foliage and wood. Ecology 67: 1002–1010.

Lenart, E. A., R. T. Bowyer, J. V. Hoef, and R. W. Ruess. 2002. Climate change and caribou: effects of summer weather on forage. Canadian Journal of Zoology 80: 664–678.

Lenarz, M. S., J. Fieberg, M. W. Schrage, and A. J. Edwards. 2010. Living on the edge: viability of moose in northeastern Minnesota. Journal of Wildlife Management 74: 1013–1023.

Lenarz, M. S., M. E. Nelson, M. W. Schrage, and A. J. Edwards. 2009. Temperature mediated moose survival in northeastern Minnesota. The Journal of Wildlife Management 73: 503–510.

Lerdau, M., M. Litvak, and R. Monson. 1994. Plant chemical defense: monoterpenes and the growth-differentiation balance hypothesis. Trends in Ecology & Evolution 9: 58–61.

Lesica, P., and E. E. Crone. 2017. Arctic and boreal plant species decline at their southern range limits in the Rocky Mountains. Ecology Letters 20: 166–174.

Lewinsohn, E., M. Gijzen, R. M. Muzika, K. Barton, and R. Croteau. 1993. Oleoresinosis in Grand Fir (*Abies grandis*) saplings and mature trees (modulation of this wound response by light and water stresses). Plant Physiology 101: 1021–1028.

Lindroth, R. L. 2012. Atmospheric change, plant secondary metabolites and ecological interactions. The ecology of plant secondary metabolites: from genes to global processes. Cambridge University Press, Cambridge, New York.

Lott, C. A., and J. P. Smith. 2006. A geographic-information-system approach to estimating the origin of migratory raptors in North America using stable hydrogen isotope ratios in feathers. The Auk 123: 822–835.

MacCracken, J. G., V. V. Ballenberghe, and J. M. Peek. 1993. Use of aquatic plants by moose: sodium hunger or foraging efficiency? Canadian Journal of Zoology 71: 2345–2351.

Marshall, J. D., J. R. Brooks, and K. Lajtha. 2007. Sources of variation in the stable isotopic composition of plants in Stable Isotopes in Ecology and Environmental Science. Blackwell Publishing, Malden.

Martínez del Rio, C., N. Wolf, S. A. Carleton, and L. Z. Gannes. 2009. Isotopic ecology ten years after a call for more laboratory experiments. Biological Reviews 84: 91–111.

McArt, S. H., D. E. Spalinger, W. B. Collins, E. R. Schoen, T. Stevenson, and M. Bucho. 2009. Summer dietary nitrogen availability as a potential bottom-up constraint on moose in south-central Alaska. Ecology 90: 1400–1411.

Mccain, C. M., and S. R. King. 2014. Body size and activity times mediate mammalian responses to climate change. Global Change Biology 20: 1760–1769.

McCann, N. P., R. A. Moen, and T. R. Harris. 2013. Warm-season heat stress in moose (*Alces alces*). Canadian Journal of Zoology 91: 893–898.

McCann, N. P., R. A. Moen, S. K. Windels, and T. R. Harris. 2016. Bed sites as thermal refuges for a cold-adapted ungulate in summer. Wildlife Biology 22: 228–237.

Mech, L. D., and J. Fieberg. 2014. Re-evaluating the northeastern Minnesota moose decline and the role of wolves. The Journal of Wildlife Management 78: 1143–1150.

Merrill, E. H. 1991. Thermal constraints on use of cover types and activity time of elk. Applied Animal Behaviour Science 29: 251–267.

Mittler, R. 2006. Abiotic stress, the field environment and stress combination. Trends in Plant Science 11: 15–19.

Monteith, K. L., R. W. Klaver, K. R. Hersey, A. A. Holland, T. P. Thomas, and M. J. Kauffman. 2015. Effects of climate and plant phenology on recruitment of moose at the southern extent of their range. Oecologia 178: 1137–1148.

Murray, B. D., C. R. Webster, and J. K. Bump. 2013. Broadening the ecological context of ungulate-ecosystem interactions: the importance of space, seasonality, and nitrogen. Ecology 94: 1317–1326.

Murray, D. L., E. W. Cox, W. B. Ballard, H. A. Whitlaw, M. S. Lenarz, T. W. Custer, T. Barnett, and T. K. Fuller. 2006. Pathogens, nutritional deficiency, and climate influences on a declining moose population. Wildlife Monographs 1–30.

Mysterud, A., N. C. Stenseth, N. G. Yoccoz, R. Langvatn, and G. Steinheim. 2001. Nonlinear effects of large-scale climatic variability on wild and domestic herbivores. Nature 410: 1096–1099.

Nash, L. J., and W. R. Graves. 1993. Drought and flood stress effects on plant development and leaf water relations of five taxa of trees native to bottomland habitats. Journal of the American Society for Horticultural Science 118: 845–850.

Newsome, S. D., M. T. Tinker, D. H. Monson, O. T. Oftedal, K. Ralls, M. M. Staedler, M. L. Fogel, and J. A. Estes. 2009. Using stable isotopes to investigate individual diet specialization in California sea otters (*Enhydra lutris nereis*). Ecology 90: 961–974.

Oates, B. A., J. A. Merkle, M. J. Kauffman, S. R. Dewey, M. D. Jimenez, J. M. Vartanian, S. A. Becker, and J. R. Goheen. 2019. Antipredator response diminishes during periods of resource deficit for a large herbivore. Ecology 100(4): e02618.

Oksanen, J., G. Blanchet, R. Kindt, P. Legendre, P. R. Minchin, G. L. Simpson, P. Solymos, M. H. H. Stevens, and H. Wagner. 2015. vegan: Community Ecology Package.

Olff, H., M. E. Ritchie, and H. H. Prins. 2002. Global environmental controls of diversity in large herbivores. Nature 415: 901–904.

Ometto, J. P. H. B., J. R. Ehleringer, T. F. Domingues, J. A. Berry, F. Y. Ishida, E. Mazzi, N. Higuchi, L. B. Flanagan, G. B. Nardoto, and L. A. Martinelli. 2006. The stable carbon and nitrogen isotopic composition of vegetation in tropical forests of the Amazon Basin, Brazil. Biogeochemistry 79: 251–274.

Omuto, C. T., and R. R. Vargas. 2015. Re-tooling of regression kriging in R for improved digital mapping of soil properties. Geosciences Journal 19: 157–165.

Otto, A., and V. Wilde. 2001. Sesqui-, di-, and triterpenoids as chemosystematic markers in extant conifers—a review. The Botanical Review 67: 141–238.

Owen-Smith, N. 2002. Adaptive herbivore ecology: from resources to populations in variable environments. Cambridge University Press, New York.

Owen-Smith, N., J. M. Fryxell, and E. H. Merrill. 2010. Foraging theory upscaled: the behavioural ecology of herbivore movement. Philosophical Transactions of the Royal Society of London B: Biological Sciences 365: 2267–2278.

Parker, K. L., P. S. Barboza, and M. P. Gillingham. 2009. Nutrition integrates environmental responses of ungulates. Functional Ecology 23: 57–69.

Parmesan, C. 2006. Ecological and evolutionary responses to recent climate change. Annual Review of Ecology Evolution and Systematics 37: 637–669.

Parnell, A. C., D. L. Phillips, S. Bearhop, B. X. Semmens, E. J. Ward, J. W. Moore, A. L. Jackson, J. Grey, D. J. Kelly, and R. Inger. 2013. Bayesian stable isotope mixing models. Environmetrics 24: 387–399.

Pavarini, D. P., S. P. Pavarini, M. Niehues, and N. P. Lopes. 2012. Exogenous influences on plant secondary metabolite levels. Animal Feed Science and Technology 176: 5–16.

Pebesma, E. J., and R. Bivand. 2005. Classes and methods for spatial data in R.

Peek, J.M., D. L. Urich, and R. J. Mackie. 1976. Moose habitat selection and relationships to forest management in northeastern Minnesota. Wildlife Monographs 3–65.

Peek, James M., D. L. Urich, and R. J. Mackie. 1976. Moose habitat selection and relationships to forest management in northeastern Minnesota. Wildlife Monographs 3–65.

Perala, D. A., and D. Alban. 1993. Allometric biomass estimators for aspen-dominated ecosystems in the upper Great Lakes. U.S. Dept. of Agriculture, Forest Service, North Central Forest Experiment Station, St. Paul, MN.

Pinheiro, J., D. Bates, S. DebRoy, D. Sarkar, and R Core Team. 2015. nlme: Linear and nonlinear mixed-effects models.

Poelman, E. H., J. J. van Loon, and M. Dicke. 2008. Consequences of variation in plant defense for biodiversity at higher trophic levels. Trends in Plant Science 13: 534–541.

PRISM Climate Group. 2017. PRISM Climate Group. Oregon State University.

Prudhomme, C., and D. W. Reed. 1999. Mapping extreme rainfall in a mountainous region using geostatistical techniques: a case study in Scotland. International Journal of Climatology 19: 1337–1356.

R Core Team. 2018. R: A language and environment for statistical computing. R Foundation for Statistical Computing, Vienna, Austria.

Raynor, E. J., A. Joern, J. B. Nippert, and J. M. Briggs. 2016. Foraging decisions underlying restricted space use: effects of fire and forage maturation on large herbivore nutrient uptake. Ecology and Evolution 6: 5843–5853.

Reich, P. B., K. M. Sendall, K. Rice, R. L. Rich, A. Stefanski, S. E. Hobbie, and R. A. Montgomery. 2015. Geographic range predicts photosynthetic and growth response to warming in co-occurring tree species. Nature Climate Change 5: 148-152.

Renecker, L. A., and C. C. Schwartz. 2007. Food habits and feeding behavior in Ecology and management of the North American moose, 2nd ed. Smithsonian Institution Press, Washington.

Renecker, L. A., and R. J. Hudson. 1986. Seasonal energy expenditure and thermoregulatory response of moose. Canadian Journal of Zoology 64: 322–327.

Renecker, L. A., and R. J. Hudson. 1989. Seasonal activity budgets of moose in aspen-dominated boreal forests. The Journal of Wildlife Management 296–302.

Renecker, L., and R. Hudson. 1990. Behavioral and thermoregulatory responses of moose to high ambient-temperatures and insect harassment in aspen-dominated forests.

ALCES, 26, 1990 – 26th North American Moose COnverence and Workshops 66-72.

Rich, R. L., A. Stefanski, R. A. Montgomery, S. E. Hobbie, B. A. Kimball, and P. B. Reich. 2015. Design and performance of combined infrared canopy and belowground warming in the B4WarmED (Boreal Forest Warming at an Ecotone in Danger) experiment. Global Change Biology 21(6): 2334-2348..

Richards, L. A., L. A. Dyer, A. M. Smilanich, and C. D. Dodson. 2010. Synergistic effects of amides from two Piper species on generalist and specialist herbivores. Journal of Chemical Ecology 36: 1105–1113.

Richards, L. A., L. A. Dyer, M. L. Forister, A. M. Smilanich, C. D. Dodson, M. D. Leonard, and C. S. Jeffrey. 2015. Phytochemical diversity drives plant–insect community diversity. Proceedings of the National Academy of Sciences 112: 10973–10978.

Ripple, W. J., T. M. Newsome, C. Wolf, R. Dirzo, K. T. Everatt, M. Galetti, M. W. Hayward, G. I. Kerley, T. Levi, P. A. Lindsey, and others. 2015. Collapse of the world's largest herbivores. Science Advances 1: e1400103.

Rizhsky, L., H. Liang, and R. Mittler. 2002. The combined effect of drought stress and heat shock on gene expression in tobacco. Plant Physiology 130: 1143–1151.

Rizhsky, L., H. Liang, J. Shuman, V. Shulaev, S. Davletova, and R. Mittler. 2004. When defense pathways collide. The response of Arabidopsis to a combination of drought and heat stress. Plant Physiology 134: 1683–1696.

Roitto, M., P. Rautio, A. Markkola, R. Julkunen-Tiitto, M. Varama, K. Saravesi, and J. Tuomi. 2009. Induced accumulation of phenolics and sawfly performance in Scots pine in response to previous defoliation. Tree Physiology 29: 207–216.

Royle, A. J., and D. R. Rubenstein. 2004. The role of species abundance in determining breeding origins of migratory birds with stable isotopes. Ecological Applications 14: 1780–1788.

Rubenstein, D. R., and K. A. Hobson. 2004. From birds to butterflies: animal movement patterns and stable isotopes. Trends in Ecology & Evolution 19: 256–263.

Sallas, L., E.-M. Luomala, J. Utriainen, P. Kainulainen, and J. K. Holopainen. 2003. Contrasting effects of elevated carbon dioxide concentration and temperature on Rubisco activity, chlorophyll fluorescence, needle ultrastructure and secondary metabolites in conifer seedlings. Tree Physiology 23: 97–108.

Samuel, W. M. 1991. Grooming by moose (*Alces alces*) infested with the winter tick, *Dermacentor albipictus* (*Acari*): a mechanism for premature loss of winter hair. Canadian Journal of Zoology 69: 1255–1260.

Samuel, W. M., D. A. Welch, and M. L. Drew. 1986. Shedding of the juvenile and winter hair coats of moose (*Alces alces*) with emphasis on the influence of the winter tick, Dermacentor albipictus. Alces 22: 345–360.

Savin, R., and M. E. Nicolas. 1996. Effects of short periods of drought and high temperature on grain growth and starch accumulation of two malting barley cultivars. Functional Plant Biology 23: 201–210.

Savsani, H. H., R. J. Padodara, A. R. Bhadaniya, V. A. Kalariya, B. B. Javia, S. N. Ghodasara, and N. K. Ribadiya. 2015. Impact of climate on feeding, production and reproduction of animals-A Review. Agricultural Reviews 36.

Schloss, C. A., T. A. Nuñez, and J. J. Lawler. 2012. Dispersal will limit ability of mammals to track climate change in the Western Hemisphere. Proceedings of the National Academy of Sciences 109: 8606–8611.

Schoeninger, M. J., and M. J. DeNiro. 1984. Nitrogen and carbon isotopic composition of bone collagen from marine and terrestrial animals. Geochimica et Cosmochimica Acta 48: 625–639.

Schwartzberg, E. G., M. A. Jamieson, K. F. Raffa, P. B. Reich, R. A. Montgomery, and R. L. Lindroth. 2014. Simulated climate warming alters phenological synchrony between an outbreak insect herbivore and host trees. Oecologia 175: 1041–1049.

Sealy, J. C., N. J. van der Merwe, J. A. L. Thorp, and J. L. Lanham. 1987. Nitrogen isotopic ecology in southern Africa: Implications for environmental and dietary tracing. Geochimica et Cosmochimica Acta 51: 2707–2717.

Sedio, B. E., J. C. Rojas Echeverri, P. Boya, A. Cristopher, and S. J. Wright. 2017. Sources of variation in foliar secondary chemistry in a tropical forest tree community. Ecology 98: 616–623.

Severud, W. J., G. D. Giudice, T. R. Obermoller, T. A. Enright, R. G. Wright, and J. D. Forester. 2015. Using GPS collars to determine parturition and cause-specific mortality of moose calves. Wildlife Society Bulletin 39: 616–625.

Shi, J., R. I. M. Dunbar, D. Buckland, and D. Miller. 2003. Daytime activity budgets of feral goats (*Capra hircus*) on the Isle of Rum: influence of season, age, and sex. Can. J. Zool. 81: 803–815.

Smith, C. A., E. J. Want, G. O'Maille, R. Abagyan, and G. Siuzdak. 2006. XCMS: processing mass spectrometry data for metabolite profiling using nonlinear peak alignment, matching, and identification. Analytical chemistry 78: 779–787.

Smith, W. B., and G. J. Brand. 1983. Allometric biomass equations for 98 species of herbs, shrubs, and small trees. Research Note NC-299. St. Paul, MN: US Dept. of Agriculture, Forest Service, North Central Forest Experiment Station 299.

Smith, W. R. 2008. Trees and shrubs of Minnesota. University of Minnesota Press, St. Paul.

Snow, M. D., R. R. Bard, D. M. Olszyk, L. M. Minster, A. N. Hager, and D. T. Tingey. 2003. Monoterpene levels in needles of Douglas fir exposed to elevated CO_2 and temperature. Physiologia Plantarum 117: 352–358.

Sreekumar, A., L. M. Poisson, T. M. Rajendiran, A. P. Khan, Q. Cao, J. Yu, B. Laxman, R. Mehra, R. J. Lonigro, Y. Li, M. K. Nyati, A. Ahsan, S. Kalyana-Sundaram, B. Han, X. Cao, J. Byun, G. S. Omenn, D. Ghosh, S. Pennathur, D. C. Alexander, A. Berger, J. R. Shuster, J. T. Wei, S. Varambally, C. Beecher, and A. M. Chinnaiyan. 2009. Metabolomic profiles delineate potential role for sarcosine in prostate cancer progression. Nature 457: 910–914.

Stefanescu, C., D. X. Soto, G. Talavera, R. Vila, and K. A. Hobson. 2016. Long-distance autumn migration across the Sahara by painted lady butterflies: exploiting resource pulses in the tropical savannah. Biology Letters 12: 20160561.

Stewart, K. M., R. T. Bowyer, J. G. Kie, B. L. Dick, and M. Ben-David. 2003. Niche partitioning among mule deer, elk, and cattle: Do stable isotopes reflect dietary niche? Ecoscience 10: 297–302.

Still, C. J., and R. L. Powell. 2010. Continental-scale distributions of vegetation stable carbon isotope ratios in isoscapes. Springer, New York.

Stock, B. C., and B. X. Semmens. 2016. Unifying error structures in commonly used biotracer mixing models. Ecology 97: 2562–2569.

Stolter, C., J. P. Ball, R. Julkunen-Tiitto, R. Lieberei, and J. U. Ganzhorn. 2005. Winter browsing of moose on two different willow species: food selection in relation to plant chemistry and plant response. Canadian Journal of Zoology 83: 807–819.

Street, G. M., J. Fieberg, A. R. Rodgers, M. Carstensen, R. Moen, S. A. Moore, S. K. Windels, and J. D. Forester. 2016. Habitat functional response mitigates reduced foraging opportunity: implications for animal fitness and space use. Landscape Ecology 1–15.

Sumner, L. W., A. Amberg, D. Barrett, M. H. Beale, R. Beger, C. A. Daykin, T. W.-M. Fan, O. Fiehn, R. Goodacre, and J. L. Griffin. 2007. Proposed minimum reporting standards for chemical analysis. Metabolomics 3: 211–221.

Tahvanainen, J., E. Helle, R. Julkunen-Tiitto, and A. Lavola. 1985. Phenolic compounds of willow bark as deterrents against feeding by mountain hare. Oecologia 65: 319–323.

Tankersley, N. G., and W. C. Gasaway. 1983. Mineral lick use by moose in Alaska. Canadian Journal of Zoology 61: 2242–2249.

Tateno, R., T. Hishi, and H. Takeda. 2004. Above-and belowground biomass and net primary production in a cool-temperate deciduous forest in relation to topographical changes in soil nitrogen. Forest Ecology and Management 193: 297–306.

Tautenhahn, R., C. Boettcher, and S. Neumann. 2008. Highly sensitive feature detection for high resolution LC/MS. BMC bioinformatics 9: 504.

Timmermann, H. R., and A. R. Rodgers. 2017. The status and management of moose in North America-circa 2015. Alces 53.

Tischler, K. B. 2004. Aquatic plant nutritional quality and contribution to moose diet at Isle Royale National Park. Ph.D. Dissertation. Michigan Technological University.

Turbill, C., T. Ruf, T. Mang, and W. Arnold. 2011. Regulation of heart rate and rumen temperature in red deer: effects of season and food intake. Journal of Experimental Biology 214: 963–970.

van Beest, F. M., and J. M. Milner. 2013. Behavioural responses to thermal conditions affect seasonal mass change in a heat-sensitive northern ungulate. PloS one 8: e65972.

van den Boogaart, K. G., R. Tolosana-Delgado, and M. Bren. 2018. compositions: Compositional Data Analysis.

van der Merwe, N. J., and E. Medina. 1989. Photosynthesis and 13C/12C ratios in Amazonian rain forests. Geochimica et Cosmochimica Acta 53: 1091–1094.

Vandegeer, R., R. E. Miller, M. Bain, R. M. Gleadow, and T. R. Cavagnaro. 2013. Drought adversely affects tuber development and nutritional quality of the staple crop cassava (*Manihot esculenta Crantz*). Functional Plant Biology 40: 195–200.

Veluri, R., T. L. Weir, H. P. Bais, F. R. Stermitz, and J. M. Vivanco. 2004. Phytotoxic and antimicrobial activities of catechin derivatives. Journal of Agricultural and Food Chemistry 52: 1077–1082.

Veteli, T. O., J. Koricheva, P. Niemelä, and S. Kellomäki. 2006. Effects of forest management on the abundance of insect pests on Scots pine. Forest Ecology and Management 231: 214–217.

Walter, W. D., D. M. Leslie, E. C. Hellgren, and D. M. Engle. 2010. Identification of subpopulations of North American elk (*Cervus elaphus L.*) using multiple lines of evidence: habitat use, dietary choice, and fecal stable isotopes. Ecol Res 25: 789–800.

Walther, G. R., E. Post, P. Convey, A. Menzel, C. Parmesan, T. J. C. Beebee, J. M. Fromentin, O. Hoegh-Guldberg, and F. Bairlein. 2002. Ecological responses to recent climate change. Nature 416: 389–395.

Welch, D. A., W. M. Samuel, and R. J. Hudson. 1990. Bioenergetic consequences of alopecia induced by Dermacentor albipictus (*Acari: Ixodidae*) on moose. Journal of Medical Entomology 27: 656–660.

West, J. B., G. J. Bowen, T. E. Cerling, and J. R. Ehleringer. 2006. Stable isotopes as one of nature's ecological recorders. Trends in Ecology & Evolution 21: 408–414.

West, J. B., G. J. Bowen, T. E. Dawson, and K. P. Tu. 2009. Isoscapes: understanding movement, pattern, and process on Earth through isotope mapping. Springer, New York.

Williams, R. S., D. E. Lincoln, and R. J. Norby. 2003. Development of gypsy moth larvae feeding on red maple saplings at elevated CO_2 and temperature. Oecologia 137: 114–122.

Wink, M. 1988. Plant breeding: importance of plant secondary metabolites for protection against pathogens and herbivores. Theoretical and Applied Genetics 75: 225–233.

Worrall, J. J., L. Egeland, T. Eager, R. A. Mask, E. W. Johnson, P. A. Kemp, and W. D. Shepperd. 2008. Rapid mortality of Populus tremuloides in southwestern Colorado, USA. Forest Ecology and Management 255: 686–696.

Wünschmann, A., A. G. Armien, E. Butler, M. Schrage, B. Stromberg, J. B. Bender, A. M. Firshman, and M. Carstensen. 2015. Necropsy findings in 62 opportunistically collected free-ranging moose (*Alces alces*) from Minnesota, USA (2003–13). Journal of Wildlife Diseases 51: 157–165.

Yates, F. 1934. Contingency tables involving small numbers and the χ 2 test. Supplement to the Journal of the Royal Statistical Society 1: 217–235.

Yin, X. 1993. Variation in foliar nitrogen concentration by forest type and climatic gradients in North America. Canadian Journal of Forest Research 23: 1587–1602.

Zackrisson, O., T. H. DeLuca, M.-C. Nilsson, A. Sellstedt, and L. M. Berglund. 2004. Nitrogen fixation increases with successional age in boreal forests. Ecology 85: 3327–3334.

Zandalinas, S. I., R. Mittler, D. Balfagón, V. Arbona, and A. Gómez-Cadenas. 2018. Plant adaptations to the combination of drought and high temperatures. Physiologia Plantarum 162: 2–12.

Supplemental Information

Table S2-1. Location and treatment data of field sampling locations. Light conditions were a binary response of whether a plot was in an area that was recently clear cut (i.e., high) or areas that have experienced no known overstory disturbance since at least 1985 (i.e., low). Mean-maximum summer temperature (MMST) is the maximum daily temperature averaged across June, July, and August from 1981 to 2000 (Sumner et al. 2007).

plot ID	easting	northing	light conditions	MMST
1	700598	5303917	high	23.86
2	700283	5308537	high	25.30
3	698786	5308655	high	25.05
4	685385	5304339	low	24.70
5	685160	5295714	low	22.86
6	678345	5291770	low	22.36
7	614050	5313377	low	25.40
8	611435	5315050	low	25.62
9	610716	5314932	low	25.68
10	599534	5312110	high	25.51
11	599427	5312111	high	25.51
12	598718	5310922	high	25.43

Table S2-2. Experimental exact mass, hypothetical mass, molecular formula and PPM error for all metabolites found to be significantly abundant (ANOVA, α = 0.001). "Level of Confidence" signifies the level of confidence in metabolite 'identification', as defined by the Chemical Analysis Working Group of the Metabolomics Standards Initiative (Sumner et al. 2007). Catechin was found to be significant in both positive and negative ionization modes, and its identity was confirmed via an authentic standard.

Identification	Species	Ionization mode	Experimental exact mass	Hypothetical exact mass	Molecular formula	PPM error	Level of Confidence
catechin	*paper birch*	-	289.0729	289.0712	$C_{15}H_{13}O_6$	5.8809	1
catechin	*paper birch*	+	291.0861	291.0868	$C_{15}H_{15}O_6$	2.4048	1
putative diterpene resin acid 1	*balsam fir*	+	317.1382	317.1389	$C_{18}H_{21}O_5$	2.2072	3
putative diterpene resin acid 2	*balsam fir*	+	331.1541	331.1545	$C_{19}H_{23}O_5$	1.2079	3
putative diterpene resin acid 3	*paper birch*	+	337.1435	337.1439	$C_{21}H_{21}O_4$	1.1864	3

Table S2-3. Results of linear mixed-effects models comparing changes in relative abundance of example compounds for different stress conditions. Statistically significant results ($\alpha = 0.05$) are identified with an asterisk (*) and change values preceded by "–" indicate a decline in mean relative abundance relative to our reference group, where as a "+" indicates an increase in mean relative abundance.

species	compound	year	stress condition	df	change (%)	t	P
balsam fir	resin acid 1	1	moderate temperature	29	-16.5	-0.724	0.4751
		1	high temperature	29	-15.9	-0.372	0.7126
		2	drought	25	+21.9	0.795	0.4343
		2	temperature	25	+28.7	1.238	0.2272
		2	drought + temperature	25	+30.0	1.234	0.2288
		3	light	8	+83.7	0.977	0.3570
		3	temperature	8	+120.2	1.484	0.1761
		3	temperature + light	8	+70.2	0.878	0.4057
	resin acid 2	1	moderate temperature	29	-14.2	-1.068	0.2944
		1	high temperature	29	-13.6	-0.919	0.3657
		2	drought	25	-3.0	-0.103	0.9188
		2	temperature	25	+5.4	0.333	0.7417
		2	drought + temperature	25	+13.1	0.736	0.4685
		3	light	8	-17.9	-0.586	0.5739
		3	temperature	8	+20.8	0.815	0.4389
		3	temperature + light	8	+39.5	1.495	0.1734
paper birch	catechin	1	moderate temperature	26	-54.3	-3.933	*< 0.0001**
		1	high temperature	26	-66.4	-4.322	*0.0002**

	2	drought	30	-23.9	-1.070	0.2931
	2	temperature	30	-33.8	-1.618	0.1161
	2	drought + temperature	30	-32.2	-1.489	0.1469
	3	light	6	+22.0	0.310	0.7670
	3	temperature	6	+44.5	0.626	0.5538
	3	temperature + light	6	+251.1	2.837	*0.0297**
terpene acid	1	moderate temperature	26	-75.8	-3.015	*0.0057**
	1	high temperature	26	-71.4	-2.877	*0.0079**
	2	drought				
	2	temperature				
	2	drought + temperature		*feature undetected*		
	3	light	6	-98.0	-1.504	0.1832
	3	temperature	6	24.9	0.283	0.7870
	3	temperature + light	6	149.1	1.664	0.1470

Table S3-1. Summary information for different forage-preference groups. For low-preference forage, "other" includes plant species that are not considered part of the routine diet of moose in Minnesota, but possibly still sampled, such as *Alnus spp., Populus balsamifera*, *Populus grandidentata*, *Fraxinus nigra*, *Thuja occidentalis*, etc.

			$\delta^{13}C$ (‰)		$\delta^{15}N$ (‰)		%N		C:N	
preference group	species	n	mean	sd	mean	sd	mean	sd	mean	sd
high	*Betula papyrifera*	348	-28.99	1.48	-2.32	2.02	2.81	0.94	18.42	6.09
	Populus tremuloides	293	-28.55	1.42	-1.78	2.19	2.92	1.18	18.76	5.72
	Salix spp.	150	-27.84	1.34	-1.58	2.12	2.82	0.96	18.92	6.30
	all species	**791**	**-28.61**	**1.50**	**-1.96**	**2.15**	**2.85**	**1.04**	**18.63**	**5.99**
medium	*Acer* spp.	281	-28.80	1.60	-4.42	2.31	2.53	0.85	19.30	6.24
	Prunus spp.	171	-28.83	1.18	-2.81	2.11	2.81	0.78	17.90	6.43
	Sorbus americana	144	-29.50	1.50	-3.61	1.98	2.71	0.71	17.92	4.76
	all species	**596**	**-28.98**	**1.49**	**-3.77**	**2.27**	**2.66**	**0.81**	**18.57**	**6.01**
low	*Abies balsamea*	344	-30.12	1.19	-3.38	2.13	1.38	0.42	38.43	9.71
	Amelanchier spp.	388	-29.57	1.42	-3.11	2.14	2.79	0.86	17.97	5.45
	Corylus cornuta	381	-29.45	1.56	-3.17	1.88	2.50	0.67	18.67	4.44
	Cornus spp.	124	-29.76	1.98	-2.43	2.07	2.41	0.68	19.66	5.64
	other	94	-28.92	1.47	-2.45	2.37	2.37	1.01	25.69	16.74
	all species	**1331**	**-29.65**	**1.51**	**-3.08**	**2.10**	**2.28**	**0.90**	**24.17**	**11.69**

Table S3-2. Summary information for fixed and random effects. When necessary, spatial covariates were converted from their original format, first into raster datasets for manipulation of resolution and extent, then into ASCII datasets for analysis in R 3.5.2. All data format conversions were performed in ArcGIS 10.3.1. Random effects are identified with an asterisk (*). In addition to the covariates listed below, we also incorporated both easting and northing as fixed effects.

covariate	definition	units description	original format	source
aspect	downslope direction with values ranging from 0.0 to 359.0 degrees	degrees	grid	LANDFIRE. 2018. Aspect. <www.landfire.gov/aspect.php> Accessed 01 May 2018.
bedrock geology*	primary and secondary bedrock type combined into a single, categorical code	categorical code	shapefile	Minnesota Geologic Survey. 2011. Geologic Map of Minnesota - Bedrock Geology (MGS Map S-21). <gisdata.mn.gov/dataset/geos-bedrock-geology-mn> Accessed on 01 May 2018.
covertype	updated classification of 2013 national landcover database using a combination of Landsat 8 data and LiDAR data	categorical code	raster	Rampi, L. P., Knight, J. F. and M. Bauer. 2016. Minnesota Land Cover Classification and Impervious Surface Area by Landsat and Lidar: 2013 Update. Retrieved from the Data Repository for the University of Minnesota <http://doi.org/10.13020/D6JP4S> Accessed on 01 May 2016.
digital elevation (DEM)	elevation in feet above mean sea level	feet	raster	USGS. 2014. Minnesota Digital Elevation Model - 30 Meter Resolution. <gisdata.mn.gov/dataset/elev-30m-digital-elevation-model> Accessed on 01 May 2018.
disturbance age	disturbance age as of 2014, characterized as discrete time periods — 1 year, 2-5 years, or 6-10 years	categorical code	raster	LANDFIRE. 2016. Disturbance. <www.landfire.gov/disturbance_2.php> Accessed 01 May 2018.

disturbance severity	disturbance severity, characterized as high, low, or moderate	categorical code	raster	LANDFIRE. 2016. Disturbance. <www.landfire.gov/disturbance_2.php> Accessed 01 May 2018.
disturbance type	disturbance type of original disturbance, characterized as fire, mechanical addition, mechanical removal, or chemical	categorical code	raster	LANDFIRE. 2016. Disturbance. <www.landfire.gov/disturbance_2.php> Accessed 01 May 2018.
disturbance*	three-digit code combining disturbance type, severity, and age as described above	categorical code	raster	LANDFIRE. 2016. Disturbance. <www.landfire.gov/disturbance_2.php> Accessed 01 May 2018.
mean-maximum summer temperature (MMST)	average daily maximum from 01 June through August 31, from 1981 to 2010	ºC	ASCII	PRISM Climate Group, Oregon State University, http://prism.oregonstate.edu, created 4 Feb 2004. Accessed on 01 May 2018.
precipitation	average annual precipitation from 1981-2010	inches	raster	State Climatology Office, DNR, MDA. 2015. Normal Annual Precipitation Average, Minnesota, 1981-2010.
slope	represents deviation from horizontal elevation, values range from 0.0 to 90.0 degrees	degrees	grid	LANDFIRE. 2018. Slope. <www.landfire.gov/slope.php> Accessed 01 May 2018.
solar insolation	characterizes the amount of direct and indirect sunlight that reaches the surface	kWh/m^2	raster	Brink, C, Gosack, B, Kne, L, Luo, Y, Martin, C, McDonald, M, Moore, M, Munsch, A, Palka, S, Piernot, D, Thiede, D, Xie, Y, and A. Walz. 2015. Solar Insolation, Minnesota (2006-2012). <conservancy.umn.edu/handle/11299/172642> Accessed on 01 May 2018

water table depth	depth to water table, categorized into seven discrete depth classes that describe distance in feet below land surface	discrete depth classes	raster	Minnesota Department of Natural Resources (DNR), County Geologic Atlas Program. 2016. Water-Table Elevation and Depth to Water Table, Minnesota Hydrogeology Atlas series HG-03. <gisdata.mn.gov/dataset/geos-hydrogeology-atlas-hg03> Accessed on 01 May 2018.

Table S4-1. Summary information for different forage-preference groups. For low-preference forage, "other" includes plant species that are not considered part of the routine diet of moose in Minnesota, but possibly still sampled, such as *Alnus spp., Populus balsamifera*, *Populus grandidentata*, *Fraxinus nigra*, *Thuja occidentalis*, etc. For the purposes of this study, we did not differentiate among species of aquatic plants.

			$\delta^{13}C$ (‰)		$\delta^{15}N$ (‰)		%N	
forage group	species	n	mean	sd	mean	sd	mean	sd
high	*Betula papyrifera*	348	-28.99	1.48	-2.32	2.02	2.81	0.94
	Populus tremuloides	293	-28.55	1.42	-1.78	2.19	2.92	1.18
	Salix spp.	150	-27.84	1.34	-1.58	2.12	2.82	0.96
medium	*Acer* spp.	281	-28.80	1.60	-4.42	2.31	2.53	0.85
	Prunus spp.	171	-28.83	1.18	-2.81	2.11	2.81	0.78
	Sorbus americana	144	-29.50	1.50	-3.61	1.98	2.71	0.71
low	*Abies balsamea*	344	-30.12	1.19	-3.38	2.13	1.38	0.42
	Amelanchier spp.	388	-29.57	1.42	-3.11	2.14	2.79	0.86
	Corylus cornuta	381	-29.45	1.56	-3.17	1.88	2.50	0.67
	Cornus spp.	124	-29.76	1.98	-2.43	2.07	2.41	0.68
	other	94	-28.92	1.47	-2.45	2.37	2.37	1.01
aquatic	n/a	105	-26.97	2.65	0.62	2.43	3.10	0.77

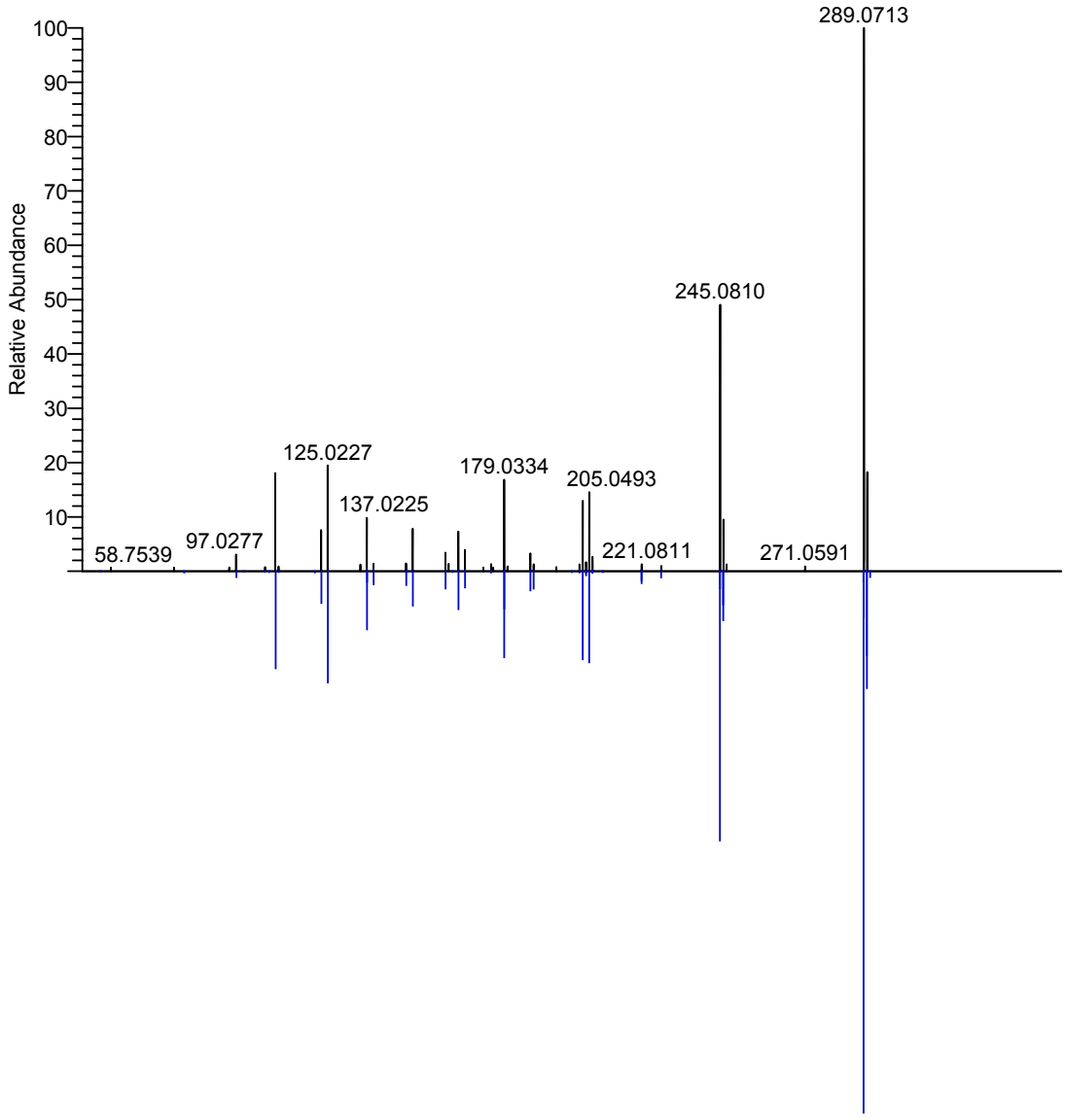

Fig.S2-1. Mirrored HCD fragmentation spectra of endogenous catechin from Year 1 paper birch (above) and a catechin standard (below) from negative ionization mode. Catechin was identified and shown to be distinct from its isomer, epicatechin, as commercial standards of each of these compounds were chromatographically resolved. HCD fragmentation was performed at a normalized collision energy of 25.

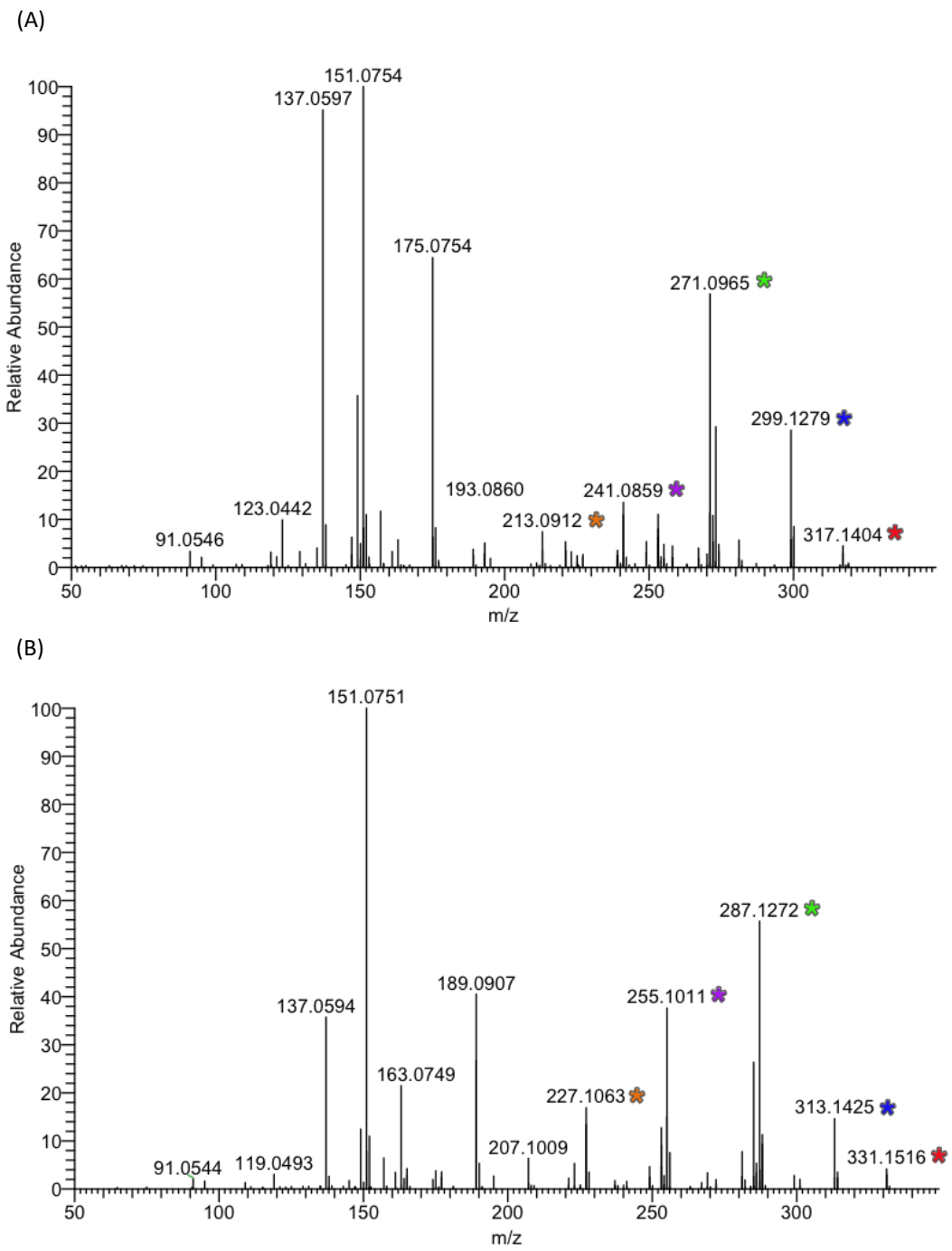

Fig.S2-2. Positive ionization mode HCD fragmentation spectra of putative diterpene resin acids with *m/z* values of 317.1382 (A) and 331.1542 (B) from balsam fir. HCD fragmentation was performed at a normalized collision energy of 10. The spectra are very similar except for a 14 AMU shift (denoted with a *), suggesting these molecules are structurally related and differ only in the length of a hydrocarbon chain or presence/absence of a methylation.

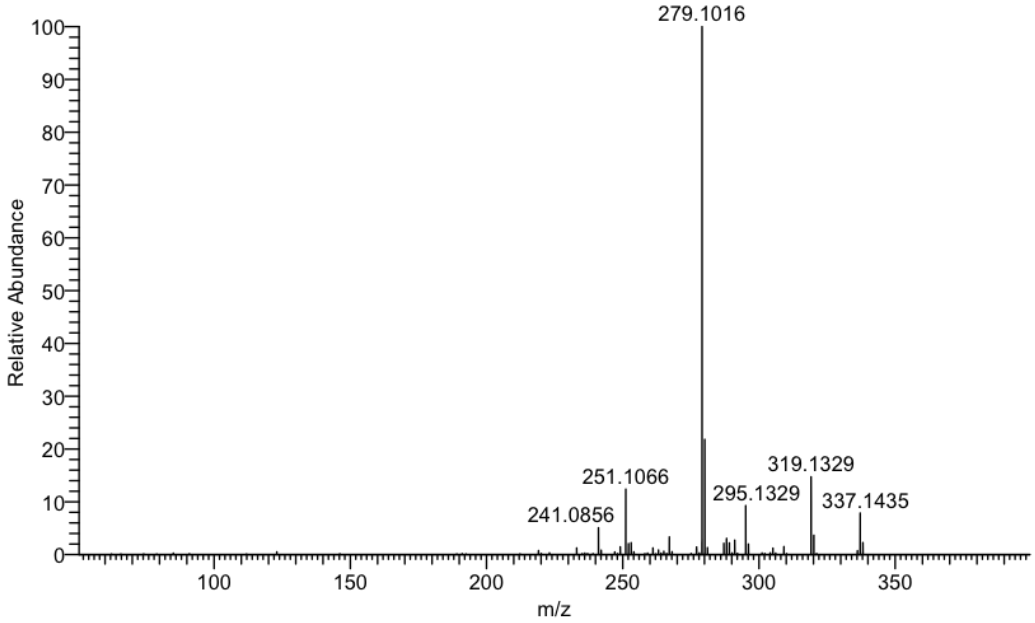

Fig.S2-3. Positive ionization mode HCD fragmentation spectra of putative diterpene resin acid from paper birch. HCD fragmentation was performed at a normalized collision energy of 25.

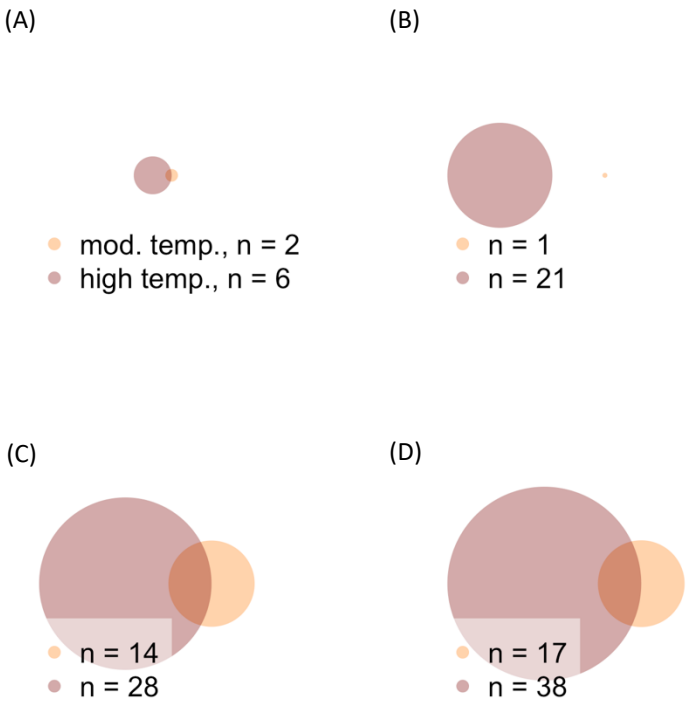

Fig.S2-4. Venn diagrams for Year 1 samples detailing the number of compounds that increase or decrease by ≥ 75% in balsam fir (A and B, respectively) and paper birch (C and D, respectively). Circles are scaled and comparable across species and treatments. Areas in which circles are overlapping are relative to the number of compounds effected by both treatments. High-temperatures appears to have a greater influence on large scale shifts in the relative abundance of compounds than moderate temperatures.

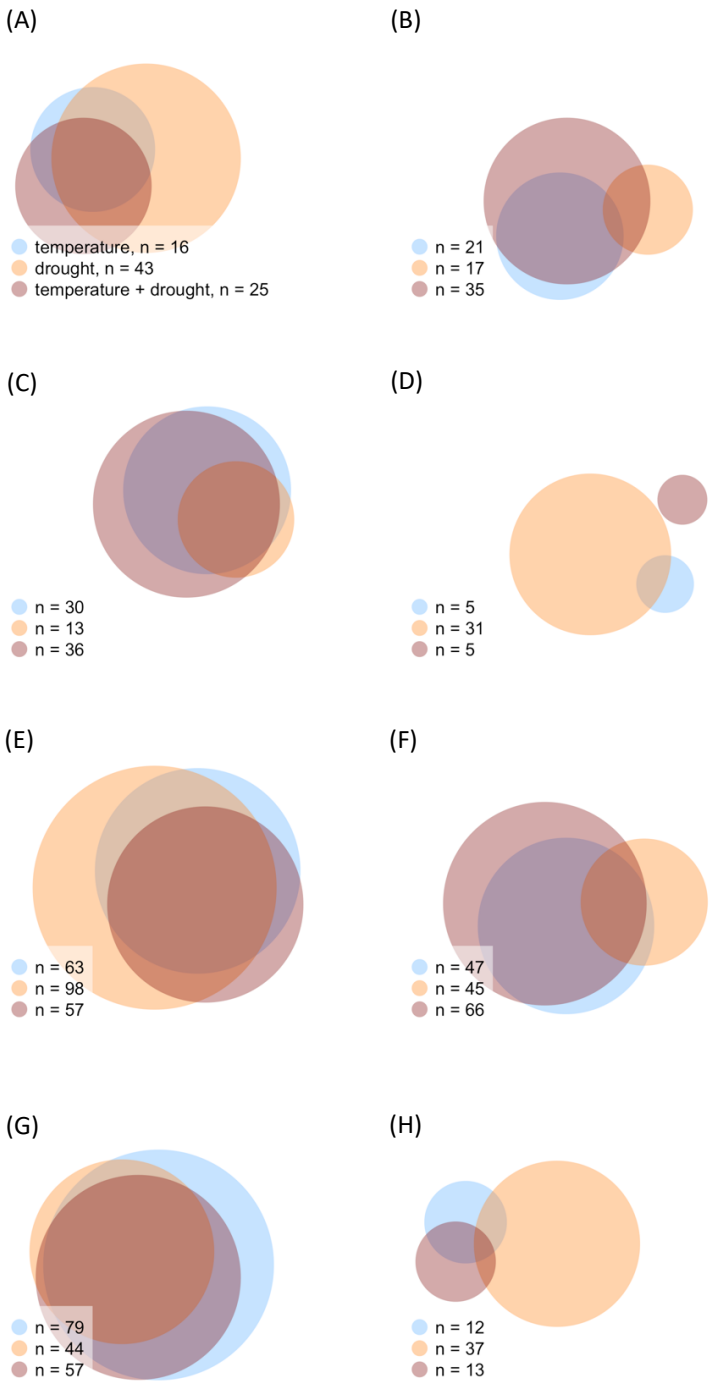

Fig.S2-5. Venn diagrams for Year 2 samples detailing the number of compounds that increase or decrease by ≥ 75% in balsam fir (A and B, respectively), red maple (C and D, respectively), paper birch (E and F, respectively), and trembling aspen (G and H, respectively). Circles are scaled and comparable across species and treatments. Areas in which circles are overlapping are relative to the number of compounds affected by all treatments.

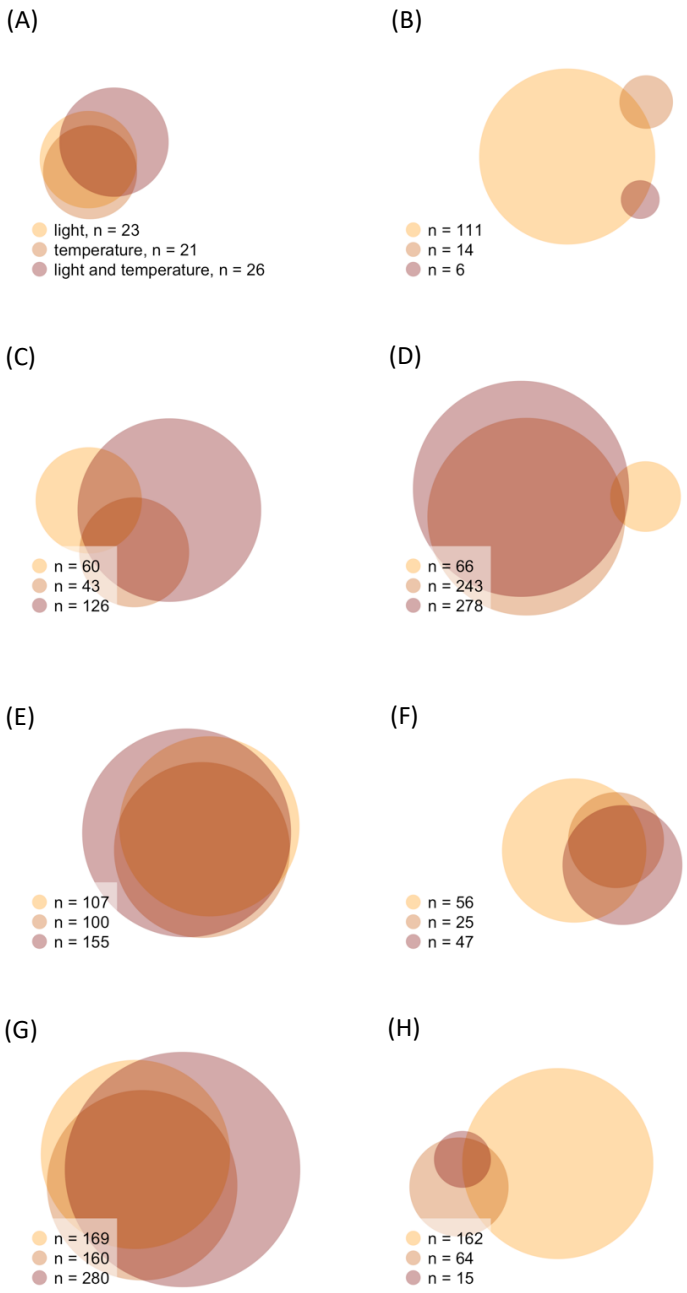

Fig.S2-6. Venn diagrams for Year 3 samples detailing the number of compounds that increase or decrease by ≥ 75% in balsam fir (A and B, respectively), paper birch (C and D, respectively), beaked hazel (E and F, respectively), and trembling aspen (D and H, respectively). Circles are scaled and comparable across species and treatments. Areas in which circles are overlapping are relative to the number of compounds affected by all treatments. In general, the combination of high-light and high-temperature results in the large-scale increase of more compounds, on average, than any other treatment. While high-light conditions result in the large-scale decrease of more compounds, on average, than any other treatment.

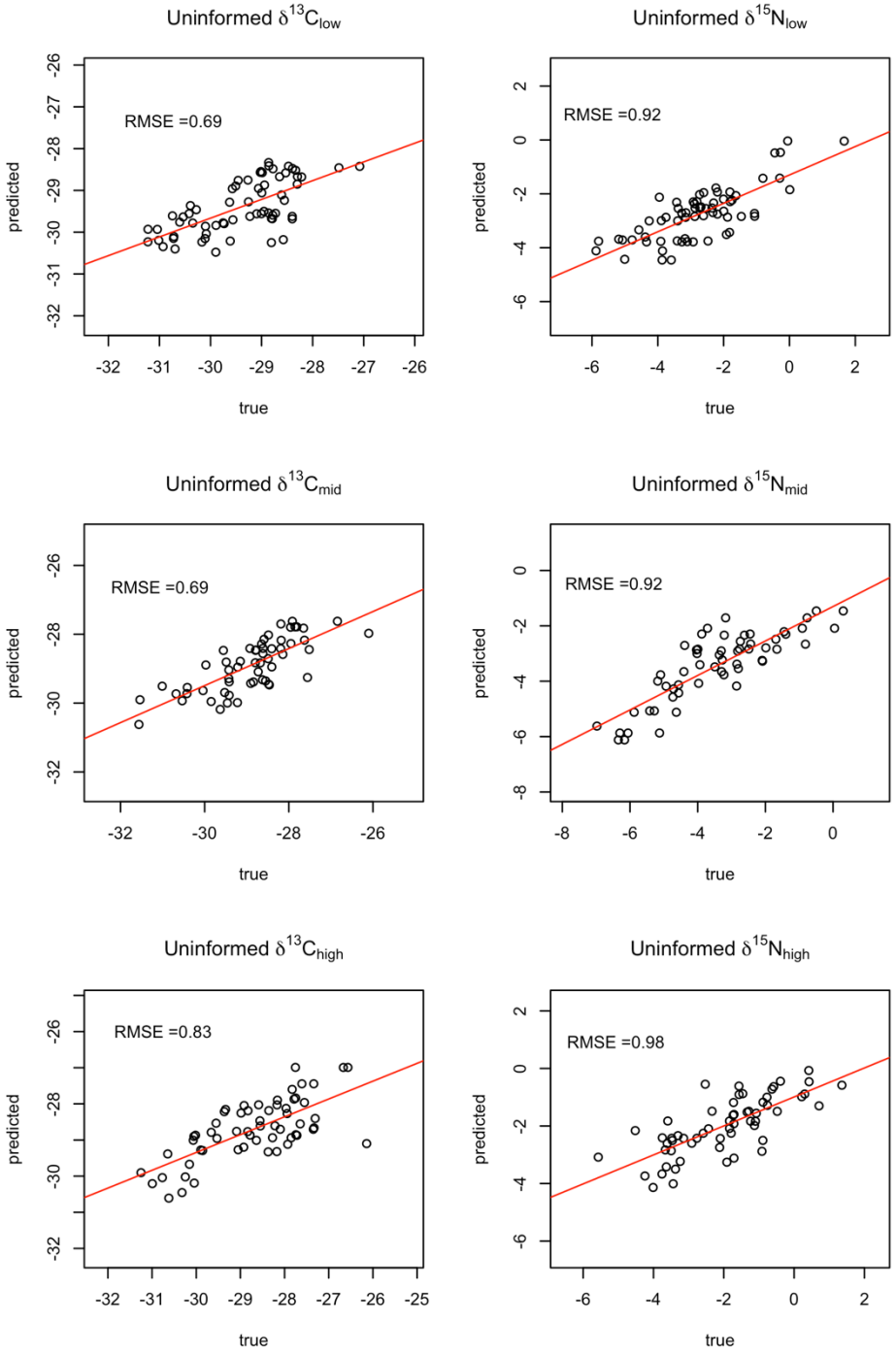

Fig.S3-1. Relationship between predicted and true values for hold-one-out cross validation from linear mixed-models predicting uninformed isotopes for $\delta^{13}C$ and $\delta^{15}N$. Points (n=67) represent predicted and true values at individual sites, while the line characterizes the linear regression between predicted and true values. RMSE is the root-mean squared error for spatial hold-one out cross validation.

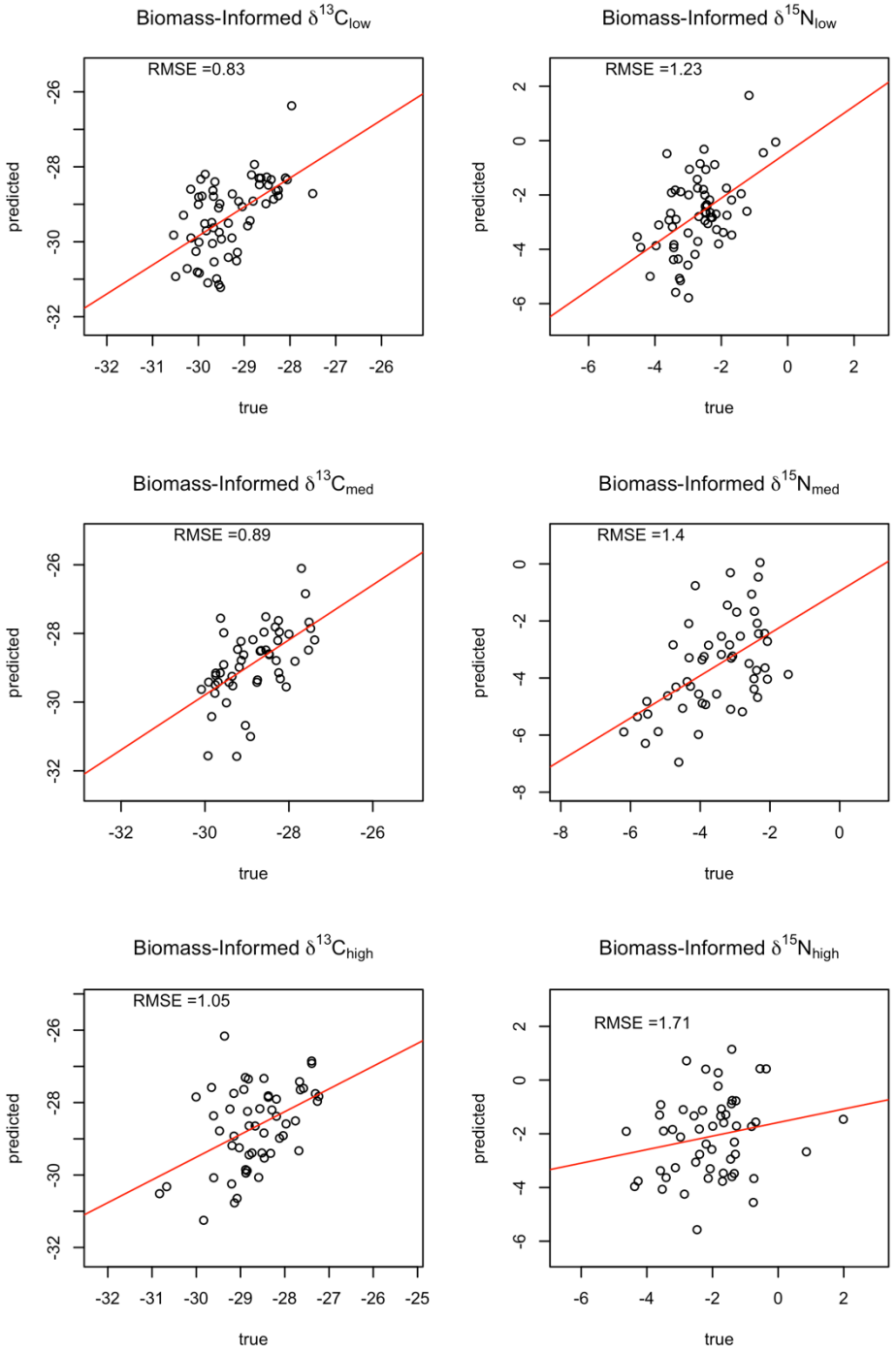

Fig.S3-2. Relationship between predicted and true values for hold-one-out cross validation from linear mixed-models predicting biomass-informed isotopes for $\delta^{13}C$ and $\delta^{15}N$. Points (n=67) represent predicted and true values at individual sites, while the line characterizes the linear regression between predicted and true values. RMSE is the root-mean squared error for spatial hold-one out cross validation.